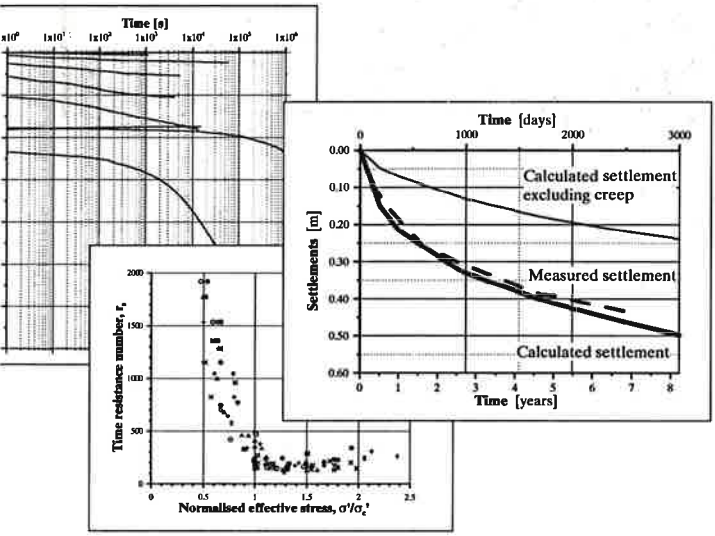

ong term settlements
soft clays

ETER CLAESSON

artment of Geotechnical Engineering
LMERS UNIVERSITY OF TECHNOLOGY
eborg, Sweden 2003

THESIS FOR THE DEGREE OF DOCTOR OF PHILOSOPHY

Long term settlements in soft clays

Peter Claesson

Department of Geotechnical Engineering
CHALMERS UNIVERSITY OF TECHNOLOGY
Göteborg , Sweden 2003

Long term settlements in soft clays

PETER CLAESSON

ISBN 91-7291-263-4

Doktorsavhandling vid Chalmers tekniska högskola

ISSN 0346-718X
Ny serie nr 1945

Department of Geotechnical Engineering
Chalmers University of Technology
SE-412 96 Göteborg
Sweden
Telephone +46 (0) 31-772 1000

Chalmers Reproservice
Göteborg, Sweden 2003

PREFACE

The work was carried out at the Department of Geotechnical Engineering at Chalmers University of Technology, under the supervision of Professor Göran Sällfors and supported by grants from FORMAS, Banverket, The Swedish National Road Administration, Skanska, The Development Fund of the Swedish Construction Industry and Chalmers.

First of all, I would like to thank Professor Göran Sällfors for his guidance, support and encouragement, which has been invaluable for carrying throughout this work.

I am most grateful to Dr. Sadek Baker for his never-ending patience during discussions about theories and differential equations and for his most competent and skilful work with the computer code.

I would like to express my sincere thanks to all those who have made important contributions to as well as influenced the work. Ingmar Svensk, Skanska Teknik, for his support and encouragement and for believing in my ability. Prof. Rolf Larsson, SGI, for valuable discussions, for kindly giving me access data available from test sites and for his critical examination of the manuscript. Dr. Claes Alén, SGI, for fruitful discussions and for proof reading parts of the manuscript. To Per-Evert Bengtsson, PEAB, for his technical support and valuable discussions. Ass. Prof. Anna-Lena Öberg-Högsta, Golder/Chalmers, for her continued support and critical examination of the manuscript.

I wish to express my special thanks to:

The project group, thank you for doing a great and skilful job:

Aaro Prionen, for manufacturing all the necessary equipment with great precision.

Ingemar Forsgren and Kjell Nätterdahl for their assistance with the field investigations.

Jacques Connant, for his help with the development of laboratory device and laboratory tests.

Simone Hellberg-Alén for taking care of the financial aspects and administration.

And not forgetting all my other departmental colleagues for support and friendship during this period.

Fredrik Svensson, Jonas Karlsson and Peter Jansson, whose assistance and contribution are greatly appreciated.

Gullvi Nilsson, her proof reading of the manuscript is greatly appreciated and also Tobias Karlsson for helping me with the figures.

Finally, I wish to express my gratitude to my nearest family: my wife Maria for her invaluable support and patience and our two children Erik and Philip for reminding me of the important things in life.

Göteborg, January 2003

Peter Claesson

TABLE OF CONTENTS

SUMMARY

Background

When buildings, roads or other structures are founded on deep layers of lightly overconsolidated soft clay large settlement often occur during a long period of time after completion of the structure, in many cases for the entire design life time. This can cause unnecessarily high costs for maintenance.

Therefore, it is of major importance to be able to calculate and predict the expected settlements with a satisfactory degree of accuracy, as this has a great impact on the design of the foundation and the possible need for soil improvement.

Objective and scope of the study

The objective of the present study was to improve the accuracy of the methods for predicting settlements over time in deep layers of soft clay with a greater accuracy, with particular attention to loads that result in an effective stress around the preconsolidation pressure.

In order to accomplish this:

- the empirical base has been extended regarding to the creep behaviour and the creep parameter.
- a number of laboratory tests have been conducted in order to document and study the behaviour of the clay under various test conditions, thereby providing a better understanding and knowledge of the consolidation process.
- a number of test sites were examined, where the soil conditions could be documented in detail and where the settlements had been monitored over a long

period of time, preferably more than 10 years. These test sites constitute a vital base for verifying the settlement calculations model.

- a computer program was developed for modelling both laboratory tests, such as incremental loading tests, and full-scale field conditions.

In addition, a study of the parameter models was conducted, with particular emphasis on the compression modulus and the creep parameter model, with the intension of making the models capable of describing the natural behaviour of clay.

Test sites

This research project includes field investigations and settlement observations from five test sites. The test sites have been chosen partly because the soil strata consist of deep deposits of soft, lightly overconsolidated clay, which is of particular relevance for this work and partly because the settlements have been monitored for periods of between 8 and 57 years. An exception is the Lundby Strand test site, where no settlement measurements have been conducted. The purpose of the Lundby Strand test site was to investigate the creep behaviour of clay at very great depths, i.e. down to about 70 m. The data from the test sites are of great importance and are vital for the verification of the proposed settlement calculation model.

The creep parameter

The findings of the laboratory tests can be summarized as follows. Firstly, the creep behaviour is strongly dependent on the effective stress. From an effective stress of about $0.7 \cdot \sigma_c'$ up to approximately $1.1 \cdot \sigma_c'$ the coefficient of secondary compression, α_s , gradually increased to the maximum value. With a further increase in the effective

stress, α_s, remained fairly constant within a certain range or showed a slight decrease, see Figure S1a.

The same general behaviour regarding α_s was also observed in clays from deep layers down to about 70 m below the ground surface, as shown in Figure S1b.

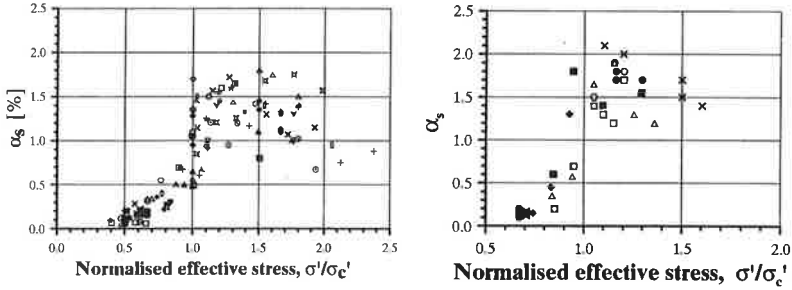

(a) The Änggården test site *(b) The Lundby Strand test site*

Figure S1 *Evaluated values of α_s from (a) the Änggården test site, depth 4 to 22 m and (b) the Lundby Strand test site, depth 10 to 70 m.*

Secondly, the drainage conditions or the load increment ratio (LIR) for IL tests appears to have no or very limited effect on the evaluated value of α_s. However, the duration of each load step should be taken into consideration, otherwise the consequence could be a miss interpretation of the value of α_s.

The relationship between effective stress, strain and strain rate

From the CRS tests conducted with various strain rates, it can be concluded that clay shows viscous effects. Each stress-strain curve is unique due to the strain rate, which confirms that, for clays under one-dimensional consolidation, there is a unique relationship between effective stress, strain and strain rate, see Figure S2a.

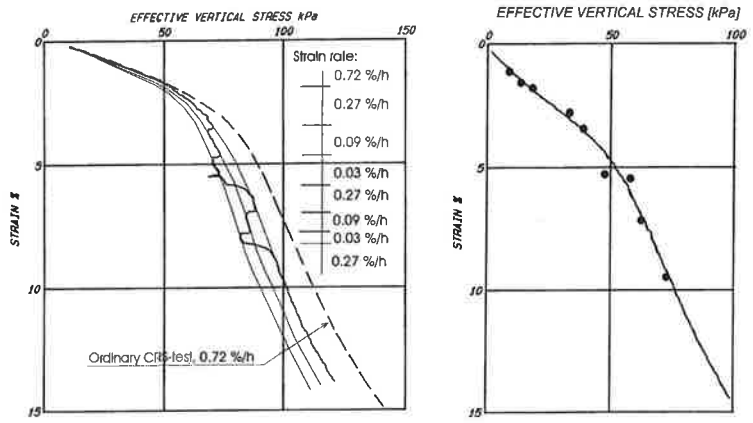

(a) (b)

Figure S2 *(a) A CRS test with different strain rates and a standard CRS test, Änggården CTH11-7m, and (b) evaluated stress – strain coordinates for strain rates 0.72 %/h compared to CRS test with corresponding strain rate 0.72 %/h, Änggården CTH11-5m.*

Furthermore, the described relationship can also be verified by evaluating the effective stress and strain of a particular strain rate from each load step of IL tests and by plotting the data obtained. The plotted data agree very well with the obtained curve from a CRS test on the same clay and with a corresponding strain rate, as illustrated in Figure S2b.

A model for settlement calculation

In 1998, Alén (1998) proposed a model for one-dimensional consolidation including creep effects. The model was intended as a tool in engineering practice. The parameter models consist of well-known parameters and are in accordance with Swedish practice. The aim of this study was to develop the computer code.

In order to improve the parameter models, the compression modulus model was modified by a gradual

change of the modulus from M_0 to M_L, see Figure S3. The calculated result will hence be less sensitive to moderate variations in the applied load where the final effective stress is close to the preconsolidation pressure.

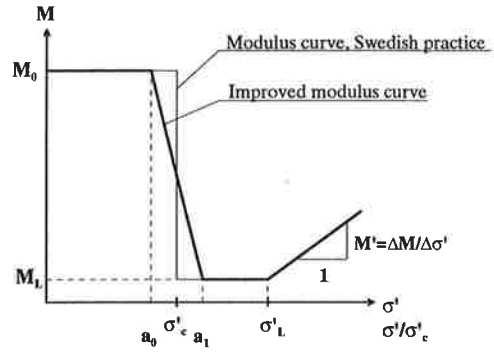

Figure S3 *Swedish practice for interpretation of the compression modulus from a CRS-test and the proposed compression modulus model. The factors a_0 and a_1 are given as values with respect to the normalised effective stress.*

For the modelling of IL tests the appropriate values of the factors a_0 and a_1 appear to be 0.9 and 1.1. However, when calculating settlements for full-scale conditions the values of a_0 and a_1 were set at 0.8 and 1.0 respectively. The reasons for the variation in the chosen values of a_0 and a_1 are the interpretation procedure for σ'_c and the strain rate effects. The strain rates during primary consolidation are obviously higher in IL tests than in field conditions for thick layers of soft clay.

If the creep parameter time resistance number, r_s, is expressed as a bi-linear function of the effective stress, the creep property of soft clays is assumed to be adequately described. The time resistance number model is defined by r_0, r_1 and the factors b_0 and b_1, see Figure S4. In the creep model, the value of factor b_1, set at 1.1 appears relevant for describing the creep behaviour when modelling both IL tests and full-scale conditions. The b_0 value is chosen due to the initial effective stress, σ'_0.

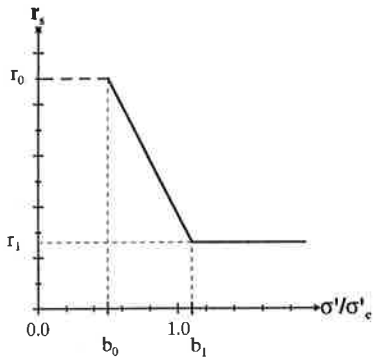

Figure S4 *Definition of the time resistance number model, including the factors b_0 and b_1 as a function of the normalised effective stress.*

The first step in the development of the model was to verify against analytical calculations excluding creep effects. Secondly, the computer code was verified by modelling IL tests, conducted under well defined conditions. An example of the modelling of an IL test load step is given in Figure S5a, where results from both time – strain and time – excess pore pressure are compared to measured data.

The next step was to compare the results of full-scale settlement calculations with measured settlements from a number of case records. As an example settlement calculations from section 0/950 at the Bratteröd test site is given in Figure S5b. Notable are firstly, the agreement between calculated and measured settlements and, secondly, the great difference between the calculations with and without the consideration of creep effects. The contribution of creep effects to settlements could be equal to or greater than the calculated settlement excluding creep effects. Creep could, under certain conditions, be a major cause of settlement.

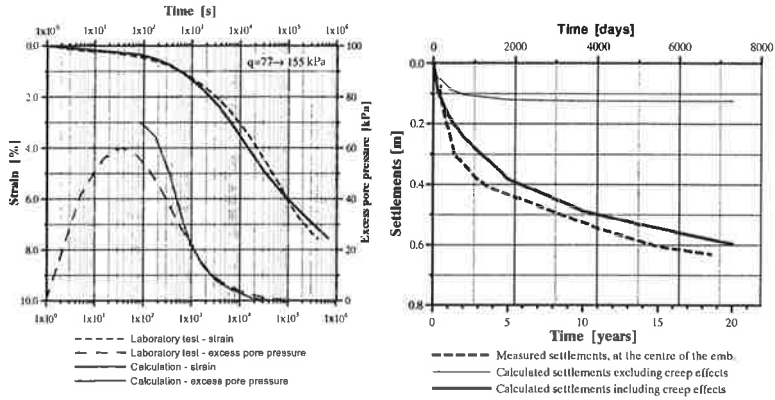

(a) (b)

Figure S5 *(a) Results from a load step of an IL test, conducted on clay specimen from Änggården, CTH12-16m, σ'_c=122 kPa The total load corresponds to an effective stress, after EOP, of $\sigma'_c \cdot 1.3$.*

(b) Calculated and measured settlements with or without consideration of creep effects for section 0/950 at the Bratteröd test site.

The model implemented in the computer code is able to predict the stress–strain behaviour and the excess pore pressure dissipation with respect to time for both incremental loading (IL) tests and full-scale calculations under varying conditions with a satisfactory degree of accuracy.

Finally, when carrying out settlement calculations for a soil profile consisting of deep layers of soft clay, at depths in excess of 20-25 m, and with a relatively broad load, minor changes in the parameters could cause differences in the calculated settlements. Hence, in order to make a reliable assessment of the predicted settlements, it is of importance to study how a variation in the input parameters affect the calculated settlements, normally with focus on the preconsolidation pressure, σ'_c; permeability, k; compression modulus, M_L; and the time resistance number, r_s.

LIST OF SYMBOLS AND ABBREVIATIONS

Roman letters

A	κ/V
a_0	factor of the modulus model
a_1	factor of the modulus model
B	m/r_s
B	$(\lambda-\kappa)/V$ (Plaxis)
b_0	factor of the time resistance number model
b_1	factor of the time resistance number model
C	$1/r_s$
C	degree Celsius
C_α	secondary compression index
C_c	compression index
C_ε	compression index
C_p	preconsolidation index
C_r	recompression index
C_s	recompression index
c_v	coefficient of consolidation
e	void ratio
e_0	initial void ratio
H	drainage length
K_0	coefficient of earth pressure in consolidated state
k	permeability or coefficient of permeability
k_v	vertical permeability
k_z	vertical permeability
$k_{\sigma'_0}$	permeability for in-situ conditions
M	compression modulus, oedometer modulus
M_0	compression modulus for effective stresses in the overconsolidated range
M_L	compression modulus for effective stresses in the normally consolidated range
M'	modulus number

m	modulus number
m'	C_α / C_c
m_e	modulus number for $\sigma' < p_c$
m_{ep}	modulus number for elastic plastic strains for $\sigma' \geq p_c'$.
p_c'	preconsolidation pressure
R	time resistance
r_s	time resistance number
r_0	initial time resistance
r_1	time resistance number for $\sigma' \geq b_1 \cdot \sigma_c'$
q	load
T_v	time factor
t	time
t'	effective creep time
t_c	time to the end of primary consolidation
t_{EOP}	time to the end of primary consolidation
t_e	equivalent time
t_r	reference time
t_0	time when the R-t curve approaches a straight line
t_0	time similar to t_{EOP}
u	pore water pressure
u'	excess pore pressure
u_{cr}	pore water pressure due to creep effects
V	specific volume
w	a force per unit volume
w_L	liquid limit
w_N	natural water content
z	depth

Greek letters

α_s	coefficient of secondary compression
$\alpha_{s\,max}$	maximum value of the coefficient of secondary compression
β_{α_s}	coefficient of change in secondary compression
β_k	coefficient of permeability change
ε	strain

ε_e	elastic strain
ε_{ep}	elastic plastic strain
ε_v	vertical strain
ε_z	vertical strain
ε_c^e	elastic strain during primary consolidation
ε_v^{vp}	strain corresponding to σ'_p
ε_z^e	vertical elastic strain
ε_z^{ep}	vertical elastic plastic strain
ε_z^p	vertical plastic strain
ε_z^{tp}	vertical time-dependent plastic strain
ε_{cr}	creep strain
ε_{ac}^{cr}	creep strain after primary consolidation
ε_c^{cr}	creep strain during primary consolidation
ε_s	creep strain
ε_z^{cr}	vertical creep strain
$\dot{\varepsilon}_{ref}$	reference strain rate
$\dot{\varepsilon}_c^e$	elastic strain rate during primary consolidation
$\dot{\varepsilon}_v$	vertical strain rate
$\dot{\varepsilon}^{cr}$	creep strain rate
$\dot{\varepsilon}_v^e$	vertical elastic strain rate
$\dot{\varepsilon}_v^{vp}$	vertical viscoplastic strain rate
$\dot{\varepsilon}_z^{cr}$	vertical creep strain rate
κ	elastic stiffness of soil
λ	elastic plastic stiffness of soil
Γ	value of $\log\sigma'_p$ at $\dot{\varepsilon}_v = 10^0\ 1/s$
γ_w	unit weight of water
σ	total stress
σ'	effective stress
σ'_c	preconsolidation pressure
σ'_L	effective stress where the compression modulus begins to increase
σ'_p	preconsolidation pressure
σ'_v	vertical effective stress
$\dot{\sigma}'_v$	rate of effective stress change

ψ	creep parameter, $1/r_s$
τ_c	the intercept with the time axis of the straight creep line

Abbreviations

CRS	constant rate of strain
CPT	cone penetration test
CTH	Chalmers University of Technologi
EOP	end of primary consolidation
EPS	expanded polystyrene
EVP	elastic viscoplastic
IL	incremental loading
LIR	load increment ratio
OCR	overconsolidation ratio
SGI	Swedish Geotechnical Institute

1. INTRODUCTION

1.1 Background

When buildings, roads or other structures are founded on layers of soft clay, large settlements often occur over a long period of time following completion of the structure, which in many cases means the entire design lifetime. This can cause unnecessarily high maintenance costs.

Therefore, it is of great relevance to be able to calculate and predict the expected settlements with a fairly high degree of accuracy, as settlement predictions have a great impact on the design of the foundation and on the possible need for soil improvement.

In order to reliably predict the settlements it is necessary for the calculation model to take account of creep effects. Many researchers have addressed this problem, in many cases quite successfully. However deep layers of normally consolidated and only lightly overconsolidated, soft clay have proved to be a special challenge, particularly when dealing with conditions such as limited loads with a relatively large extension, where the final effective stress is of the same order of magnitude as the preconsolidation pressure. Under such conditions, the creep strains can account for a relatively large part of the total settlements.

1.2 Objective and scope of the study

The objective of this thesis was to improve the possibility of accurately predicting the settlement over time for deep layers of clay, especially for loads resulting in an effective stress around the preconsolidation pressure after dissipation of the excess pore pressure. In order to accomplish this:

- a number of laboratory tests were conducted in order to test and document the behaviour of the clay under

various conditions, thus leading to an increased understanding and knowledge of the consolidation process and, in addition, extending the base for the creep parameter.

- a number of full-scale case histories were examined, where the settlements had been monitored over a long period of time, preferably more than 10 years and where the soil conditions could be documented in detail and these test sites contribute an essential base for verifying and improving the model for settlement analysis.

- a computer program was developed capable of modelling both laboratory tests and full-scale case records.

Furthermore, the work with the computer model involved a general study of a number of other methods and theories for settlement calculations including creep effects.

Moreover, a study was conducted of the parameter models, in particular for the compression modulus and the creep parameter, with the intention of making the models capable of describing the natural behaviour. Estimates of how changes in the different parameters influence the results are also included.

An additional objective was to improve the laboratory test procedures and the methods of interpreting the creep behaviour of soft clay.

2. SURVEY OF LITERATURE

2.1 Introduction

The compressibility behaviour of soft clay has been of major concern over the past 100 years. The literature contains a considerable number of research papers on the subject of consolidation models, with or without creep effects, which highlight the importance of increasing the knowledge and understanding of the complex consolidation process. Thorough knowledge of the consolidation process is essential when developing tools for predicting settlements. A great number of theories with varying degrees of complexity have also been presented.

The consolidation process is often divided into primary and secondary consolidation in the literature. Due to practical aspects this terminology is used also in this thesis. Creep strains are assumed to be involved in both the primary and the secondary consolidation process, i.e. creep is not necessarily equal to secondary consolidation.

In the literature survey the vast number of available papers on consolidation have been limited to those focusing on areas relevant to this work. The first part of this chapter contains a summary of papers dealing with experiences of and theories concerning the compressibility behaviour of clays.

In the concluding part of the survey a brief description of different consolidation models for computer application is presented. Some models are well known worldwide within the geotechnical community whereas others are specially developed for Swedish or Norwegian conditions with respect to standard compression parameters. Some models have been studied more thoroughly than others because of the degree of relevance.

2.2 Theories and models of the process of consolidation

2.2.1 The classical consolidation theory

The classical theory of consolidation was developed by Terzaghi (1923) and first published in 1923. Today, this theory is still the foundation of one-dimensional consolidation theory. The theory is based on the assumption that there is a unique relationship between effective stress and strain independent of time. Furthermore, Terzaghi assumes that the modulus as well as the permeability is constant with time.

The assumption that the relationship between stress and strain, or void ratio, is independent of time is a rough simplification used for high plastic clays since those clays show a large amount of time dependent strains. This can be established by laboratory tests, e.g. incremental loading tests. Numerous long term field observations from e.g. Sweden have also shown that measured settlements and pore water pressures strongly deviates from the classical theory of consolidation when it comes to magnitude as well as duration (Larsson 1986).

Terzaghi's equation for one-dimensional consolidation can be expressed as:

$$\frac{\partial u}{\partial t} = \frac{M}{\gamma} \cdot \frac{\partial}{\partial z}\left(k \cdot \frac{\partial u}{\partial z} \right) \quad \text{or} \tag{2.1}$$

$$\frac{\partial u}{\partial t} = c_v \frac{\partial^2 u}{\partial z^2} \tag{2.2}$$

if k does not vary with depth,

where the coefficient of consolidation, c_v, is defined as:

$$c_v = \frac{k \cdot M}{\gamma_w} \tag{2.3}$$

where k = permeability [m/s]

M = compression modulus [kPa]

γ_w = unit weight of water [kN/m^3]

The hydraulic conductivity, k, is in the geotechnical field referred to as permeability or coefficient of permeability.

Equation (2.2) is valid under the following conditions:

- the soil is saturated and homogeneous
- the flow of pore water flow and the strain are one-dimensional.
- Darcy´s law is valid
- the change in pore water pressure is equal to the change in effective stress
- the pore water and soil particles are incompressible
- the strain is only dependent on the effective stress

In 1925 Terzaghi introduced the first oedometer device and suggested a test procedure where a specimen is loaded step-wise, each load step doubling the previous value, until the excess pore pressure has dissipated. For clays, a duration of 24 h is quite common. This procedure is still widely used, and is commonly referred to as a standard incremental load oedometer test.

In 1936 Terzaghi proposed a model for calculating the degree of consolidation, see Figure 2.1.

The degree of consolidation is determined by calculating the time factor, T_v:

$$T_v = \frac{c_v}{H^2} \cdot t \qquad (2.4)$$

where c_v = coefficient of consolidation [m^2/s]

H = drainage length [m]

t = time [s]

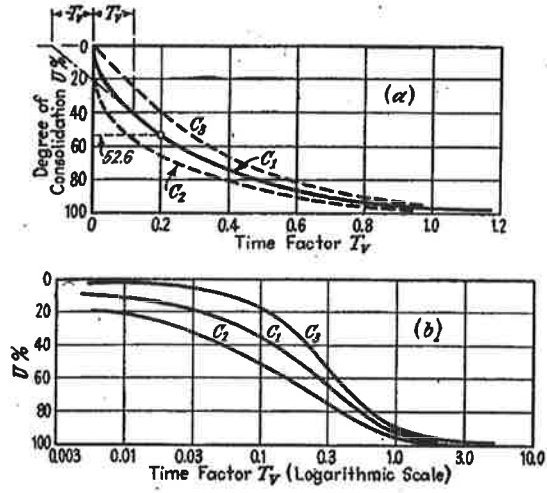

Figure 2.1 Relationship between the time factor and degree of consolidation. In (a) the time factor is plotted on the abscissa in an arithmetic scale and in (b) on a logarithmic scale. The three curves C_1 to C_3 correspond to three different cases of excess pore pressures and drainage conditions. (After Terzaghi and Frölich, 1936)

Casagrande (1936) proposed an oedometer test procedure for determining the end of primary consolidation, EOP, of each load increment, i.e. when the excess pore pressure has completely dissipated.

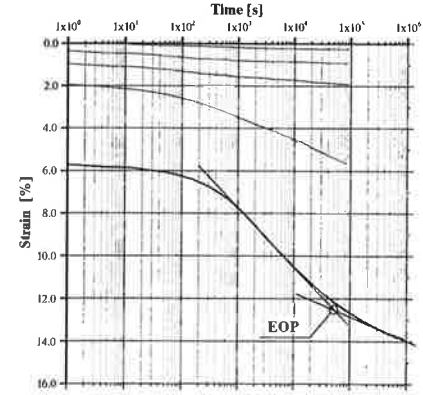

Figure 2.2 The Casagrande method of determining EOP, 100 % of primary consolidation.

It assumes that the time – strain curve is plotted in a semi-logarithmic diagram. The EOP is defined as the point of intersection between the two tangents to the curve as shown in Figure 2.2.

Another commonly used method of determining the EOP was suggested by Taylor (1948). In this method, the strain is plotted versus the square root of time.

2.2.2 Early models for consolidation including creep effects

Originally consolidation settlements were calculated according to Terzaghi's theory and possibly creep settlements starting after that full excess pore pressure dissipation had occurred, e.g. Buisman (1936).

Taylor and Merchant (1940) formulated the first theory where creep effects were at least partly involved in the process of dissipation of excess pore pressure.

Two years later, in 1942, Taylor developed a first model of a general variation of void ratio, e, versus effective stress, σ', and time, t. The model was applicable for oedometer tests.

When consolidation models have been presented in the literature, the consolidation process has almost always been divided into primary and secondary consolidation. The basic assumption is that primary consolidation occurs during an increase in the effective stress and a simultaneous decrease in excess pore pressure and volume. The process of secondary consolidation is defined as a decrease in volume under constant effective stress. Over a long period of time creep strains were separated from the primary consolidation and thus considered equal to secondary consolidation. In 1957, Šuklje presented a model, described below, where creep strains also were assumed to occur during primary consolidation. This is the dominating concept for models presented over the last 20-30 years.

The model presented by Šuklje (1957), where the relationship between effective stress, void ratio and strain rate defined the consolidation curve. This relationship was presented by a set of isotaches, see Figure 2.3.

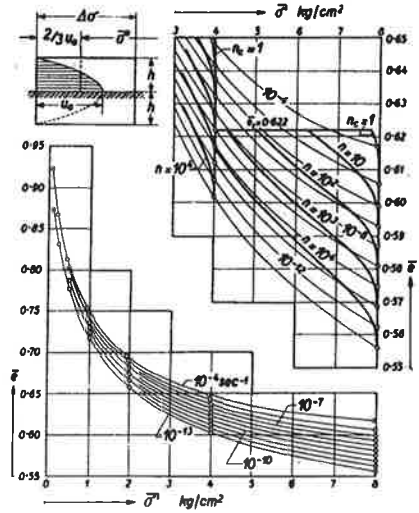

Figure 2.3 Set of isotaches, each line representing a constant strain rate. n denotes the ratio between the initial thickness of the layer and the sample. (Šuklje, 1957).

Šuklje was the first to suggest that the behaviour of clay at one-dimensional compression is governed by a unique relationship between effective stress, void ratio and strain rate.

The model developed by Šuklje assumes that creep occurs during the entire consolidation process. It thus assumes that primary consolidation and creep effects are not two separate processes, occurring before and after the dissipation of excess pore pressure. Šuklje also accounted for the fact that the time-dependent strains are influenced by the thickness of the clay layer, permeability and drainage conditions.

2.2.3 The Bjerrum model

In 1967 Bjerrum presented a conceptual model, which, in a similar fashion to Šuklje's model, also assumes that primary consolidation and creep strains are not divided into separate processes. It should be observed that the model is primarily intended for settlements that have developed over a long period of time, i.e. a period of time in a geological perspective. The engineer however, is normally concerned with a shorter period of time, often 50-100 years or shorter. Consequently, in engineering practice, it is essential that the design takes account of the time delay caused by permeability and the drainage conditions.

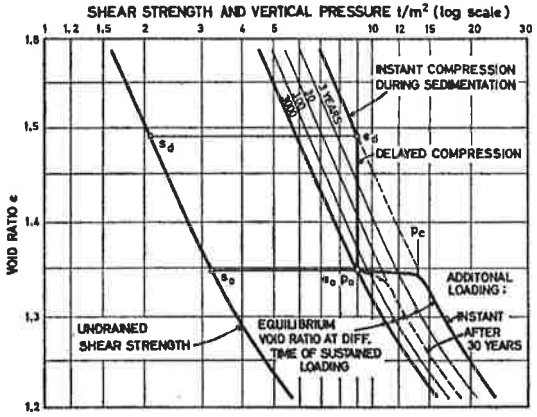

Figure 2.4 *A diagram describing the conceptual model developed by Bjerrum. A series of parallel time lines on a log σ' – e diagram, describing the compressibility and shear strength of clay, which shows delayed consolidation (Bjerrum, 1967).*

The Bjerrum model was intended to explain the apparent preconsolidation pressure and overconsolidation ratio of virgin clays, resulting from geological ageing. The model also explains settlements and creep effects occurring over time, in spite of the fact that the preconsolidation pressure has not been exceeded. In Figure 2.4 the unique relationship between void ratio, pressure (effective stress)

and time is represented by a series of parallel time lines on the vertical pressure – void ratio diagram.

Bjerrum separated strains into "instant" and "delayed" compression and used "time lines" to model the reduced creep rates resulting from the increased duration of loading.

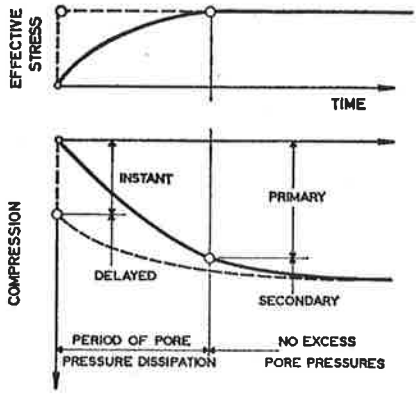

Figure 2.5 Definition of the two parts of settlements, "instant" and "delayed" compression, compared with "primary" and "secondary" compression illustrated by the broken and the solid line respectively (Bjerrum, 1967).

Figure 2.5 shows how the compression of a clay layer is assumed to develop with time for an applied load if the applied load is transferred instantaneously to the clay structure, i.e. as effective stress. This is termed "instant" compression and the broken line curve illustrates how the strains would occur if the pore water in the saturated clay could be disregarded. The subsequent compression, i.e. under unchanged effective stress, is the "delayed" compression. Due to the viscosity of water the effective stresses will gradually increase when the excess pore pressures dissipate and consequently compression will occur along the solid line.

Bjerrum (1967) also stated that there is an obvious relation between preconsolidation pressure and undrained shear strength. The relation is assumed to

remain unchanged at changing void ratio (or strain). Hence, a decrease in void ratio, or increasing strains, increases the undrained shear strength.

The magnitude of the overconsolidation ratio, OCR, depends, according to Bjerrum, on the plasticity of the clay and its geological history.

2.2.4 The creep parameters C_α and α_s

A widely used parameter for describing the creep behaviour of clay is the *secondary compression index*, C_α, (Taylor 1942) defined as:

$$C_\alpha = \frac{\Delta e}{\Delta \log(t)} \tag{2.5}$$

where e = void ratio

The creep parameter that is commonly used in Sweden, the *coefficient of secondary consolidation*, α_s, relates to the *secondary compression index*. The only difference in the definition of the two parameters is that α_s is described as a function of strain, ε, and C_α as a function of void ratio, e. The relationship between the two creep parameters can be expressed as:

$$\alpha_s = \frac{C_\alpha}{1+e_0} \tag{2.6}$$

where $1+e_0$ = the specific volume, V

e_0 = initial void ratio

The coefficient of secondary compression, α_s, is thus defined as:

$$\alpha_s = \frac{\Delta \varepsilon_{cr}}{\Delta \log(t)} \tag{2.7}$$

where α_s = coefficient of secondary compression

ε_{cr} = creep strain

t = time

Figure 2.6 illustrates the evaluation of α_s from an incremental loading (IL) test.

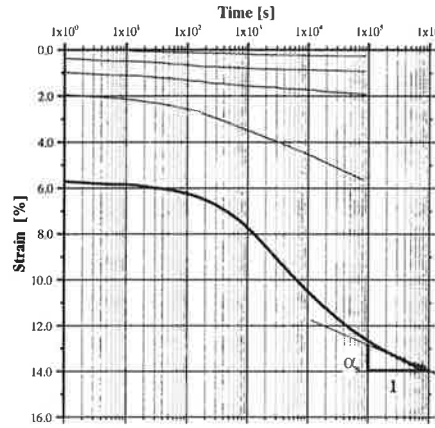

Figure 2.6 Evaluation of α_s from an incremental loading test.

The creep behaviour is often described by the coefficient of secondary compression, α_s, as a function of strain. Figure 2.7 shows a general model of α_s and its variation with strain. The coefficient β_{a_s} define the change in α_s with increasing strain.

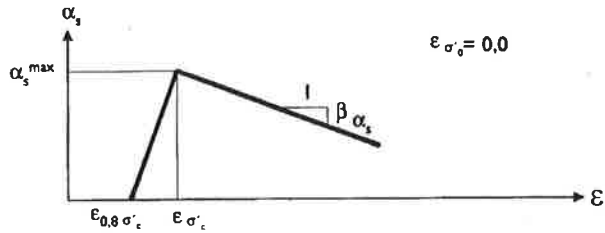

Figure 2.7 The model of the coefficient of secondary compression, α_s, according to Swedish practice (Bengtsson and Larsson, 1994).

2.2.5 The time resistance concept

Another parameter that describes the creep behaviour is the time resistance, R, introduced by Janbu (1969). If an applied stress is to be considered as an action, then the

strain will be considered as a reaction. In the case of creep, the time will be considered as an action and the creep strain is its reaction. This relationship is defined as:

$$R = \frac{dt}{d\varepsilon} \tag{2.8}$$

where R = time resistance [s]

ε = strain

In laboratory tests it has been found that the time resistance of clays increases about linearly with time, as is illustrated in Figure 2.8, and can be expressed as:

$$\frac{dR}{dt} = r_s \tag{2.9}$$

where r_s is the time resistance number. It can be seen from Figure 2.8 that after a certain time t_0 the time resistance is assumed to increase linearly with time. Thereafter the relation may be expressed as:

$$R = r_s \cdot (t - t_r) \tag{2.10}$$

where t = time

t_r = reference time

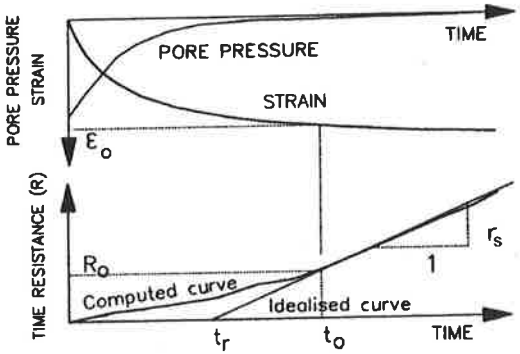

Figure 2.8 Time resistance as a function of time for one load increment (Svanø et al., 1991).

The creep strain rate $\dot{\varepsilon}$ at time t is equal to the inverse of the time resistance R:

$$\dot{\varepsilon}_{cr} = \frac{\partial \varepsilon_{cr}}{\partial t} = \frac{1}{R} = \frac{1}{r_s \cdot (t - t_r)} \tag{2.11}$$

where $\dot{\varepsilon}_{cr}$ = creep strain rate [1/s]

ε_{cr} = creep strain

By integration of equation (2.11) from t_0 to t, the strain due to creep can be expressed as:

$$\Delta\varepsilon_{cr} = \frac{1}{r_s} \int_{t_0}^{t} \frac{dt}{(t - t_r)} = \frac{1}{r_s} \ln \frac{t - t_r}{t_0 - t_r} \tag{2.12}$$

where t_0 = time when the R-t curve approaches a straight line

From equation (2.12), the time resistance number, r_s, can hence be defined as:

$$\frac{1}{r_s} = \frac{\partial \varepsilon_{cr}}{\partial \ln t} \tag{2.13}$$

Finally, the relationship between the time resistance number and the coefficient of secondary consolidation is given by:

$$\alpha_s = \frac{\partial \varepsilon_{cr}}{\partial \log(t)} = \frac{\partial \varepsilon_{cr}}{\partial \ln(t)} \cdot \frac{\partial \ln(t)}{\partial \log(t)} = \frac{\partial \varepsilon_{cr}}{\partial \ln(t)} \cdot \ln 10 \tag{2.14}$$

$$\alpha_s = \frac{\ln 10}{r_s} \approx \frac{2{,}3}{r_s} \tag{2.15}$$

2.2.6 Relationship between parameters for primary and secondary consolidation

A parameter commonly used worldwide to describe the compression behaviour of clay for effective stresses greater than the preconsolidation pressure is the *compression index*, C_c, which is defined as:

$$C_c = \frac{\Delta e}{\Delta \log \sigma'} \tag{2.16}$$

where e = void ratio

Mesri and Godlewski (1977) claimed that there is a unique relationship between C_α and C_c that holds true for any type of soil and that will be valid for all combinations of time, effective stress and void ratio:

$$\frac{C_\alpha}{C_c} = constant \tag{2.17}$$

For a majority of inorganic soft clays the relationship equals (Mesri and Castro, 1987):

$$\frac{C_\alpha}{C_c} = 0.04 \pm 0.01 \tag{2.18}$$

In 1985 Janbu defined the relation between the *modulus number, m,* and *time resistance number,* r_s, as:

$$\frac{C_\alpha}{C_c} = \frac{m}{r_s} \tag{2.19}$$

where $m = \dfrac{M(\sigma')}{\sigma'}$

$M(\sigma')$ = oedometer modulus [kPa]

σ' = effective stress [kPa]

The stiffness of the clay is assumed to increase linearly with stress in the normally consolidated domain, i.e. $M = m \cdot \sigma'$. This is in accordance with the concept of Janbu's tangent modulus (Janbu, 1963).

As has been shown, the three creep parameters described in this section are strongly related to each other, despite the fact that there can be some significant differences.

2.2.7 The relationship between effective stress, strain and strain rate

In 1985 Leroueil et al. conducted a comprehensive study of different tests on various types of clays with the objective of determining the rheological behaviour of soft clays. They proposed that the rheological behaviour of

one-dimensional consolidation of clays is controlled by a unique relationship between stress, strain and strain rate ($\sigma' - \varepsilon - \dot{\varepsilon}$). This relationship can be described by just two functions. The first gives the relationship between the preconsolidation pressure and the strain rate, equation (2.20). The second relationship describes the normalised effective stress – strain curve by means of equation (2.21), see Figure 2.9:

$$\sigma'_p = f(\dot{\varepsilon}_v) \tag{2.20}$$

$$\frac{\sigma'_v}{\sigma'_p} = g(\varepsilon_v) \tag{2.21}$$

where σ'_p = preconsolidation pressure

σ'_v = vertical effective stress [kPa]

ε_v = vertical strain

$\dot{\varepsilon}_v$ = vertical strain rate [1/s]

$f(\dot{\varepsilon}_v)$ = a function of vertical strain rate

$g(\varepsilon_v)$ = a function of vertical strain

This rheological model is in line with the model including sets of isotaches proposed by Šuklje (1957).

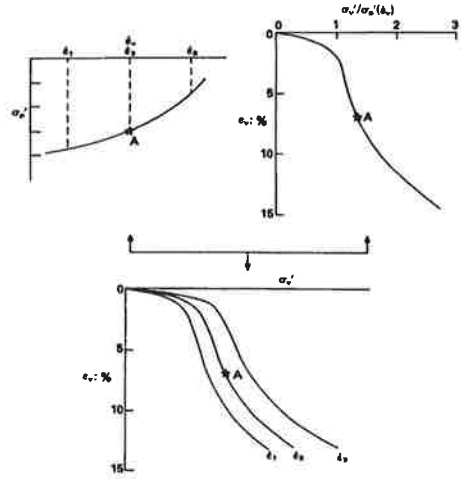

Figure 2.9 Suggested model for natural clays (Leroueil et al., 1985).

The observation that the preconsolidation pressure is dependent on the strain rate has been recognised by many researchers, e.g. Sällfors (1975), Larsson (1981), Graham et al. (1983) and Leroueil et al. (1985) to mention but a few. This behaviour can be exemplified by CRS-tests with different stain rates, as shown in Figure 2.10.

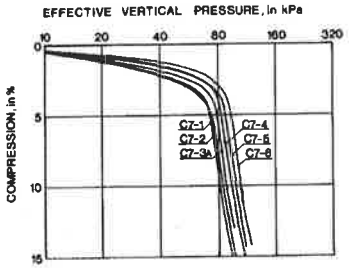

Legend

Test	Depth m	Rate of def. mm/min
C7-1	7	0,0006
C7-2	7	0,0012
C7-3A	7	0,0024
C7-4	7	0,0040
C7-5	7	0,0090
C7-6	7	0,0200

Figure 2.10 CRS-tests with different strain rates from Bäckebol, depth 7m (Sällfors, 1975).

In Figure 2.11 another important test result (Mesri et al. 1995) is presented, which confirms the behaviour described. For a 500 mm long sample the effective stress – strain curves of four different sub-layers were monitored. The stress – strain curves vary, depending on the distance of each sub-element to the drainage boundary. For sub-element 1, close to the drainage surface, the strain rate is higher than in the other sub-elements. The resulting effect is that, for a higher strain rate, a higher magnitude of effective stress was obtained in the initial branch of the curve, i.e. the apparent preconsolidation pressure increased. Analogous results were reported already by Berre and Iversen (1972). Moreover, the results presented in Figure 2.11 show clearly how the consolidation process and the apparent preconsolidation pressure vary in the clay strata due to different drainage conditions.

It can also be noted that the point of EOP, in Figure 2.11, seems to be equal for all sub-elements. Mesri and Choi (1985) proposed that there is a unique EOP e - $\log\sigma'$ curve for any soft clay. This statement is not in line with e.g. Šuklje (1957), Berre and Iversen (1972) and Yin and Graham (1996), who concluded that the relationship between strain and effective stress at the EOP depends on the thickness of the clay specimen/layer.

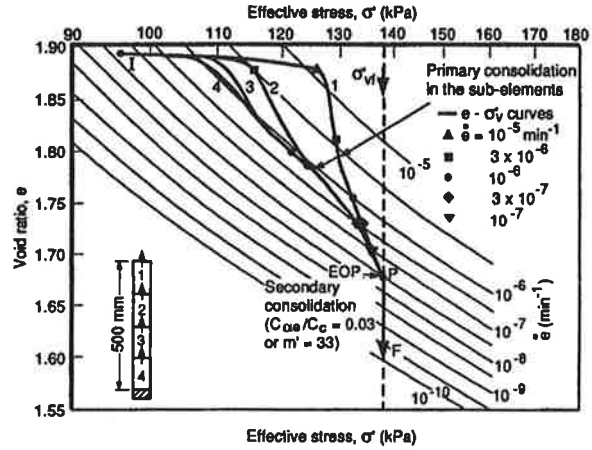

Figure 2.11 Consolidation of Saint-Hilaire clay for pressure increment from 97 to 138 kPa (results from Mesri et al. (1995), reinterpreted and presented by Leroueil and Marques, 1996). C_α, secondary compression index; C_c, compression index; $\dot{e}$, rate of void ratio and $m' = C_c/C_\alpha$.

In 2001 Leroueil and Kim proposed a non-linear viscoplastic model for one-dimensional consolidation, where the strain is divided into two parts: elastic strains and viscoplastic strains. This model is a further development of the model presented by Leroueil et al. (1985) and is described in Section 2.3.5.

2.2.8 The effect of temperature on the compressibility

The behaviour of natural clay during consolidation is evidently not influenced only by the strain rate. Temperature is also an important factor, especially in the normally consolidated range and also in terms of the magnitude of the preconsolidation pressure. The influence of temperature on the compressibility of natural clays has been investigated by authors such as for example Tidfors and Sällfors (1989) and Boudali et al. (1994). In 1994, Boudali et al, proposed a generalization of the model suggested by Leroueil (1985), which takes the temperature into consideration.

Tidfors and Sällfors (1989) found that if the temperature increased from about +7°C, which is the normal temperature in-situ, to about 20°C, the preconsolidation pressure for a high plastic clay decreases with 6 to 10%. Leroueil and Marques (1996) obtained results that were in agreement with that.

However, the temperature in a clay deposit is normally constant and the temperature effects can be neglected in this project because the laboratory tests have been carried out under temperature conditions corresponding to field conditions.

2.2.9 Determination of the creep parameter from CRS tests

Länsivaara (1995, 1999) proposed a model that made it possible to determine the creep parameter *time resistance number,* r_s, from CRS-tests with different strain rates. However, the model assumed that the compression modulus increases linearly with effective stress. For Swedish clays the compression modulus is evaluated as constant from σ'_c to σ'_L. This implies that the relation becomes more complex and thus more difficult to solve. Länsivaara utilised the unique relation between preconsolidation pressure and effective stress at a given strain (see equations (2.20) and (2.21)) and derived:

$$\frac{\sigma'_{v1}}{\sigma'_{cv1}} = \frac{\sigma'_{v2}}{\sigma'_{cv2}} \tag{2.22}$$

where σ'_{v1} = the effective stress for the strain rate $\dot{\varepsilon}_1$

σ'_{cv1} = the preconsolidation pressure for the strain rate $\dot{\varepsilon}_1$

σ'_{v2} = effective stress for the strain rate $\dot{\varepsilon}_2$

σ'_{cv2} = the preconsolidation pressure for the strain rate $\dot{\varepsilon}_2$

In addition to the strain rate relation the equation can be expressed as (Länsivaara 1995):

$$\frac{\sigma'_{v1}}{\sigma'_{v2}} = \frac{\sigma'_{cv1}}{\sigma'_{cv2}} = \left(\frac{\dot{\varepsilon}_1}{\dot{\varepsilon}_2}\right)^B \tag{2.23}$$

where the parameter B was determined. Länsivaara proposed that parameter B is equal to equation (2.19), i.e.

$$B = \frac{m}{r_s} = \frac{C_\alpha}{C_c} \tag{2.24}$$

which describes the relation between the creep and primary compression parameters in the equation.

Hence the time resistance number can be determined from:

$$r_s = \frac{M(\sigma')}{\sigma' \cdot B} \tag{2.25}$$

Länsivaara (1999) found that the value of B for Finnish clays is about 0.073.

Leroueil and Kim (2001) suggested an elastic viscoplastic (EVP) model. The model utilises the relationship between the preconsolidation pressure and strain rate to describe the viscous behaviour. By conducting CRS tests with different strain rates, determining the preconsolidation pressure at each strain rate and then plotting the results in a diagram as shown in Figure 2.12, thus making it possible

to interpret a linear relationship from the plotted results. This procedure is used in Section 6.3.2. The equation describing the relation between preconsolidation pressure and viscoplastic strain rate, $\sigma'_p = f(\dot{\varepsilon}_v^{vp})$, can be expressed as a linear function in a $\log\sigma'_p$–$\log\dot{\varepsilon}_v^{vp}$ diagram, see Figure 2.12:

$$\log\sigma'_p = \Gamma + C_p \cdot \log\dot{\varepsilon}_v^{vp} \tag{2.26}$$

where Γ = the value of $\log\sigma'_p$ at $\dot{\varepsilon}_v^{vp} = 10^0\ 1/s$

$\dot{\varepsilon}_v^{vp}$ = viscoplastic strain rate

$$C_p = \left(\frac{\partial\log\sigma'_p}{\partial\log\dot{\varepsilon}_v^{vp}}\right) \tag{2.27}$$

the preconsolidation index is denoted C_p and is equal to the value of C_α/C_c, which according to Mesri and Castro (1987) is between 0.03-0.05.

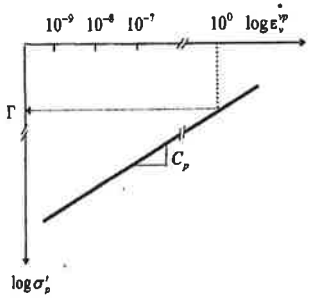

Figure 2.12 Definition of the parameters C_p and Γ (Kim and Leroueil, 2001).

These two parameters define the viscous behaviour of the clay and are necessary parameters in the model described more thoroughly in Section 2.3.5.

2.3 Different models for settlement calculations including creep effects

2.3.1 Introduction

Eight different models for one-dimensional settlement analysis including creep effects for settlement calculation are briefly described in this section. The general features of each model are described as e.g. differential equations, parameters and creep model.

For all of the models presented, the basic equation for primary consolidation is Terzaghi's classic equation for one-dimensional consolidation, see Section 2.2.1 and equation (2.2).

A computer program, GEOFEM-G, was developed as early as 1978 by Runesson (1978). It was a finite element program based on the Modified Cam Clay theory and expanded by means of anisotropy. GEOFEM-G is a complex program that takes creep effects into account. The program appeared to predict settlements and excess pore pressure in very good agreement with measured data but unfortunately there is no version of the program available today.

2.3.2 Alén model

In 1998 Alén (1998) presented a model for one-dimensional consolidation including creep effects. The purpose was to develop a simpler model that could reliably predict settlements in soft clays and be used as a tool in engineering practice. The model is based on a hypothesis that the time dependent settlement in clay can be adequately described by three separate physical phenomena; consolidation, elastic-plastic strain and creep strain. The assumed interaction between these phenomena is described by a rheological model, see Figure 2.13.

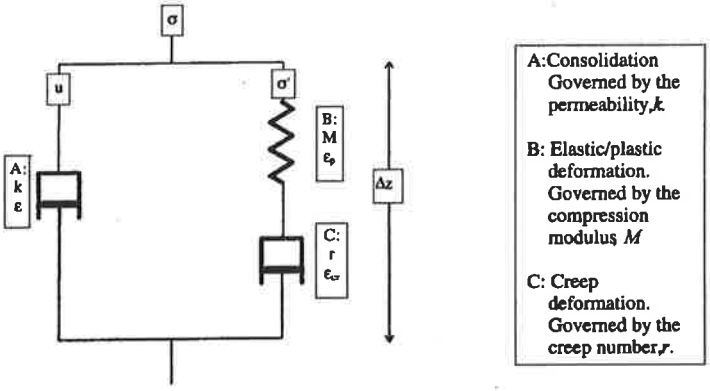

Figure 2.13 Rheological soil model describing long term strains in clay (Alén, 1998).

The compression parameters are σ_c', M, k and the creep behaviour is given by the parameter time resistance number, r_s.

The consolidation process is governed by:

$$\frac{\partial \varepsilon_z}{\partial t} = -\frac{\partial}{\partial z}\left[\frac{k_z}{\gamma_w}\cdot\left(\frac{\partial u}{\partial z}\right)\right] \tag{2.28}$$

and the total vertical strain is equal to the sum of elastic-plastic strain and creep strain:

$$\varepsilon_z = \varepsilon_z^{ep} + \varepsilon_z^{cr} \tag{2.29}$$

where ε_z^{ep} = elastic and plastic strains

ε_z^{cr} = creep strain

A comprehensive description of the theory and the differential equations is given in Chapter 7.

Settlement calculations with a finite difference code gave very good results for a couple of case records analysed (Alén, 1998). For the tested sites, the loads corresponded to effective stresses that with good margin exceeded the preconsolidation pressure. The relative simplicity and relevance of the model makes it very attractive for further

application development, something that has been accomplished within this work, and the result is presented in Chapters 7 and 8.

2.3.3 Embankco

The Embankco computer program was developed by the Swedish National Road Administration (SNRA) and the Swedish Geotechnical Institute (SGI) in 1994 (Bengtsson and Larsson, 1994). The purpose of the finite difference Embankco program was to develop a user friendly computer program for prediction of settlements, including creep, in soft clays/fine grained soils beneath embankment constructions.

The original code, known as CONMULT, was developed in France (Magnan et al., 1979) and subsequently further developed at the Laval University of Quebec in Canada and at SGI. The program was rewritten for e.g. compression parameters, evaluated from CRS tests used in Sweden, and a new creep model was adopted.

The compressibility is defined by the parameters:

σ_c' = preconsolidation pressure [kPa]

σ_L' = effective stress where the compression modulus begins to increase [kPa]

M_0 = compression modulus for $\sigma_v' < \sigma_c'$ [kPa]

M_L = compression modulus for $\sigma_c' \le \sigma_v' \le \sigma_L'$ kPa]

$M' = \Delta M / \Delta \sigma'$, modulus number, for $\sigma_v' > \sigma_L'$

The permeability is given by the parameter k and factor β_k, the latter describing the decrease in permeability with increasing strain.

The creep behaviour is defined by the coefficient of secondary compression, α_s:

$$\alpha_s = \frac{d\varepsilon}{d \log t} \tag{2.30}$$

How α_s varies with strain is described in Section 2.2.4.

The classical differential equation for one-dimensional consolidation was complemented by an expression for creep effects and the following equation was obtained:

$$\frac{\partial u}{\partial t} = \frac{M}{\gamma_w} \cdot \frac{\partial}{\partial z}\left(k \cdot \frac{\partial u}{\partial z}\right) - \frac{\partial u_{cr}}{\partial t} \tag{2.31}$$

where ∂u_{cr} is an increase in pore water pressure due to creep effects. This is obtained by first determining the strain due to creep, equation (2.32), that would have occurred if the soil was freely drained. From this fictitious creep strain and the modulus at hand the resulting increases in pore pressure is calculated according to equation (2.33).

$$\Delta\varepsilon_{cr} = \int_{t}^{t_1} \frac{\alpha_s}{2{,}3} \frac{dt}{t} \tag{2.32}$$

$$\Delta u_{cr} = \Delta\varepsilon_{cr} \cdot M \tag{2.33}$$

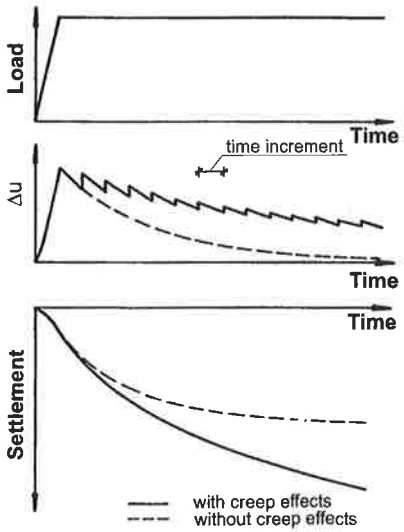

Figure 2.14 Illustration of computed course of consolidation (Larsson et al., 1994)

Some characteristic features of the model are firstly that the soil parameters are up-dated after each time increment. Secondly, the excess pore water pressure due to creep effects is restricted to the dissipation for the calculated time increment according to equation (2.31), i.e. $\partial u/\partial t \leq 0$. Finally, the model does not consider creep effects when the strain rate exceeds a certain value, $\dot{\varepsilon}_{ref} = \alpha_s \cdot 5 \cdot 10^{-6}\,[1/s]$, which approximately corresponds to the standard strain rate at which the oedometer stress-strain curve is evaluated in Sweden.

The program has been used for almost 10 years in the design of embankment constructions and found to have good reliability in the prediction of settlements. It has also been tested previously as well as within this project. However, under certain conditions, e.g. with an increase in effective stress resulting in a value close to the preconsolidation pressure, the calculation results can to a certain extent depend on the chosen number of sub-layers and the excess pore pressure may exceed the initial excess pore pressure.

Moreover, the experience within this research project is that when dealing with time-dependent settlements, including creep effects, a minor change in the parameters can, when using Embankco results in large differences in calculated settlements after long period of times. In many cases, under the conditions as those described above, creep causes surprisingly large settlements both as calculated and as measured in long term (decades) observations. A reliable answer in terms of the geological perspective is missing.

2.3.4 Krykon

Krykon ver. 02 (Svanø and Emdal, 1987) is a FEM program for one-dimensional consolidation analysis including creep effects. The program was developed at SINTEF, Div. of Geotechnical Engineering, Trondheim, Norway.

The stress-strain-time model for one-dimensional consolidation is based on Janbu's tangent moduli formulation (1963), coupled with the time resistance concept. In this model the modulus is stress dependent and the permeability is strain or stress dependent.

Basic equation: $$\frac{\partial \sigma'}{\partial z} + \frac{\partial u}{\partial z} + w = 0 \qquad (2.34)$$

where w = a force per unit volume

The equation of continuity is given by:

$$\frac{\partial}{\partial z}\left(\frac{k}{\gamma_w}\frac{\partial u}{\partial z}\right) + \frac{\partial v}{\partial z} = 0 \qquad (2.35)$$

v = displacement velocity of the soil skeleton [m/s]

The total strain is decoupled into an elasto plastic immediate contribution and a time dependent viscous creep contribution.

The total strain is given by:

$$\varepsilon = \varepsilon(\sigma') + \varepsilon(t) = \varepsilon_e + \varepsilon_{ep} + \varepsilon_s = \frac{1}{m_e}\ln\left(\frac{p_c'}{\sigma_0'}\right) + \frac{1}{m_{ep}}\ln\left(\frac{\sigma'}{p_c'}\right) + \frac{1}{r_s}\ln\left(\frac{t+t_r}{t_r}\right) \qquad (2.36)$$

where: ε_e = elastic strain

ε_{ep} = elasto-plastic strain

ε_s = creep strain

m_e = modulus number for $\sigma' < p_c$

m_{ep} = modulus number for elasto-plastic strains for $\sigma' \geq p_c'$.

p_c' = preconsolidation pressure [kPa]

r_s = time resistance number

When using critical state soil mechanics terminology it becomes:

$$\frac{1}{m_e} = \frac{\kappa}{V} \tag{2.37}$$

and $$\frac{1}{m_{ep}} = \frac{\lambda}{V} \tag{2.38}$$

where $$\kappa = \frac{\Delta e}{\Delta \ln \sigma'}$$

$$\lambda = \frac{\Delta e}{\Delta \ln \sigma'}$$

2.3.5 Elastic-viscoplastic (EVP) model (Leroueil et al. 1985, 1996, 2001)

Leroueil et al. (1985, 1996, 2001) proposed that the rheological behaviour of natural clays is controlled by a unique stress–strain–strain rate relationship. This relationship can be completely described by two equations (2.20) and (2.21). The theory is described in Subsection 2.2.7.

The continuity equation for the consolidation is given by:

$$-\frac{\partial \varepsilon_v}{\partial t} = \frac{1+e_0}{\gamma_w} \frac{\partial}{\partial z}\left(\frac{k_v}{1+e} \frac{\partial u}{\partial z} \right) \tag{2.39}$$

where k_v = vertical permeability [m/s]

z = depth [m]

e_0 = initial void ratio

e = current void ratio

u = excess pore pressure [kPa]

t = time [s]

γ_w= unit weight of water [kN/m^3]

The rate of total strain with respect to time at any stage can be expressed by the constitutive equation as:

$$\dot{\varepsilon}_v = \dot{\varepsilon}_v^e + \dot{\varepsilon}_v^{vp} \tag{2.40}$$

where $\dot{\varepsilon}_v$ = rate of total strain

$\dot{\varepsilon}_v^e$ = elastic strain rate

$\dot{\varepsilon}_v^{vp}$ = viscoplastic strain rate

The elastic strain rate can be obtained from:

$$\dot{\varepsilon}_v^e = \frac{\partial \varepsilon_z}{\partial t} = \frac{\kappa}{1+e_0}\frac{1}{\sigma_v'}\dot{\sigma}_v' \tag{2.41}$$

where e_0 = initial void ratio

$\dot{\sigma}_v'$ = rate of effective stress change

$$\kappa = \frac{\Delta e}{\Delta \ln \sigma'} = \frac{C_s}{\ln 10}$$

and $C_s = \frac{\Delta e}{\Delta \log t}$, denoted recompression index.

The viscoplastic strain rate, $\dot{\varepsilon}_v^{vp}$, can be expressed as:

$$\dot{\varepsilon}_v^{vp} = 10^{\left[\left(\log \sigma_v' - \Gamma - \varepsilon_{0i} - C_\varepsilon \cdot \varepsilon_v^{vp}\right)/C_p\right]} \tag{2.42}$$

where Γ = the value of $\log \sigma_c'$ at $\dot{\varepsilon}_v^{vp} = 10^0\ 1/s$ [kPa]

$C_\varepsilon = \frac{\Delta e}{\Delta \log t}$, denoted compression index

ε_{0i} = intercept of the linear segment with slope C_ε

C_p = preconsolidation index

Leroueil and Kim (2001) utilised the relationship between the strain rate and the corresponding preconsolidation pressure to describe the viscous behaviour of clay by means of the parameters Γ and C_p. The parameters are described in Section 2.2.9.

The other parameters are illustrated by Figure 2.15.

And consequently, the total vertical strain rate can be written as:

$$\dot{\varepsilon}_v = \frac{\kappa}{1+e_0}\frac{\dot{\sigma}_v'}{\sigma_v'} + 10^{\left[\left(\log \sigma_v' - \Gamma - \varepsilon_{0i} - C_\varepsilon \cdot \varepsilon_v^{vp}\right)/C_p\right]} \tag{2.43}$$

By integration of equation (2.43) with respect to time the total vertical strain is obtained.

The proposed model is attractive, due to, among other things, the procedure for defining viscous behaviour with the help of CRS tests. The computer program is flexible and can model both laboratory tests and field behaviour with a high degree of accuracy according to the authors (Kim and Leroueil, 2001).

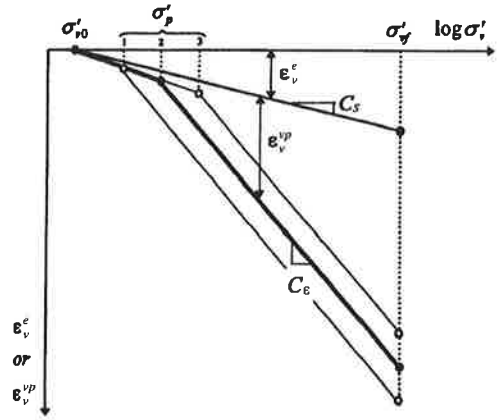

Figure 2.15 Schematic diagram, σ'_v versus ε_v^e or ε_v^{vp}, of the non-linear viscoplastic model. σ'_{v0} is the initial effective stress (Kim and Leroueil, 2001).

2.3.6 Elastic-viscoplastic model (EVP) with "equivalent time" (Yin and Graham, 1994, 1996)

In 1989 and 1994 Yin and Graham presented an elastic viscoplastic model (EVP) for one-dimensional consolidation analysis using the concept of time lines. Time lines are equal in value to the equivalent times, t_e, see Figure 2.16. The model describes one-dimensional stress or strain responses under general conditions in laboratory tests.

In 1996 the same authors (Yin and Graham, 1996) presented an improved model, which included the calculation of excess pore water pressure as well as

settlements. This one-dimensional EVP model was then extended to a generalised three-dimensional model in 1999 (Yin and Graham, 1999). However, as this three-dimensional model was calibrated by using results from tests conducted on a densely compacted sand-bentonite mixture, the results are not compatible with those obtained on soft clay, and therefore, the model will not be described in this section.

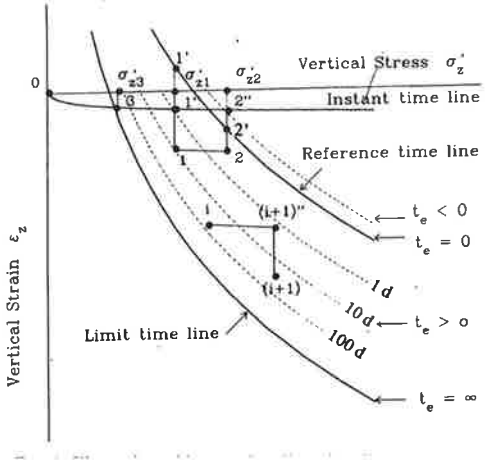

Figure 2.16 Illustration of the instant time line, time lines, equivalent time, reference time line and limit time line (Yin and Graham, 1994)

For the one-dimensional EVP model a time-line model is used to define the relationship between vertical strain, ε_z, vertical effective stress, σ_z', and time, t.

In this model the compressibility parameters are given by the logarithmic functions (natural logarithm) κ and λ, from critical state soil mechanics. The model allowed for the modelling of creep strains in both the overconsolidated and normally consolidated ranges using a constant creep parameter ψ, see Figure 2.17.

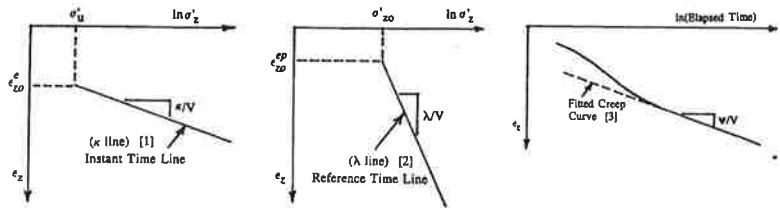

(a) (b) (c)

Figure 2.17 Schematic evaluation of fitting functions for (a) instant time line, (b) reference time line, and (c) creep behaviour (Yin and Graham, 1994)

The basic assumption is that the strains consist of three components:

$$\varepsilon_z = \varepsilon_z^e + \varepsilon_z^{ep} + \varepsilon_z^{tp} \tag{2.44}$$

where ε_z^e = recoverable elastic strain

ε_z^{ep} = vertical elastic plastic strain

ε_z^{tp} = vertical time-dependent plastic strain

Strains along the instant time line, see Figure 2.17a, are elastic and recoverable and can be expressed as:

$$\varepsilon_z^e = \varepsilon_{z0}^e + \frac{\kappa}{V} \ln\left(\frac{\sigma_z'}{\sigma_u'}\right) \tag{2.45}$$

where σ_u' = unit effective stress [kPa]

ε_{z0}^e = the strain at $\sigma_z' = \sigma_u'$

$$\kappa = \frac{\Delta e}{\Delta \ln \sigma'}$$

$V = 1+e_0$, specific volume

The time-independent elastic-plastic strain, see Figure 2.17b, can be written as:

$$\varepsilon_z^{ep} = \varepsilon_{z0}^{ep} + \frac{\lambda}{V} \ln\left(\frac{\sigma_z'}{\sigma_{z0}'}\right) \tag{2.46}$$

where ε_{zo}^{ep} = the strain at $\sigma_z' = \sigma_{z0}'$

ε_{z0}^{ep} = strain corresponding to σ_p'

$$\lambda = \frac{\Delta e}{\Delta \ln \sigma'}$$

The creep strains, see Figure 2.17c, when the excess pore pressure has completely dissipated, are assumed to be described by:

$$\varepsilon_z^{tp} = \frac{\psi}{V} \ln\left(\frac{t_0 + t_e}{t_0}\right) \quad \text{for } -t_0 < t_e < \infty \tag{2.47}$$

where t_e = equivalent time [s]

t_0 = time similar to t_{EOP} [s]

$\psi = 1/r_s$ creep parameter, constant for a given clay

The *equivalent time, t_e,* is defined as the time required for the creep process to bring the clay from a reference time line to the current ε and σ'_v under constant effective stress. However, it is necessary to determine a *reference time*, see Figure 2.16.

A finite difference method was used to solve the resulting differential equation

General equations:

If the equivalent time, t_e , is known, the strain is defined by:

$$\varepsilon_z = \varepsilon_z^{ep} + \varepsilon_z^{tp} = \varepsilon_{z0}^{ep} + \frac{\lambda}{V} \cdot \ln\left(\frac{\sigma_z'}{\sigma_{z0}'}\right) + \frac{\psi}{V} \cdot \ln\left(\frac{t_0 + t_e}{t_0}\right) \tag{2.48}$$

Further, a stress – strain model for any one-dimensional loading condition can be obtained and the vertical strain rate given as:

$$\dot{\varepsilon}_z = \frac{\partial \varepsilon_z}{\partial t} = \frac{\kappa}{V} \frac{1}{\sigma_z'} \left(\frac{\partial \sigma_z'}{\partial t}\right) + \frac{\psi}{V \cdot t_0} \exp\left[-\left(\varepsilon_z - \varepsilon_{z0}^{ep}\right)\frac{V}{\psi}\right] \left(\frac{\sigma_z'}{\sigma_{z0}'}\right)^{\lambda/\psi} \tag{2.49}$$

The parameters in equation (2.49) are described above.

The model can predict the behaviour of viscous soils in one-dimensional compression loadings, e.g. creep aging, relaxation and stress rate effects.

This model employs parameters that seldom are used in Sweden for settlement analysis. The model also seemed to predict the behaviour of clay in laboratory tests well, while full-scale behaviour according to the model was not verified.

2.3.7 Länsivaara model

In 1999, Länsivaara (1999), presented a one-dimensional model for settlement calculations, based on the theory described in Section 2.2.9 and implemented it in a spreadsheet program. One significant feature of the model is that the preconsolidation pressure is strain rate dependent, and is up-dated according to the actual strain rate.

The model calculates the change in excess pore pressure by means of the classical theory of consolidation.

Thereafter the primary strain are calculated according to:

$$\varepsilon_p(t) = \frac{q - u(t)}{M(\sigma')} \tag{2.50}$$

$u(t)$ = excess pore pressure calculated with the classical theory of consolidation

The next step is to calculate the creep strains, ε_c, due to a decrease in the strain rate during the present time increment, which for the normally consolidated range is obtained by:

$$\varepsilon_{c(i,k)} = \frac{B}{m} \ln\left(\frac{\dot{\varepsilon}_{(i,k-1)}}{\dot{\varepsilon}_{(i,k)}}\right) \tag{2.51}$$

where $B = \frac{m}{r_s} = \frac{C_\alpha}{C_c}$ rate parameter

m = modulus number

$\dot{\varepsilon}_{(i,k-1)}$ = strain rate at depth *i* and time *k-1*

$\dot{\varepsilon}_{(i,k)}$ = strain rate at depth *i* and time *k*

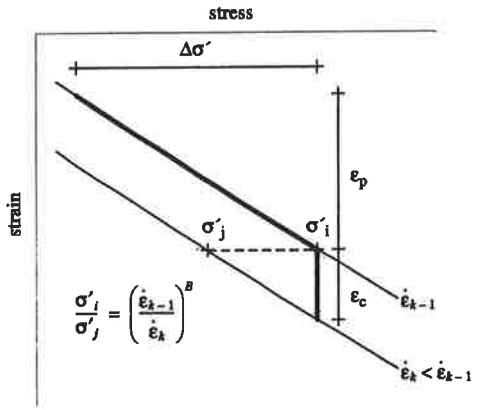

Figure 2.18 The basic concept for the calculation of creep strain (Länsivaara, 1999).

Figure 2.18 presents the concept for creep strain calculation. The creep strain in the overconsolidated range is calculated in a similar way.

The next step is to calculate the preconsolidation pressure for the subsequent time increment in accordance with equation (2.52), as the model takes the strain rate dependence of the preconsolidation pressure value into account.

$$\sigma'_{cv(i,k+1)} = \max\left(\sigma'_{cv(i,k)} \cdot \left(\frac{\dot{\varepsilon}_{(i,k)}}{\dot{\varepsilon}_{(i,k-1)}}\right)^B, \sigma'_{v(i,k)}\right) \quad (2.52)$$

where $\sigma'_{cv(i,k)}$ = preconsolidation pressure estimation used for the present time increment corresponding to the strain rate $\dot{\varepsilon}_{(i,k-1)}$

$\sigma'_{v(i,k)}$ = effective stress at depth *i* after time *k*

Under conditions with large stress increments, usually close to the drainage boundaries, equation (2.52) can

reduce the calculated preconsolidation pressure below the in situ effective stress. In the next time increment this calculated preconsolidation value will be checked and the preconsolidation pressure is restricted to be equal to or greater than the vertical in situ effective stress, $\sigma'_{v0(i)}$. The procedure will be repeated until the defined total time, t, is reached.

2.3.8 Plaxis – Soft-Soil-Creep model, version 8.0

Plaxis is a finite element code and the computer program covers most areas of geotechnical engineering. The development of the program began in 1987 at the Technical University of Delft. The program has been continuously developed. In Sweden it is used more frequently, but so far mainly in the design of sheet pile walls for deep excavations. The now available version of the program includes both the one- and the three-dimensional model including creep (Brinkgreve and Vermeer, 2002).

In the Soft-Soil-Creep model it is assumed that all inelastic strains are considered to be creep. In the one-dimensional model the total strain is given by equation (2.53) (Emdal, 2000) and the parameters are illustrated in Figure 2.19 and Figure 2.20.

$$\varepsilon = \varepsilon_c^e + \varepsilon_c^{cr} + \varepsilon_{ac}^{cr} = -A \cdot \ln\left(\frac{\sigma'}{\sigma'_0}\right) - B \cdot \ln\left(\frac{\sigma'_{pc}}{\sigma'_{p0}}\right) - C \cdot \ln\left(\frac{\tau_c + t'}{\tau_c}\right) \qquad (2.53)$$

where ε_c^e = elastic strain during primary consolidation

ε_c^{cr} = creep strain during primary consolidation

ε_{ac}^{cr} = creep strain after primary consolidation

τ_c = the intercept with the time axis of the straight creep line, see Figure 2.20

t' = effective creep time, see Figure 2.20

and $$\varepsilon_c^e = A = \frac{C_r}{(1+e_0)\cdot \ln 10} = \frac{\kappa}{V} \quad (2.54)$$

$$\varepsilon_c^{cr} = B = \frac{(C_c - C_r)}{(1+e_0)\cdot \ln 10} = \frac{\lambda - \kappa}{V} \quad (2.55)$$

$$\varepsilon_{ac}^{cr} = C = \frac{C_\alpha}{(1+e_0)\cdot \ln 10} = \frac{1}{r_s} \quad (2.56)$$

where C_r = recompression index

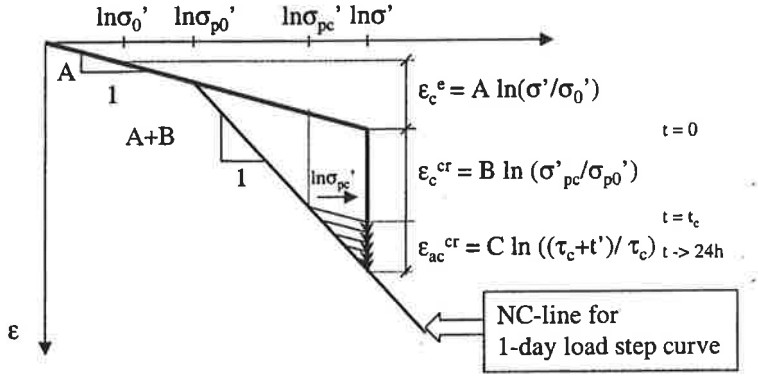

Figure 2.19 Idealised stress-strain curve with the strain increment divided into an elastic and a creep component. (Emdal, 2000)

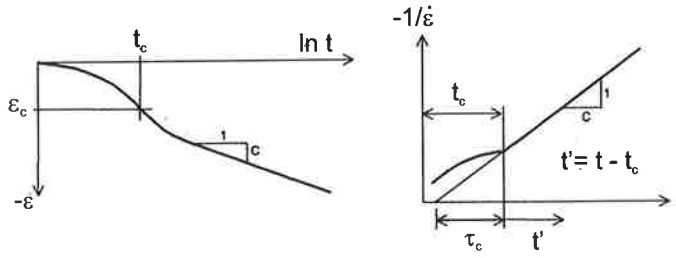

Figure 2.20 Definition of C and the relevant time parameters. t_c is defined as the time to EOP (Brinkgreve and Vermeer, 2002).

The differential equation can than be derived as:

$$\dot{\varepsilon} = \dot{\varepsilon}^{e} + \dot{\varepsilon}^{cr} = -A\frac{\dot{\sigma}'}{\sigma'} - \frac{C}{\tau_c + t'} \tag{2.57}$$

The Soft-Soil-Creep model in Plaxis is recommended to be used for calculations in the normally consolidated range for clays, clayey silts and peat. Thus when calculating settlements for lightly overconsolidated, soft clay the model may not describe the natural behaviour with sufficient accuracy, especially for loads that implies a final effective stress around the preconsolidation pressure. The creep parameter C is given as a constant. However, the consequence of using a constant creep parameter is of minor importance for the result if calculations are conducted as recommended, in the normally consolidated region.

2.3.9 Illicon (1989, 1995)

Mesri et al. (1989, 1995) developed the *Illicon* computer program, which is a finite difference model for one-dimensional settlement analysis with or without vertical drains.

The major features of the model are:

- the consolidation process is divided into the primary and the secondary stages. The model includes time-compressibility during both primary followed by secondary consolidation.
- for any clay, a unique relationship is assumed to exist for the void ratio – effective stress curve until the end of primary consolidation (EOP) (Mesri and Choi, 1985).
- *Time-compressibility and secondary* compression: the model includes time-compressibility during primary consolidation followed by secondary consolidation. To define this, C_α/C_c is required as an input parameter. However, the computer program does not consider creep effects (C_α/C_c = 0) during the primary consolidation stage.

The theory of consolidation is based on Terzaghi's classical equation for one-dimensional consolidation.

The resulting hydrodynamic equation, excluding the terms related to vertical drains, is:

$$\frac{\partial e}{\partial t} = \frac{(1+e_0)^2}{e+1}\frac{1}{\gamma_w}\cdot\left[\frac{\partial k_v}{\partial z}\frac{\partial u'}{\partial z} + k_v\cdot\left(\frac{\partial^2 u'}{\partial z^2} - \frac{1}{e+1}\frac{\partial u'}{\partial z}\frac{\partial e}{\partial z}\right)\right] \quad (2.58)$$

where e = void ratio

e_0 = in situ void ratio

k_v = vertical permeability [m/s]

u' = excess pore pressure [kPa]

z = height [m]

The general constitutive equation for one-dimensional compression is:

$$\frac{\partial e}{\partial t} = \left(\frac{\partial e}{\partial \sigma'_v}\right)_t \cdot \frac{d\sigma'_v}{dt} + \left(\frac{\partial e}{\partial t}\right)_{\sigma'_v} \quad (2.59)$$

where $\left[\frac{\partial e}{\partial \sigma'_v}\right]_t \cdot \frac{d\sigma'_v}{dt}$ = the decrease in void ratio over time associated with an increase in effective stress

$\left[\frac{\partial e}{\partial t}\right]_{\sigma'_v}$ = the decrease in void ratio over time following a structural disruption caused by effective stress

The equation (2.59) can be integrated over time to obtain the total change in the void ratio:

$$\Delta e = \int_{t_0}^{t}\frac{\partial e}{\partial t}\,dt = \int_{t_0}^{t_p}\left[\left(\frac{\partial e}{\partial \sigma'_v}\right)_t \cdot \frac{d\sigma'_v}{dt} + \left(\frac{\partial e}{\partial t}\right)_{\sigma'_v}\right]dt + \int_{t_p}^{t}\left(\frac{\partial e}{\partial t}\right)_{\sigma'_v} dt \quad (2.60)$$

where t_p is the duration of the primary consolidation stage and the two terms on the right hand side of equation (2.60), from time t_0 to t_p and from t_p to t, are primary and secondary consolidation respectively.

A special feature that should be noted is that all layers in the given soil profile have to complete primary consolidation before any layer goes into the secondary compression stage, i.e. creep strain is separated from the primary consolidation.

3. HYPOTHESIS CONCERNING COMPRESSION PARAMETERS INCLUDING CREEP

Settlement calculations are strongly dependent not only on the calculation model as such, but also on the interpreted parameters and how well they describe the natural behaviour.The most common computer program in Sweden for clay settlement calculations is Embankco (Larsson et al. 1994) The program employs a model for describing the compression modulus according to Figure 3.1a. The modulus changes from M_0 to M_L at an effective stress equal to the preconsolidation pressure. The concept is classical and similar approaches of describing compression behaviour are very common, such as the κ and λ parameters in the Modified Cam Clay model, see Figure 3.1b, or alternatively by the compression index C_r and C_c.

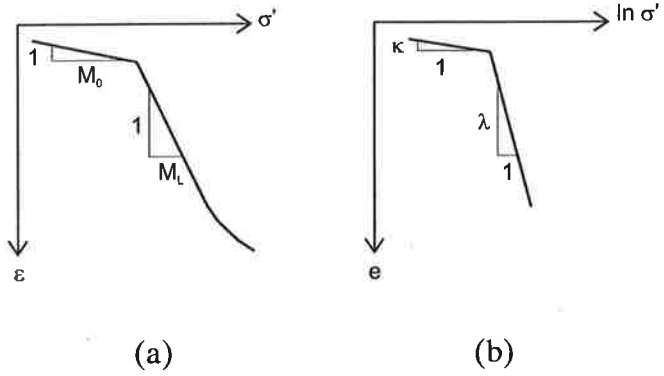

Figure 3.1 *Illustrations of the compression parameters as a function of the effective stress according to (a) Swedish standard practice and (b) the MCC model.*

However, the described modulus model leads to a drastic change in the modulus when the effective stress passes the preconsolidation pressure. It can thus, under conditions when the final effective stress is close to the preconsolidation pressure, imply that a minor change in

the effective stress results in larger variations in calculated settlements than expected.

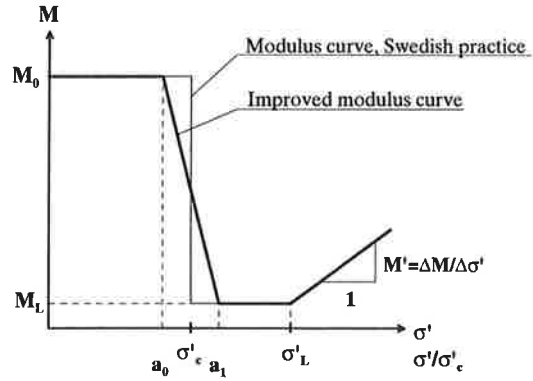

Figure 3.2 *An illustration of the variation in the compression modulus according to Swedish standard practice and with the suggested modification.*

A part of this work was to identify a suitable. It also involved improvement of the description of compression behaviour with emphasis on the models for compression modulus and the creep parameter.

By modelling laboratory tests under different conditions a better understanding of the compression behaviour is obtained, which is necessary in order to improve the parameter models. This gives a possibility to develop a model for full-scale analysis, which will be able to accurately predict settlements.

Among the creep parameters, the coefficient of secondary compression, α_s, is the most commonly used creep parameter today in Sweden. This is related to the secondary compression index, C_α, as described in Chapter 2. Figure 3.3 shows the model for α_s recommended by Larsson (1986), where the α_s is given as a function of strain.

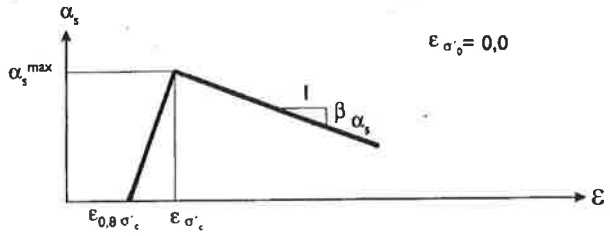

Figure 3.3 *The model of the coefficient of secondary compression, α_s, according to Swedish standard practice (Bengtsson and Larsson 1994).*

Another often used creep parameter is the time resistance number, r_s. Because r_s is inversely proportional to α_s, a search of linear functions with the effective stress for α_s and r_s respectively will give somewhat different results, as illustrated in Figure 3.4

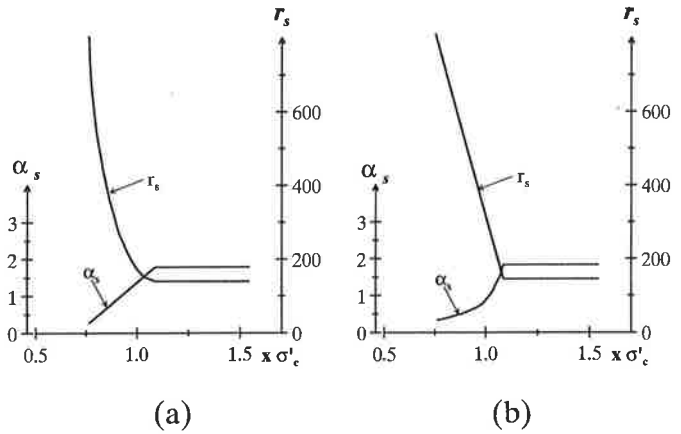

Figure 3.4 *(a) r_s as a function of stress when α_s is assumed to vary linearly with stress.*

(b) α_s as a function of stress when r_s is assumed to vary linearly with stress.

It was most important to thoroughly study and increase the understanding and determining the properties that govern the stress-strain behaviour for laboratory tests carried out under different conditions. It was also

important to study full-scale conditions and find ways to transfer the experience from small-scale laboratory tests to the field conditions.

Predicted and occurred settlements for full-scale behaviour sometimes show quite large variations. It is well known that the properties of natural deposits are complex and difficult to describe in detail. The reason for the discrepancy may thus not lie in the theory, but in the way the soil profile is simplified for the analyses. Hence, it is important to study the effect of a change of parameters on the calculated result.

4. LABORATORY TESTS

4.1 Introduction

In this chapter the test equipment used in the laboratory and the test procedures are described. The relationship between effective stress – strain – strain rate is studied in Chapter 6. Finally, the magnitude of the coefficient of secondary consolidation and the variation with the effective stress is analysed and presented in Chapter 6.

One important objective of this research project was to extend the empirical base concerning the creep behaviour of natural lightly overconsolidated, soft clays and to further investigate the creep parameter describing the creep behaviour. To achieve the above mentioned objectives, a broad experimental base was necessary and for that reason a great number of tests were carried out under different conditions.

All the tests were carried out in climate-controlled rooms with a temperature of +8°C.

4.2 CRS tests

In order to determine the preconsolidation pressure, compression modulus and the coefficient of permeability CRS tests were conducted according to Swedish standard (SIS SS 02 71 26, 1991).

Sällfors (1975) developed the CRS test and for the last 20 years this test has been extensively used in Sweden for determining the preconsolidation pressure and the corresponding compression properties.

For the CRS tests the clay specimen was ϕ50 mm and 20 mm of height and placed into a confining ring made of teflon. The very smooth ring was lubricated with silicon grease to obtain a minimum of friction between the

sample and the confining ring. The teflon ring was then mounted and fixed in an outer ring made of stainless steel. The strain rate used in most of the tests was the standard rate, i.e. 0.0024 mm/min (0.72 %/h).

The monitored strain was plotted in a diagram with effective stress on the horizontal axis and strain on the vertical axis, both in linear scales. The technique for interpreting the preconsolidation pressure takes account of strain rate effects (Sällfors, 1975), so the determined value of the preconsolidation pressure has been found to be an appropriate value when compared to the clay behaviour at full-scale loadings in the field.

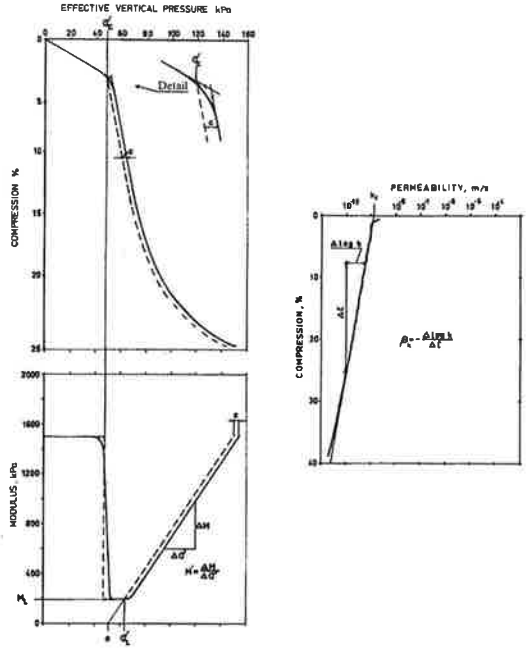

Figure 4.1 Plotted results from CRS test and evaluated compression parameters (Larsson, 1981).

The standard Swedish practice of evaluating the effective stress – strain behaviour is given in Figure 4.1. The parameters thus obtained are the preconsolidation pressure σ'_c, the effective stress, σ'_L, where the

compression modulus starts increase again, the compression modulus M_0 and M_L and the modulus number M'. The permeability is also obtained, with the parameters k and β_k.

As pointed out in Chapter 2, the preconsolidation pressure evaluated as described in Figure 4.1 is to a certain extent a function of the strain rate. This will be analysed in the Chapter 6.

The test procedure and the technique for interpreting the preconsolidation pressure have mainly been tested for clays down to depths of about 20-25 m. For clay samples from greater depths, the determination of the preconsolidation pressures may require special attention. However, within this work CRS tests, according to Swedish standard, were conducted on clay specimens to depths of 55 m and with a modified strain rate, the half standard rate; 0.0012 mm/min, for specimens from 60-70 m depths. The results appeared to be very good and in concordance with corresponding triaxial tests.

4.3 CRS tests with different strain rates

For the purpose of studying the effective stress–strain–strain rate behaviour and also to identify and develop a method for evaluating a creep parameter, CRS tests with different strain rates were conducted. Länsivaara (1999) proposed a model for evaluating the creep parameter from a CRS test with different strain rates. However, this model assumed that the compression modulus increases linearly with stress. For Swedish soft clays it has generally been found that the compression modulus is constant for a stress range between σ_c' and σ_L'.

The laboratory equipment that was used for the tests with different strain rates was the same device as for normal CRS tests, as described in Section 4.2.

For the tests performed within this project, the strain rates varied from 0.03 to 1.44 %/h (0.0001-0.0048 mm/min),

where the lowest rate is 24 times slower than the standard rate for a standard CRS test (0,72 %/h or 0,0024 mm/min). In most of the tests a procedure was adopted in which the strain rate was altered after the effective stress had exceeded the preconsolidation pressure. The duration of each strain rate was adjusted so that the developed strain was about 1%. The intention behind this procedure was to obtain a result where the clay sample had clearly adjusted to the prevailing conditions and the length of the plotted curve was long enough to allow for a reliable evaluation. In Figure 4.2 it can be seen that the stress–strain curve underwent distinct changes when the strain rate was altered and also how consistently the plotted curves follow a certain pattern for the respective strain rates.

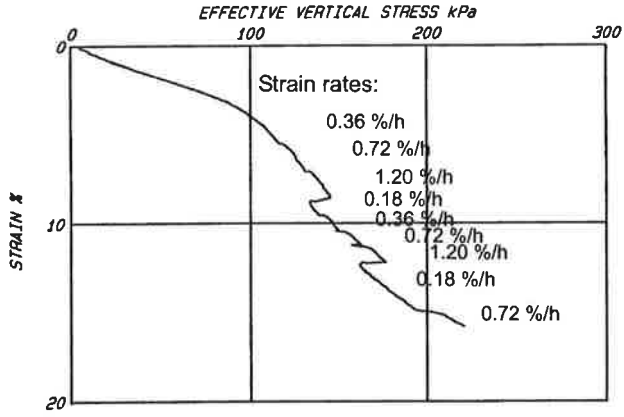

Figure 4.2 *Änggården CTH12-14m. CRS test with different strain rates.*

Further results and analyses from conducted tests are given in Chapter 6.

4.4 Incremental loading (IL) tests

The oedometer test with incremental loading (IL) is used all over the world for determination of compression characteristics including the creep properties. The

procedure involves an incremental loading of the specimen, each increment being equal to the previous consolidation load, i.e. a load increment ratio (LIR) of $\Delta q/q=1.0$. The duration of each load is normally 24 hours.

Within this project the IL test was utilised to determine the creep parameter of the clay. The same type of apparatus as the CRS device was used. In order to improve the test equipment some modifications were made. Figure 4.3 contains a schematic sketch and a photo of the oedometer apparatus.

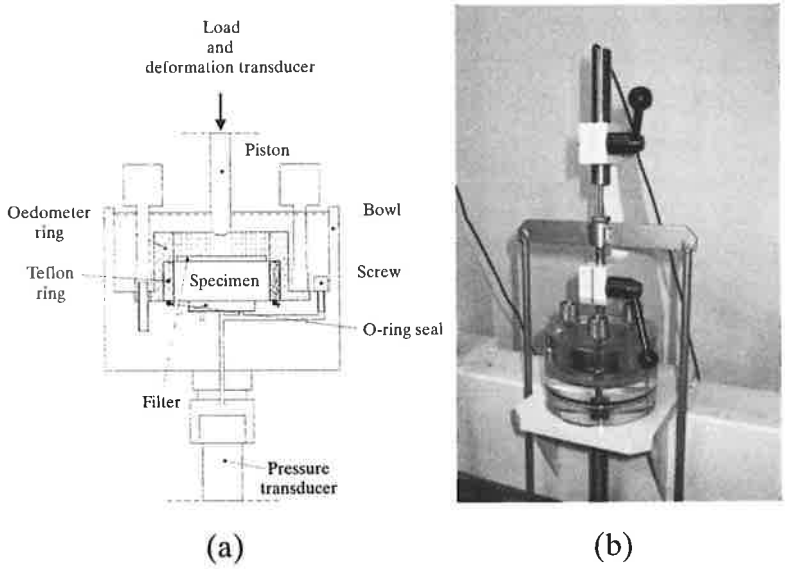

Figure 4.3 *(a) A schematic sketch of the modified oedometer.*

(b) A photo of the oedometer.

A pore pressure transducer was mounted in the bottom plate of the oedometer, which allowed monitoring of the dissipation of excess pore pressure. Hence, a more detailed analysis of the consolidation process was possible to obtain, when the prevailing effective stress at a given point in time was known. The test was thus conducted under one-sided drainage conditions. In Figure 4.4 an example is given where the excess pore pressure was

monitored during a load step. It was, of course, possible to conduct the tests also under two-sided drainage conditions.

The accuracy of the pore pressure transducer and the strain gauge was examined. The maximum error of the pore pressure transducer was determined to ±0.03 kPa at 100 kPa, and the error of the strain gauge was less than ±1.5 μm.

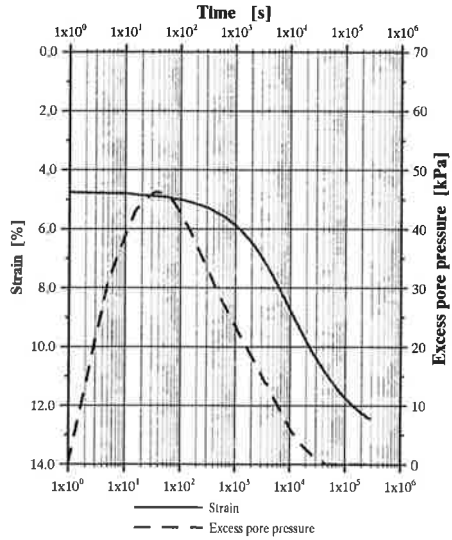

Figure 4.4 *Änggården CTH11-14m, q=120→ 180 kPa and σ'_c= 108 kPa. Semi-logarithmic diagram with time versus strain and time versus excess pore pressure.*

During a test the monitoring interval of the vertical strain and the excess pore pressure was adjusted with respect to the processes during the test, i.e. short intervals between registrations at the beginning of the test, which increased over time.

The normal test procedure involves loading of the specimen in increments, each increment equal to the previous consolidation load, with each load step acting over a 24-hour period. Within this project, tests were

carried out under different boundary conditions, load increment ratios and durations of load steps.

Depending on if the excess pore pressures were to be monitored, the tests were conducted under one-sided or two-sided drainage conditions, as mentioned above. Next, different load increment ratios were applied, generally varying between 0.3 and 1.0. The purpose was to investigate the effect of using load increment ratios below 1.0. By using load increment ratios of 0.3-0.5 the determination of the creep parameter was feasible for more than one load increment during each test within the range of effective stress of 0.8-1.3· σ_c'.

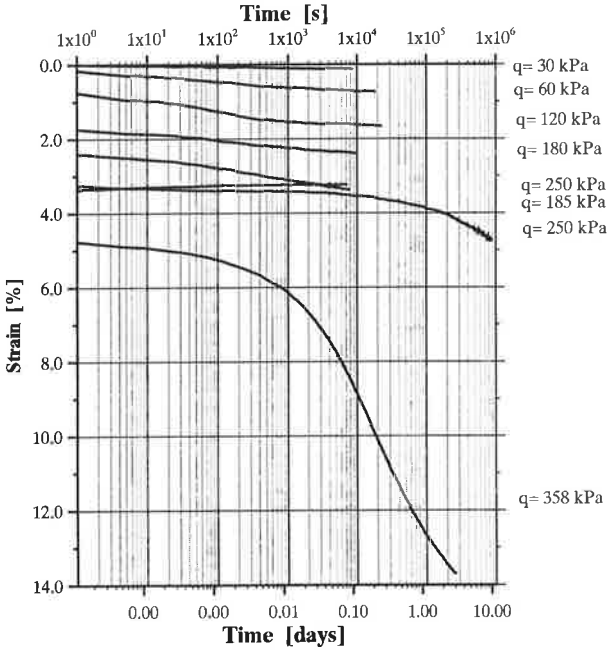

Figure 4.5 *An example of an IL test where the sample was reconsolidated. Clay from the Lundby Strand test site, depth 30m, in-situ stress σ'_0 = 185 kPa and the σ'_c= 260 kPa.*

In order to improve the test procedure and thereby obtain greater similarity between the laboratory tests and in situ conditions, a modified procedure was used. The intention was to reconsolidate the sample to in situ conditions. To

achieve this state the sample was loaded in a step-wise manner up to about $0.95 \cdot \sigma_c'$. The load $0.95 \cdot \sigma_c'$ was applied on the sample just until the excess pore pressure had dissipated. After that the specimen was unloaded to an effective stress, which corresponded to the in-situ conditions. The next load step was applied when the swelling was practically zero. Figure 4.5 shows the result from such a test where the specimen was reconsolidated.

The described test procedure was beneficial in some aspects. First of all, it provided better information about the expected field condition strains for a particular applied load than a standard IL test. Secondly, these tests were of particular interest in terms of the validation of the proposed calculation model, because of their similarity to the in-situ behaviour of clay.

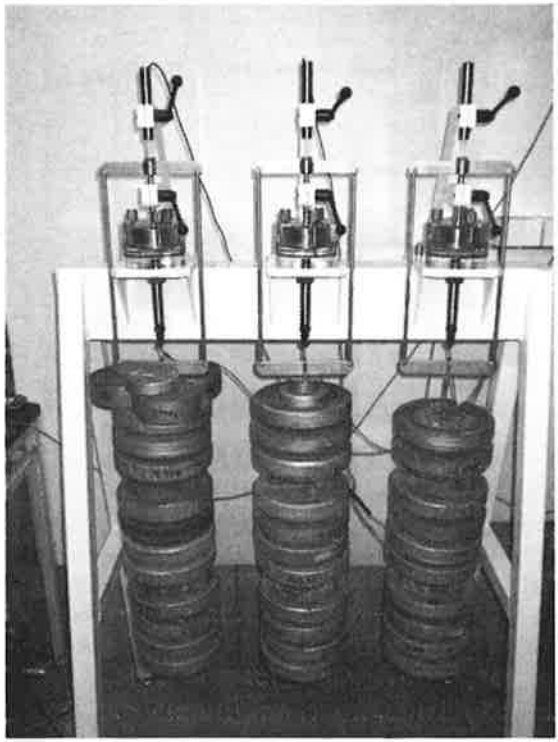

Figure 4.6 *Three IL tests, load step 10 for each test, with q= 720, 690 and 630 kPa respectively. The clay specimen is from 70 m depth, the Lundby Strand test site,.*

Within this project, the maximum applied load corresponded to an effective stress of 720 kPa. This occurred when an IL-test was conducted on clay from a depth of 70 m (the Lundby Strand test site). The evaluated in-situ stress was about 465 kPa. Figure 4.6 shows a photo of the equipment for load step 10 on the specimen from 70 m depth, where q= 720, 690 and 630 kPa respectively.

4.5 Triaxial tests

A number of K_0-consolidated, undrained triaxial-tests were conducted. The purpose of these tests was primarily to determine the preconsolidation pressure and to check the results from the CRS tests. The determination of the preconsolidation pressure for clay specimen from deep layers, i.e. about 25-30 m or deeper, was of particular concern. The height and the diameter of the specimen were 100 mm and 50 mm respectively. The triaxial tests were performed in accordance with Swedish practice. After the specimens had been K_0-consolidated, the tests were performed with a strain rate of 0.60 %/h.

5. TEST SITES

5.1 Introduction

This research project includes field investigations and settlement observations from four test sites in the western part of Sweden and also one test site north of Stockholm. Figure 5.1 shows where the test sites are located. The test sites have been chosen partly because the soil strata consist of deep deposits of soft, lightly overconsolidated clay, which is of particular interest for this work and partly because the settlements have been monitored over periods between 8 and 57 years, with the exception of the Lundby Strand test site, where no measurements have been conducted. The purpose of the Lundby Strand test site was to investigate the creep behaviour of clay from very large depths. The five test sites differ from one another in respect of type of applied load, which is important when it comes to settlements.

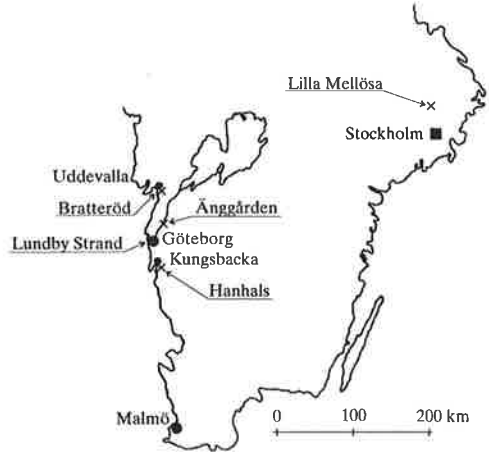

Figure 5.1 Location of test sites within this project.

Furthermore, the extensive investigations were conducted at four test sites in order to determine in situ conditions, pertaining to consolidation and the parameters that govern settlements and their time dependency. The Lilla Mellösa test site has been thoroughly investigated at several occasions by the Swedish Geotechnical Institute (SGI) since the test site was constructed in 1945. The data from the test sites are of great importance and are vital in order to verify the proposed model for settlement calculation.

The first test site is Änggården in Nol, situated in the Göta River valley about 23 km north of Göteborg, see Figure 5.1. The observed structure is the one-storey building on a fill. The building is a day-care centre called Änggårdens Förskola, which can be seen in Figure 5.2. Since the completion of the building, settlements of up to about 0.5 m have occurred beneath the building.

Figure 5.2 *The Änggården day-care centre with the eastern and southern facing.*

Embankments and the behaviour of the soft soil beneath them are another category of problems in terms of settlements. The developed settlements have been measured since the construction of the road embankments at the two test sites with such structure included in this thesis, Bratteröd junction and Hanhals.

The Bratteröd test site is situated adjacent to one of the exit ramps at Bratteröd junction, south of Uddevalla, see Figure 5.1. Until the year 2000 it was a part of Highway

E6. The height of the embankment is up to about 5 m and it is designed with lightweight fill of expanded polystyrene, EPS, in order to reduce settlements along the 60 m section of the ramp in connection with a bridge, see Figure 5.3. Settlements have been measured since 1984 (Åhnberg and Holm, 1988, Andersson and Åhnberg, 1996), when the construction of the junction was completed.

Figure 5.3 The westerly view of the exit ramp at Bratteröd test site.

The third test site is also a road embankment, situated at Hanhals about 4 km south of Kungsbacka. The location of the Hanhals test site is shown in Figure 5.1. The embankments are connected with a bridge at the junction of the new stretch of road 927/928 and the new double track railway line, the so-called Västkustbanan, see Figure 5.4. The junction was constructed in 1994-95. In order to reduce settlements, the embankments were in general designed using lightweight fill of expanded polystyrene, EPS. The maximum height of the embankments is about 5.5 m. In connection with the bridge, lime/cement columns were installed to reduce the differential settlements. The strata of natural soil consist mainly of soft clay to a depth of 9-36 m in the studied sections.

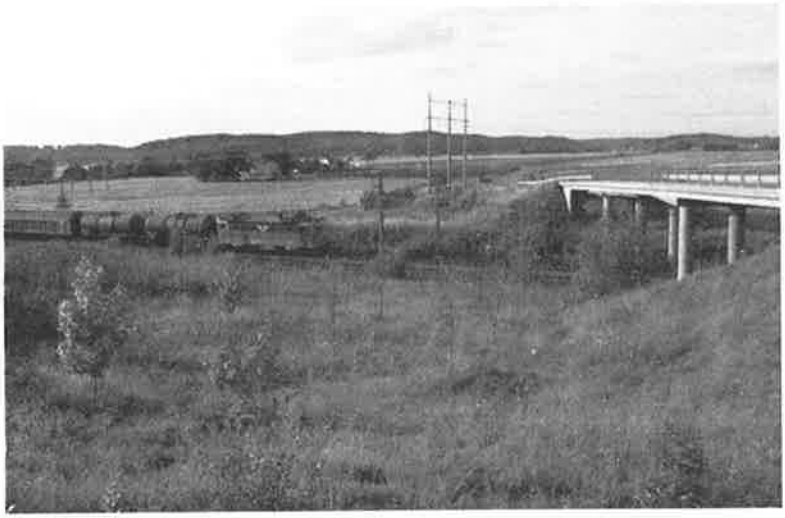

Figure 5.4 *The road embankments and the double track railroad line at the Hanhals test site seen from a southerly perspective.*

However, settlements occurred shortly after the southern embankment was completed at the end of 1994. Therefore levelling measurements of the embankment road surface were started a few months after its completion (Kjessler & Mannerstråle AB, 1999). Monitoring at the road embankment north of the bridge started directly after the construction was completed in June 1995. The monitored settlements up to August 2002 are about 0.5 m and they monitored settlements are compared to calculated settlements in two sections.

A test site with very deep deposits of soft clay was also investigated. This site is located on the island of Hisingen in Göteborg, near the Göta River and it is named Lundby Strand, see Figure 5.5. The deposit, which is about 100 m deep, was investigated to a depth of 70 m. The main purpose was to examine the creep behaviour of soft clay from very deep layers, i.e. 20-70 m below ground surface.

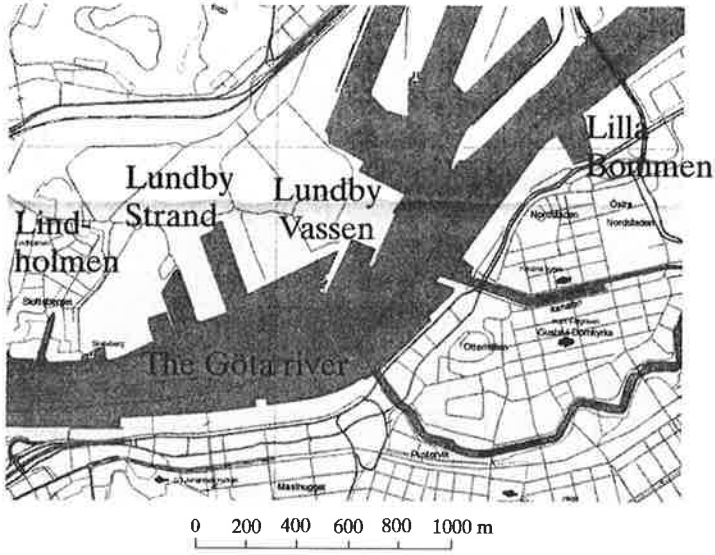

Figure 5.5 An overview of the location of Lundby Strand test site.

Finally, the well-known test site at Lilla Mellösa has been studied. The Lilla Mellösa test site is a full-scale loading test site for consolidation of soft clay over a long period of time constructed by SGI in 1945.

The test site is situated in a flat area at the farm of Lilla Mellösa, near the village Upplands Väsby and about 30 km north of the city of Stockholm, see Figure 5.1. A comprehensive description of the background and history of the test site is given by Chang (1981). The settlement data has at numerous occasions been used in geotechnical literature to verify models for settlement calculations for soft clay.

The deposit of soft clay was not as deep at this site, about 14 m, compared to the other presented test sites. But with consideration of the long term monitoring of settlements and pore pressures, the test site was of great interest.

5.2 Geology

About 20 000 years ago, the Scandinavian Peninsula was covered by a huge ice sheet. When the climate became milder the ice sheet retreated north. This implies that the area around Göteborg was ice free about 13 000 years ago but large areas were situated under the sea level. The region is dominated by a broken terrain in which bare bedrock areas are crossed by deep valleys. During the following period the Baltic Ice Lake was drained off by the north part of the province of Västergötland. The water from the Baltic Ice Lake discharged large quantities of fine-grained sediments in the deep valleys with salt water conditions, when the flow of water decreased near the open ocean and also because of changed conditions (Fridén 1994). A study of the clay due to period of sedimentation and as conditions where then is presented by Bergsten (1989) and Alte et al. (1989).

For this reason the soil profiles mainly consist of sediments of glacial and postglacial marine clay, which is relative homogenous. At the test sites, studied in this thesis, the depth of deposits of soft clay varies between 10 to about 100 m.

5.3 The Änggården test site

The test site at Änggården in Nol is, as mentioned above, situated in the Göta River valley north of Göteborg, see Figure 5.1 and Figure 5.6. The building is located about 500 m east of the Göta River. Before the site was developed, the ground level in the area was about 4-5 m above sea level and the area was used for agricultural purposes.

In order to adjust the foundation level a fill of about 0.1-0.8 m was placed on the site of the proposed building. The foundation of the building consists of an 840 m^2 concrete ground slab. The frame and the facing of the building are made of wood, except for a reinforced concrete shelter at

the centre of the building. To compensate for the extra weight of the concrete shelter, a local EPS (expanded polystyrene) fill was designed with the aim of limiting the increase of effective stress in the underlying deposit of soft clay. The construction of the building was completed in 1992.

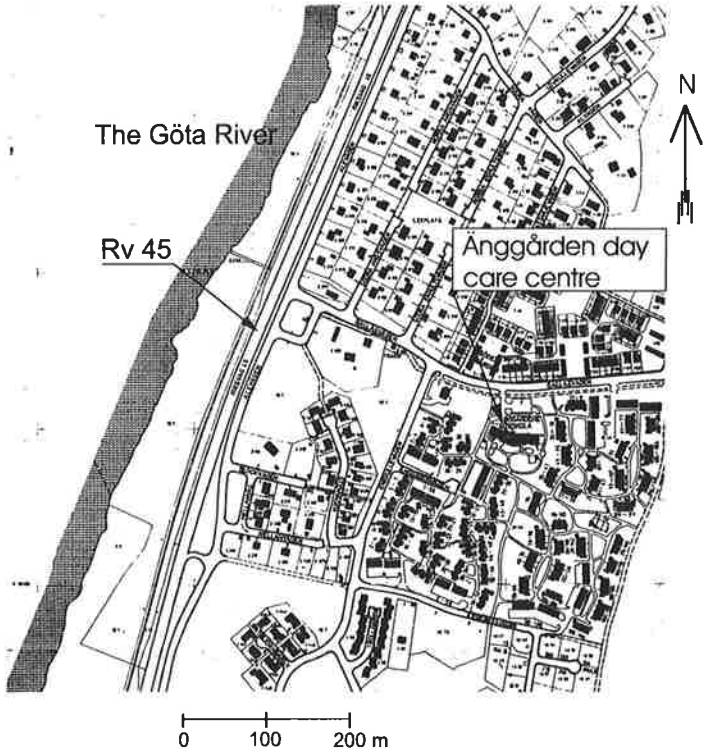

Figure 5.6 Location of the Ånggården test site at Nol.

However, over the years large settlements have occurred. The estimated settlements along the building are up to about 0.5 m. In 1999 the building was lifted, because something had to be done about the damage caused by differential settlements. In some places, excavations were also made close to the building, in order to decrease the effective stresses in the underlying clay strata and thereby

reduce the rate of settlement. The results are presented by Svensson (2000).

5.3.1 Site investigations

No geotechnical investigation was carried out at the Änggården site before the building was constructed. However, in 1997 GF Konsult AB (1997) conducted a geotechnical investigation because of large differential settlements. During 1999 the Department of Geotechnical Engineering at Chalmers conducted additional site investigations. At the test site Cone Penetration Tests (CPT), undisturbed sampling, and field vane tests down to a depth of 24 m were carried out at two different boreholes. The location of the two boreholes can be seen in Figure 5.7. Furthermore, piezometers were installed at both boreholes at different levels below the ground water table to determine the pore pressure profile. Finally, additional levelling measurements were also conducted and these are described in Section 5.3.3.

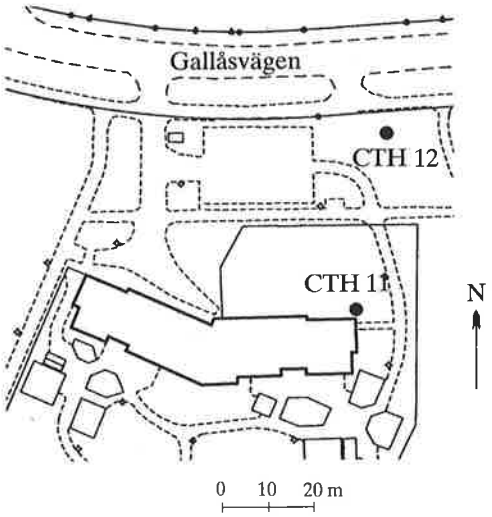

Figure 5.7 *A plan over the test site with the location of the two boreholes, CTH11 and CTH12.*

The soil consists mainly of soft clay to depths of 22-24 m. Under the fill the uppermost 1-2 m of clay consists of dry crust. The Cone Penetration Tests (CPT) indicated that the natural deposit mainly consists of soft, fairly homogeneous, clay. However, at depths of 6-12 m below the ground surface, distinct layers of 0.1-1.0 m of silty sand or shell deposits were found, see Figure 5.8. Beneath the soft clay there is a layer of coarse soil directly on the bedrock.

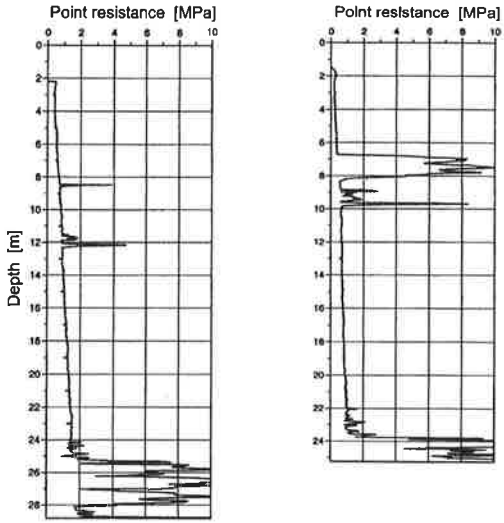

Figure 5.8 *Result of CPT tests, point resistance versus depths, borehole (a) CTH11 and (b) CTH12, at the Änggården test site.*

In order to examine the consolidation for the soil profile with appropriate accuracy, it was necessary to measure the pore pressure at different levels over a period of time in order to determine the pore pressure distribution and fluctuation in the soil profile. For that purpose six piezometers were installed at borehole CTH11 and five piezometers at borehole CTH12. The piezometers were installed at various depths. The results of the measurement are shown in Figure 5.9 and Figure 5.10.

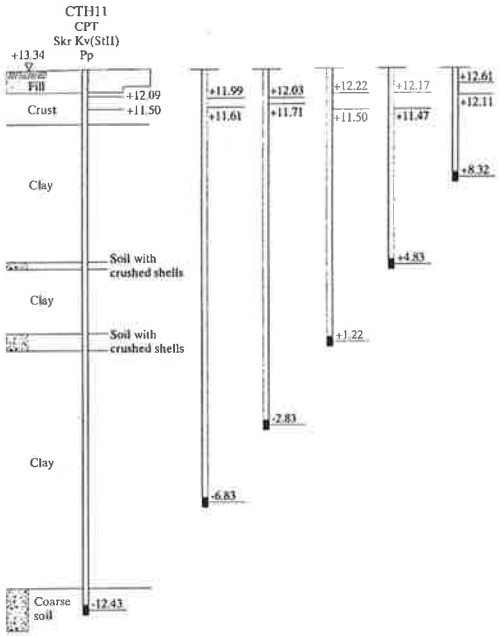

Figure 5.9 *Piezometers installed at borehole CTH11. Level of each piezometer and the corresponding pressure level for measured pore pressure are shown.*

The pore pressures were measured on five separate occasions during the period from January 2000 to April 2002. The monitored pore pressure corresponded to a pressure level at about +11.5 – +12.2, i.e. about 1.1–1.8 m below the ground surface with hydrostatic distribution, with only small variations over time, see Figure 5.9. However, the piezometers on the uppermost aquifer showed a pore pressure level at about+12.1 to +12.6, i.e. 0.7 to 1.2 m below the ground surface.

As can been seen in Figure 5.10, the monitored pore pressures at borehole CTH12 had an almost hydrostatic distribution and corresponded to a groundwater table just below or close to the ground surface, i.e. at a level of +11.5 to +12.1. Hence, the pore pressure profiles are fairly similar for the two boreholes at corresponding levels, except for the piezometers at level +8.32, borehole CTH11.

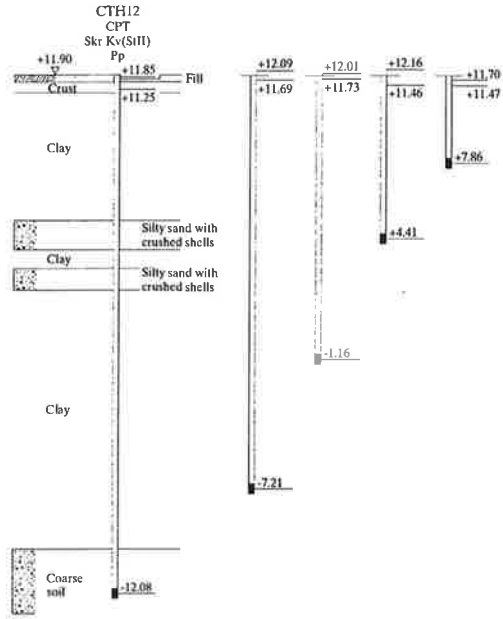

Figure 5.10 Piezometers installed at borehole CTH12. Level of each piezometer and the corresponding pressure level for measured pore pressure are shown.

5.3.2 Geotechnical properties

5.3.2.1 Routine laboratory tests

The geotechnical properties were determined at two boreholes, CTH11 and CTH12. The geotechnical parameters for borehole CTH11 are given in Figure 5.11 and for borehole CTH12 in Appendix A. When comparing the results from the laboratory investigations of borehole CTH12 with those of borehole CTH11, it can be observed that the parameters are fairly similar. However, the extent of thin layers of silt and sand or shell deposits differed. At CTH11, only two thin layers were detected, compared with CTH12, where a larger part of

the soil between the depths of 7 and 10 m consists of coarser-grained soil, see Figure 5.8.

In general, the bulk density of the soft clay is about 1.55-1.65 t/m^3 in the upper 10 m, increasing with depth to about 1.8 t/m^3 at a depth of 20 m below the ground surface. Both the natural water content, w_N, and the liquid limit, w_L, of the clay, beneath the dry crust were about 80% and decreased with depth to about 50% at a depth of 20 m below the ground surface. The determined parameters for borehole CTH12 is presented in Appendix A.

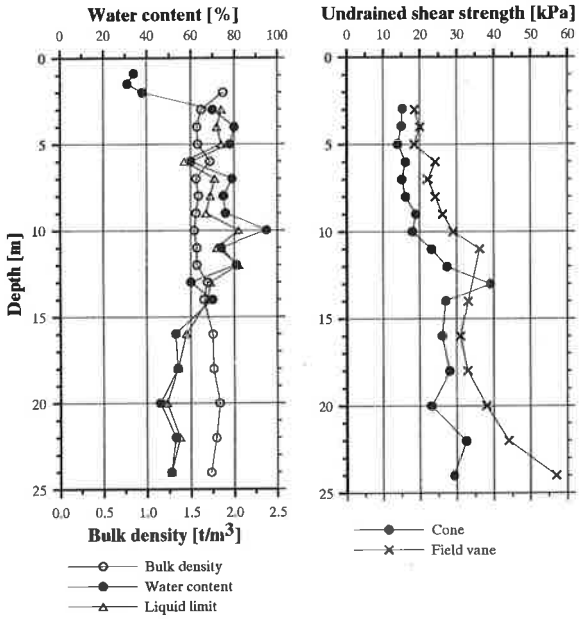

Figure 5.11 Soil parameters for borehole CTH11.

5.3.2.2 CRS and triaxial tests

The compression properties were determined by CRS tests, and also in one case by a triaxial test (borehole CTH12). When considering the present conditions with

the applied load the evaluated OCR is approximately 1.0 and somewhat higher in the deeper layers of clay.

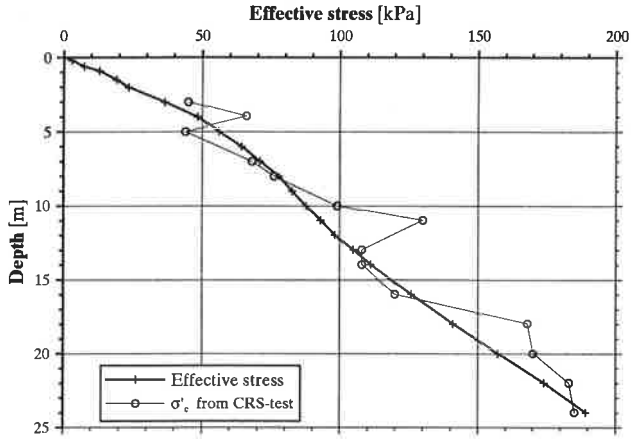

Figure 5.12 Evaluated in-situ effective stress, including fill and building, and preconsolidation pressures for borehole CTH11.

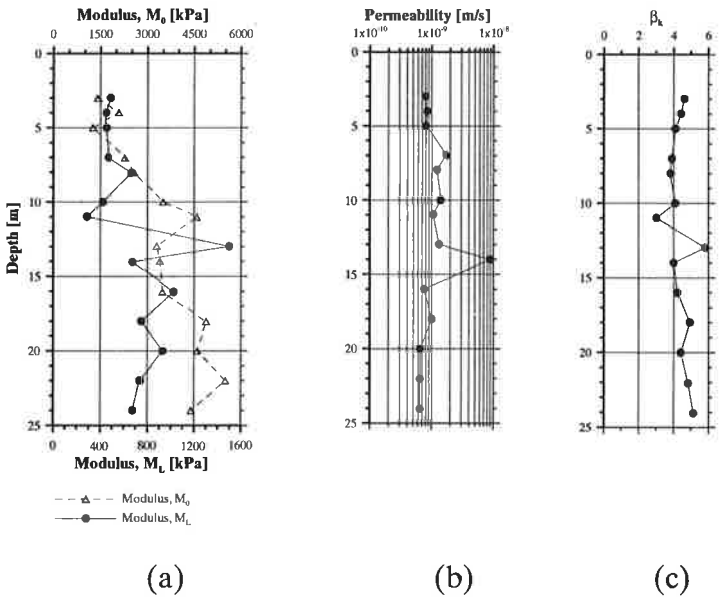

Figure 5.13 Änggården borehole CTH11, values of compression moduli, permeability and the coefficient of permeability change.

The preconsolidation pressure and in-situ stresses are shown in Figure 5.12. It should be noted that since the construction of the building, the properties of the clay strata at borehole CTH11 have changed somewhat over time due to the settlements.

The interpreted properties for borehole CTH11, as compression modulus and permeability are presented in Figure 5.13.

The compression behaviour properties for borehole CTH12 are presented in Appendix A.

5.3.2.3 Results from incremental loading tests

In order to examine the creep behaviour of the clay, incremental loading tests were carried out. The purpose of these tests was to obtain site specific data and to extend the empirical base regarding creep properties.

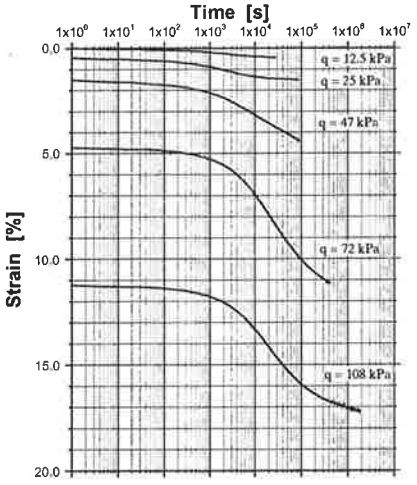

Figure 5.14 An incremental loading test for a sample from borehole CTH12, depth 5.0 m, with σ'_c of about 37 kPa.

Moreover, different conditions were studied, such as drainage conditions, ratio of load increment and/or duration, in order to ascertain whether or not they

affected the magnitude of the creep parameter. An example from an incremental loading test is provided in Figure 5.14.

The coefficient of secondary compression, $\alpha_s=\Delta\varepsilon/\Delta\log t$, could be evaluated from the conducted tests. For a strain less than 2-3%, the coefficient of secondary compression was about 0.1-0.3 %, which, from a practical point of view, is negligible in most cases. It is also exaggerated since no reconsolidation to in-situ conditions had been made. Thereafter, the value of the coefficient of secondary compression gradually increased up to a maximum value of about 1.2-1.7 %, at a strain of about 4-8 %, which corresponded to an effective stress of about $1.0\text{-}1.3\cdot\sigma_c'$. For larger strains, α_s appears to be almost constant or slightly decreasing with increasing strain. However, at very large strains, i.e. 10-15% or more, α_s decreased significantly. The variation of α_s with the magnitude of strain for this clay is shown in Figure 5.15.

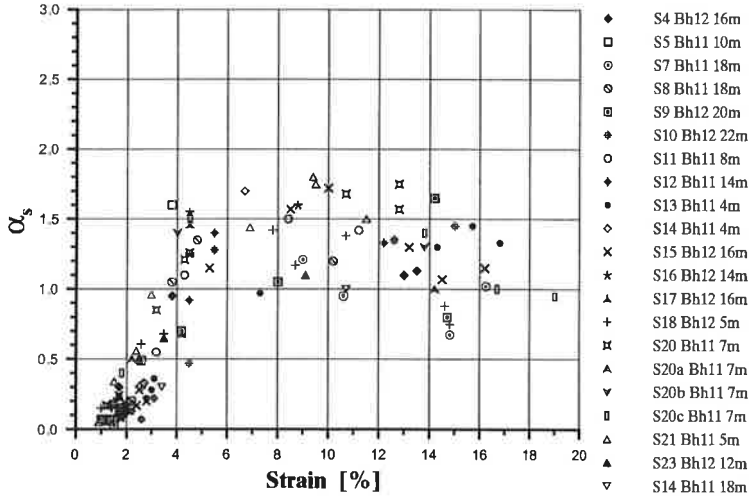

Figure 5.15 *Coefficient of secondary compression versus strain for conducted incremental loading tests for the Änggården test site.*

Another way of describing the creep behaviour is to define α_s as a function of effective stress normalised in

respect of preconsolidation pressure. The reason for this is that the laboratory specimens have a different stress situation compared to in-situ conditions. The results in Figure 5.16 are taken from the same tests as shown in Figure 5.15, but are instead plotted with the normalised effective stress on the x-axis. In this way, a somewhat more uniform pattern, of how α_s varies with normalised effective stress, is obtained.

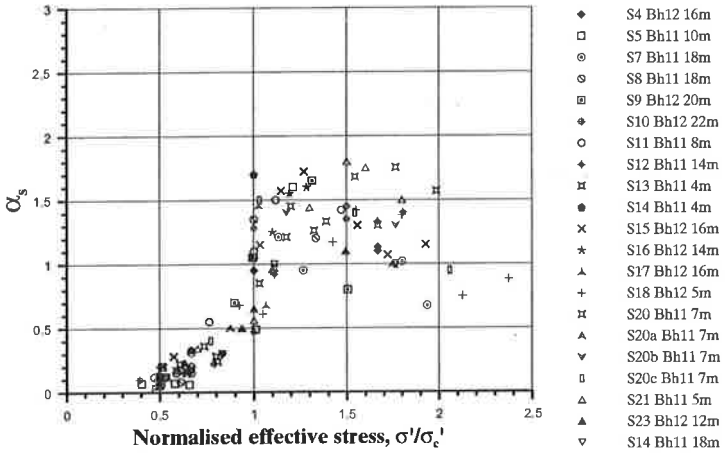

Figure 5.16 *Presentation of the coefficient of secondary consolidation versus normalised effective stress for conducted incremental loading tests for the Änggården test site.*

The creep behaviour can also be given in terms of time resistance number, r_s (Janbu 1969), described in Chapter 2. The results from the same incremental loading tests as shown in Figure 5.16 is given by the time resistance number parameter in Figure 5.17.

The incremental loading tests were conducted under different conditions, as described in Section 4.2 in order to determine whether or not different conditions have any effects on the creep behaviour and hence the determination of the creep parameter. A comprehensive presentation of the results is given by Claesson (2003) and an analyse of the tests are given in Chapter 6.

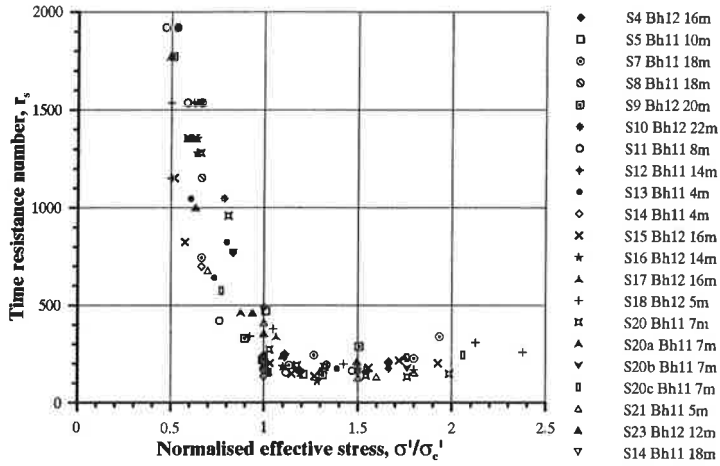

Figure 5.17 *The time resistance number, r_s, versus normalised effective stress for incremental loading tests for the Änggården test site.*

5.3.2.4 Results of CRS tests with different strain rates

A modified CRS test procedure has been used, as described in chapter 4. By changing the strain rate at appropriate points in time during the test, the effective stress – strain curve will obtain a certain position in the stress–strain plot. The strain rate affects the curve and thereby also the interpreted preconsolidation pressure. The strain rate for the tests varied within a range of 0.03-1.44 %/h (0.0001-0.0048 mm/min), which is both below and above the Swedish standard rate for a CRS test (0.72 %/h or 0.0024 mm/min). As can be seen in Figure 5.18, the effective stress – strain curve shows distinct changes when the strain rate was altered. A higher strain rate leads to a higher effective stress at corresponding strain compared to a lower strain rate.

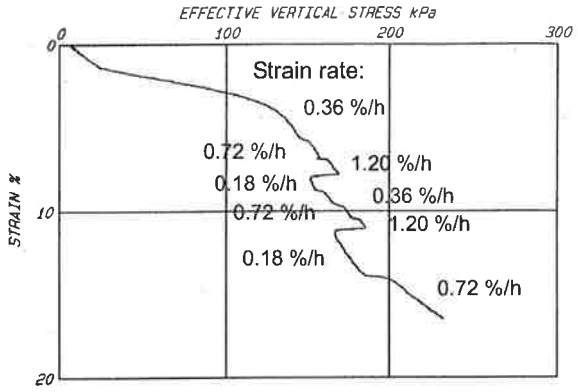

Figure 5.18 Änggården CTH12-16m. A plot of effective stress versus strain in linear scales.

This behaviour showed that, for each strain rate, the effective stress-strain curve has a particular shape or, perhaps a more adequate description would be "position" in the diagram. In addition, when the strain rate was changed during the test, the effective stress in the specimen was almost instantly adjusted to become in line with the unique curve for that particular strain rate. These results confirmed the theory proposed by Leroueil et al (1985), that the behaviour is controlled by a unique relationship between strains, effective stress and strain rate.

5.3.3 Evaluated and measured settlements

The settlements, which occurred in the soil strata beneath the building between 1992-97, were estimated by comparing a levelling in 1997 with contour maps, construction and relation drawings (GF Konsult AB, 1997). Additional levelling was carried out on three occasions after the building was lifted and excavations were made in the immediate area, in the summer of 1999.

During the period from 1992, when the building was completed, to 1997 the thus estimated amount of

settlement was about 0.05 m at the west corner of the building, increasing along the building to about 0.50 m at the east corner. This means that the maximum mean value of the rate of settlement was about 0.10 m/year that five-year period.

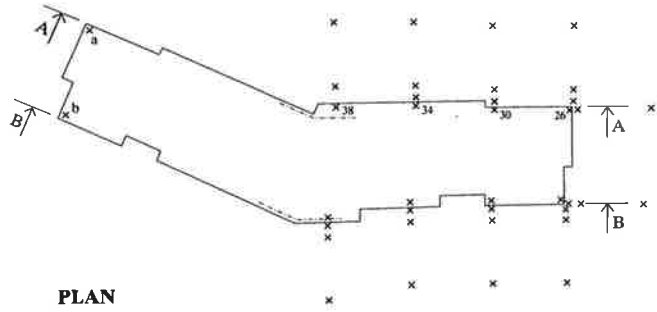

(a)

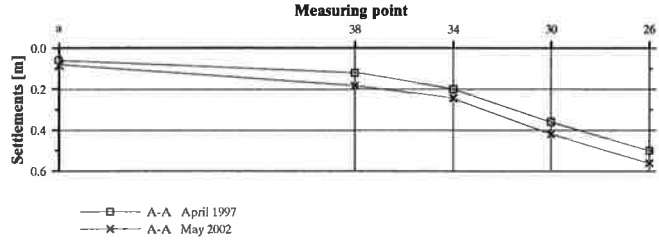

(b)

Figure 5.19 *(a) Plan with building and levelling points. (b) Section A-A with estimated/ measured settlements in the year of 1997 and 2002. Note that the building was lifted and in some places soil was excavated close to the building in 1999.*

Further levelling of the building indicated that, in general, the rate of settlement decreased over time. At the east corner the rate of settlement decreased from about 0.10 m/year (1992-1997) to about 0.012 m/year from April 2001 to May 2002.

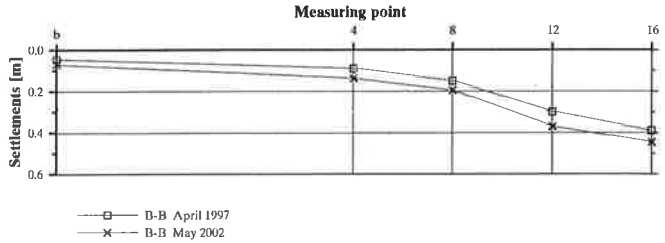

Figure 5.20 *Section B-B (Figure 5.19a), along the southern facing with estimated/ measured settlements in the year of 1997 and 2002*

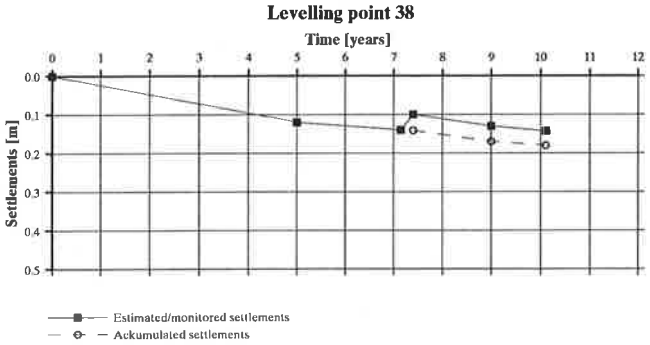

(a)

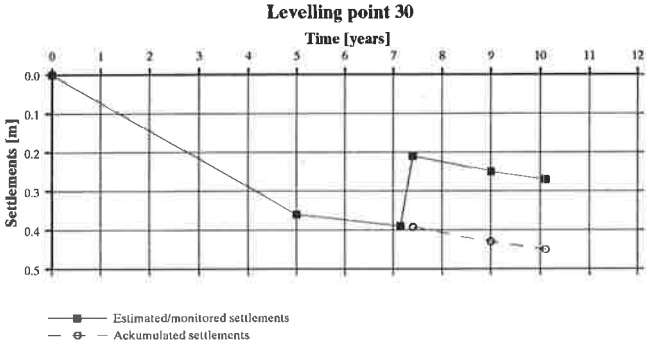

(b)

Figure 5.21 *Results from levelling of points (a) no 38 and (b) no 30. The location of the levelling points can be seen in Figure 5.19.*

When the building was lifted, the space between the ground slab and the ground surface was filled with foam. The rate of settlement increased at this time at most of the levelling points, compared to the period just before the building was adjusted. This was probably partly due to deformations in the foam. The results of conducted levelling at point nos. 30 and 38 are given in Figure 5.21. The outcome of the measurements indicates that the rate of settlement decreases over time.

5.4 The Bratteröd test site

The Bratteröd test site is a junction situated about 60 km north of Göteborg and to the south of Uddevalla, see Figure 5.1. Until the year 2000, this junction was a part of the stretch of Highway E6, constructed in 1983/84.

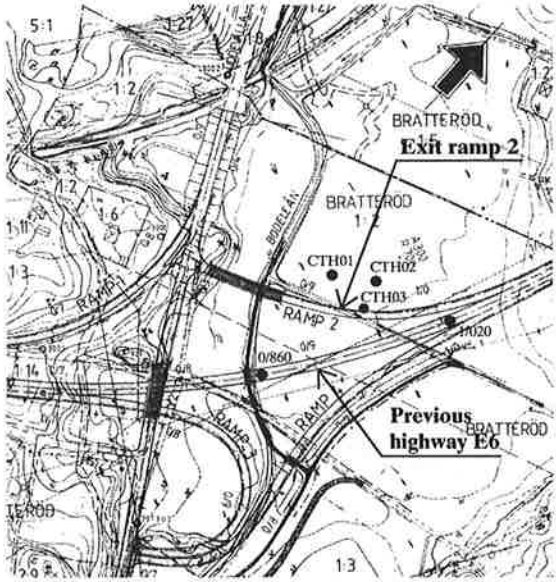

Figure 5.22 Exit ramp 2 at the Bratteröd test site.

Bratteröd is a clay filled valley surrounded by high areas with bare rock. The depth of the clay deposits varies

across the valley and is about 35 m at the investigated boreholes, see Figure 5.22 and Figure 5.23.

A 60 m long section of Exit Ramp 2 is a road embankment designed using EPS (expanded polystyrene) to ensure stability against failure and to reduce settlements beneath the ramp. The height of the studied section of the embankment is between 2.7 and 5.7 m and the thickness of the EPS is between 0,2 and 4,2 m, see Figure 5.23. In line with normal Swedish practice for road embankment design in the early 1980s, the predicted settlements did not take creep effects into consideration. Horizontal settlement hoses were placed below the exit ramp along the embankment as well as across the embankment

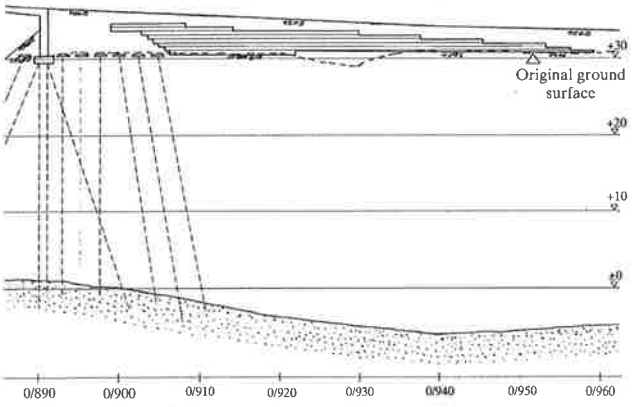

Figure 5.23 Principal cross-section of embankment with EPS-fill and the deposits of soft clay for the exit ramp 2.

Settlements were measured between 1984-88 and the results were analysed by the Swedish Geotechnical Institute (SGI). The results were presented in a report in 1988 (Åhnberg and Holm, 1988). Additional monitoring was carried out in 1995 (Andersson and Åhnberg, 1996) and also within this research project in 1998 and finally in 2002.

Although the predicted total settlement was calculated to about 0.1-0.2 m, the actual total settlement up to May 2002 was up to 0.8 m.

However, within this research project there were no incremental loading tests or CRS tests with different strain rates performed on clay from this test site. The reason was that the deposit of clay was not sufficiently homogenous to provide an appropriate foundation for the study of creep effects and stress-strain behaviour in this research project. Nevertheless, the test site is interesting in view of the levelling measurements conducted over a period of almost 20 years. Despite the lack of homogenous soil deposits, the test site is a useful complement to the other test sites in verifying the settlement calculation program.

5.4.1 Site investigations

For the design of the embankment geotechnical investigations were conducted by SGI, at the proposed location of the Bratteröd junction. The results of the investigations and the design of the Exit Ramp 2 embankment were reported by SGI (1981).

In order to carefully determine the soil properties, further geotechnical investigations were carried out during 1998-99 as a part of this research project. The soil deposit at three boreholes, CTH01-CTH03, were investigated, see Figure 5.22. At each borehole a Cone Penetration Test (CPT), undisturbed sampling and field vane tests were carried out down to a depth of 25-35 m. In addition, five piezometers were installed in borehole CTH1. Further measurements were also conducted to determine occurred settlements, and these are presented in Section 5.4.3.

The CPT-tests indicated that the natural deposit of soft soil has a thickness of about 25-35 m. Below the layers of soft soil, which consists mainly of clay, there is a layer of coarser soil. At a depth of between 6 and 12 m, and also at about 16-17 m, thin layers of soil with larger grain sizes than clay were detected. In Figure 5.24 the results from the CPT-test carried out at borehole CTH01 are shown. The other CPT tests are presented in Appendix B.

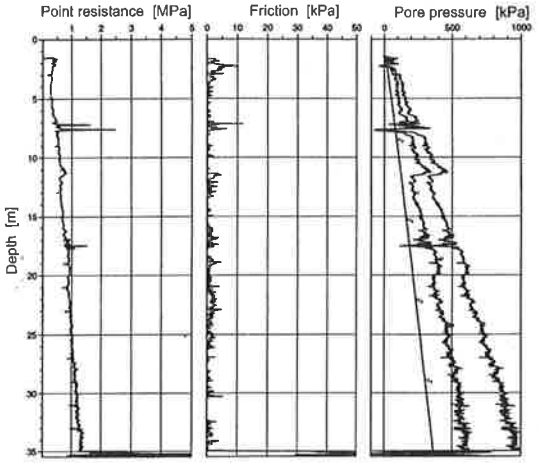

Figure 5.24 *Results of the CPT-test at borehole CTH01, Bratteröd test site.*

The pore pressure distribution in the soil profile was investigated in borehole CTH1 by measurements at 5 different depths between 8 and 35 m.

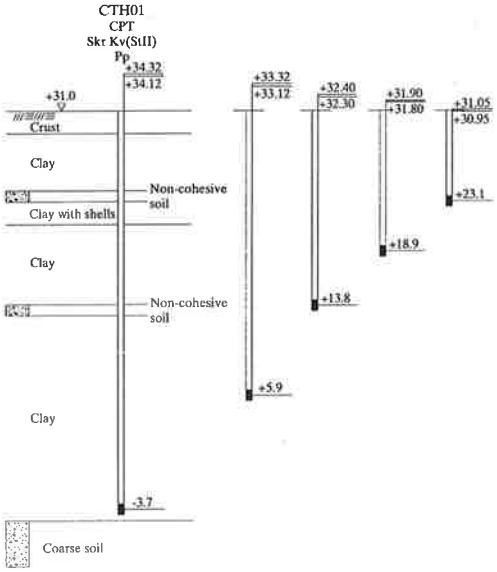

Figure 5.25 *Soil profile and measured pore pressures for the five installed piezometers at borehole CTH01.*

The measured pore pressures showed an artesian pore pressure increasing with depth, corresponding to a pressure level about 3.1 m above the ground surface at a depth of 35 m. The measured pore pressures were in agreement with results of previous investigations conducted by SGI (1981).

5.4.2 Geotechnical properties

5.4.2.1 Routine laboratory tests

As mentioned above the geotechnical properties were determined for the soil profile at three boreholes, denoted CTH1, CTH02 and CTH3. Figure 5.22 shows a map of the test site including the location of the boreholes. The results were compared with the results obtained from the investigation carried out by SGI.

For borehole CTH01, the soil profile consists mainly of sediments of clay to a depth of about 35 m below the ground surface. The uppermost 1.5-2.0 m consists of a dry crust of silt or silty clay. At depths from about 6 to 12 m below the ground surface, there are thin layers of sandy silt and/or shells deposits in the clay. The clay also contains silt and shell. At a depth of about 16-17 m below the ground surface there is another distinct layer of coarser-grained soil, which was also detected by means of CPT-tests, see Figure 5.24. The investigated clay has a bulk density of about 1.6-1.8 t/m^3 and a water content that varies between approximately 40 and 80 %. Figure 5.26 shows the determined properties of the clay. Beneath the clay there is a layer of coarser soil resting on the bedrock. The thickness of the coarser bottom soil layer was not determined.

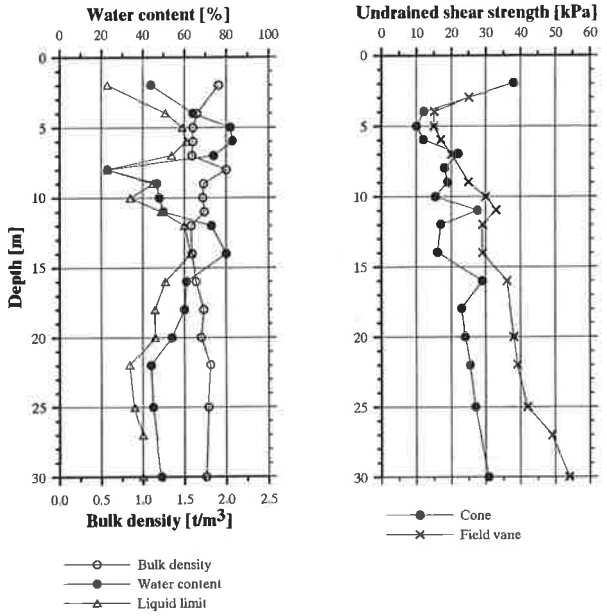

Figure 5.26 Soil properties of borehole CTH01.

At the eastern part of the test site, where boreholes CTH02 and CTH03 were located, the clay generally contained more silt and shell compared to the other part of the test site. Larger bulk density, modulus and overconsolidation ratio were also determined for the clay. In this area, the water content was lower, about 45-55 %. The determined properties are presented in Appendix B.

5.4.2.2 CRS tests

CRS tests were carried out in order to determine the preconsolidation pressure, compression modulus and permeability. The results show that the evaluated OCR for the clay layers was mostly between 1.2-1.5 at borehole CTH01, about 2.0-2.5 at borehole CTH02 and finally at borehole CTH03, the OCR was evaluated at approximately 1.5-2.0. The evaluated condition,

pertaining to the in situ effective stresses and preconsolidation pressures from borehole CTH01 and also borehole 0/860 and 1/020 (SGI, 1981) is given in Figure 5.27. The location of boreholes 0/860 and 1/020 is shown in Figure 5.22. The compression characteristics, the compression modulus and permeability are presented in Figure 5.28. A presentation of the soil conditions for boreholes CTH02 and CTH03 are given in Appendix B.

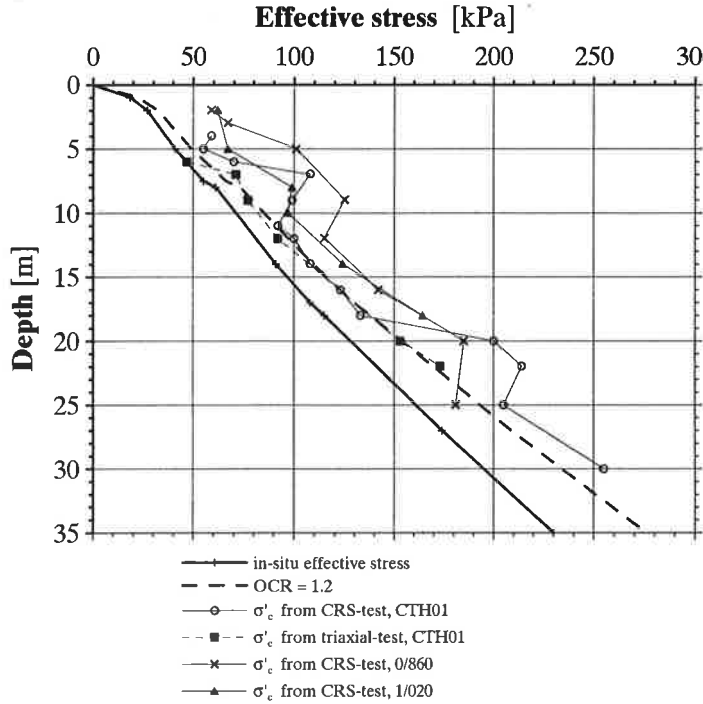

Figure 5.27 Evaluated in situ effective stress and preconsolidation pressure for borehole CTH01, 0/860 and 1/020.

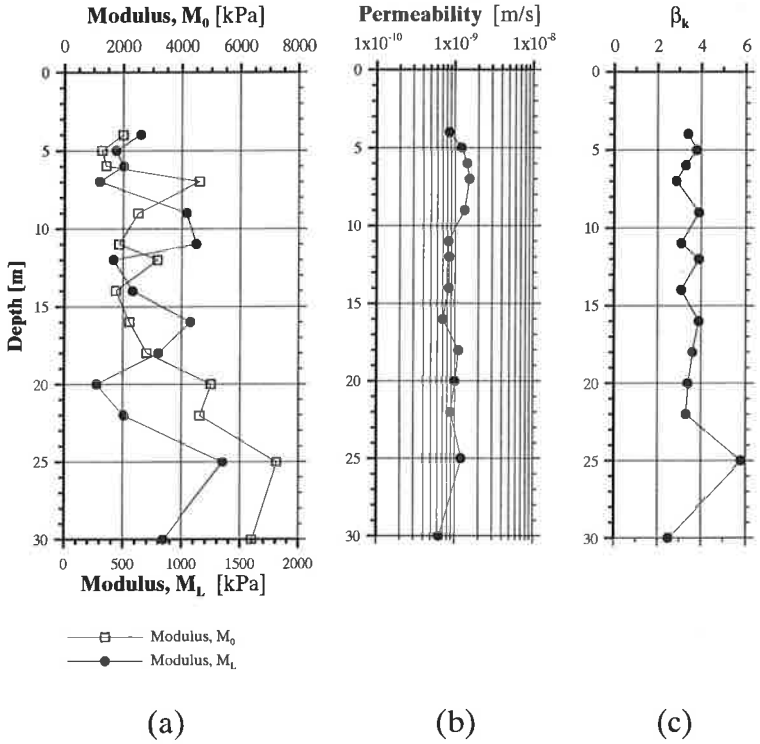

Figure 5.28 Determined values of compression moduli, permeability and the coefficient of permeability change for borehole CTH01 at the Bratteröd test site.

5.4.3 Measured settlements

Four different settlement hoses were laid out at the test site before the construction of the embankment started. The settlement hoses were located under the part of the embankment with lightweight fill, between section 0/906 and 0/960.

The developed settlements were measured from 1984 to 1988, and again in 1995 by SGI. Further monitoring was carried out within this research project in 1998 and 2002.

The magnitude of the measured settlements increased along the stretch, from about 0.05-0.10 m in section 0/906,

close to the bridge abutment, to about 0.7 m in section 0/960, at the end of the EPS fill.

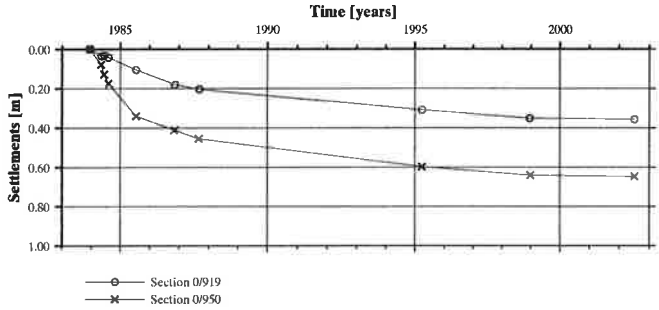

Figure 5.29 Measured settlements in sections 0/919 and 0/950 during the period December 1983 to June 2002.

The rate of settlement is also of great interest. In section 0/950 the rate of settlement has decreased from an average of about 0.3 m/year in the first year, 1984, to about 0.01 cm/year between 1998 and 2002.

5.5 The Hanhals test site

The Hanhals test site is a junction constructed in 1994-95, due to the upgrading of the rail raod to a double track railway line. A new stretch of road, designated 927/928, was designed in connections with the upgrading of the railway. The junction, which is situated about 4 km south of Kungsbacka, see Figure 5.1 and Figure 5.30, consists of a 50 m long bridge, denoted N804, spanning the Västkustbanan double track railway line and connecting the embankment on both sides of the bridge, see Figure 5.31. At the studied stretch of road, the height of the embankment is about 4.0-5.5 m.

The area around the junction is used for agricultural purposes. The ground surface is generally fairly flat, with an inclination of approximately 1:50, and lies about 5-7 m above sea level. However, from section 0/290, it rises by

1:7 in a southerly direction, and in section 0/250 there are outcrops of bare bedrock.

In view of the ground conditions, which consist of deep deposits of soft clay, it was of great concern to design the embankments in such way as to prevent large settlements and to obtain a sufficiently high level of stability to ensure safety (Kjessler & Mannerstråle AB, 1993). For this reasons the embankments were designed with a lightweight fill material of expanded polystyrene, EPS. In addition, lime/ cement columns and fill material of expanded clay were used for soil improvement in some sections, see Figure 5.31.

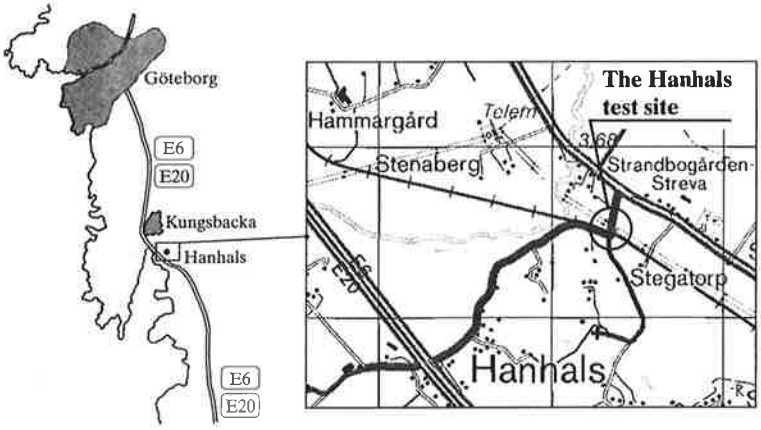

Figure 5.30 An overview and a plan over the Hanhals test site.

The N804 road bridge is founded on point bearing piles. At the southern side of the bridge, between section 0/320 and 0/371, the embankment was designed using EPS fill to a height of 4.0 to 6.0 m, with the greatest height close to the abutment. The height of the EPS fill close to the northern side of the bridge at section 0/423 is 5.0 m. The height of the EPS fill decreases in a stepwise manner further north along the studied stretch. From section 0/495 the EPS fill changes to expanded clay stabilized by cement. In Figure 5.31 the design of the embankments is illustrated.

effective stress in the clay. The location of borehole CTHA1 is given in Figure 5.32. The investigation included a Cone Penetration Test (CPT) to a depth of 35.5 m, undisturbed sampling from 12 levels to a depth of 20 m, and measuring of pore pressure using the piezometers installed by Kjessler & Mannerstråle AB in 1998.

The CPT-test at borehole CTHA1 showed a natural deposit of soft and fairly homogeneous clay to a depth of about 35 m below the ground surface, see Figure 5.33. The depth of soil profile along the studied stretch varied from about 8 m in section 0/320 to around 40 m in section 0/500, see Figure 5.31. Under a thin layer of topsoil there is a layer of about 1.0 m of dry crust. Beneath the clay there is a layer of coarse-grained soil resting on the bedrock.

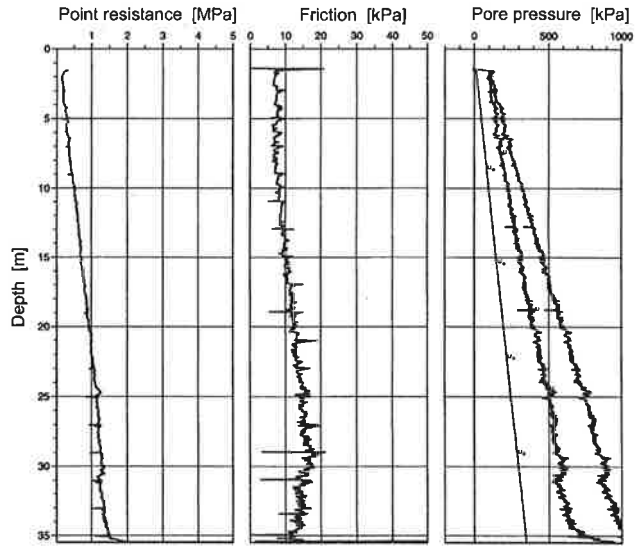

Figure 5.33 Results from CPT-test at borehole CTHA1, the Hanhals test site.

Kjessler & Mannerstråle AB measured the pore pressure at 4 and 10 m depths at borehole F1 (Kjessler & Mannerstråle AB, 1999). The pore pressure level was measured about 0.9 m below the ground surface.

5.5.2 Geotechnical properties

5.5.2.1 Routine laboratory tests

The geotechnical properties have been determined for the soil profile at 12 different levels to a depth of 20 m below the ground surface at borehole CTHA1 (Jansson, 2001). The results have been compared to corresponding results from the investigations carried out by Kjessler & Mannerstråle AB in 1993 and 1999 and the results were in fairly good agreement.

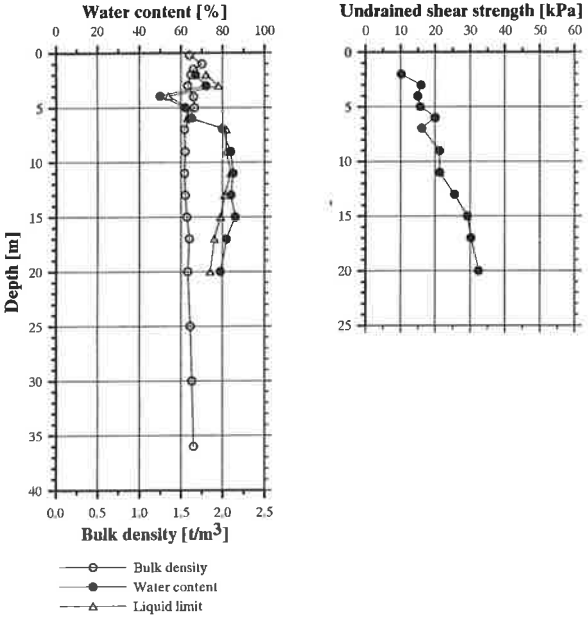

Figure 5.34 Soil properties of borehole CTHA1.

The bulk density of the soft clay varies between 1.55 and 1.70 t/m^3. A summary of the determined soil properties is presented in Figure 5.34. The water content is generally in the region of 70-85 %, with some divergence at a depth of about 4.0-6.0 m where the water content is lower, about 50-65 %, which coincides with the higher bulk density.

The liquid limit has about the same value as the water content at corresponding depth.

5.5.2.2 CRS tests

The compression characteristics were determined by CRS tests. According to the determined preconsolidation pressures, the OCR is generally about 1.3-1.4 for the soil profile. Figure 5.35 shows the evaluated in situ effective stresses and preconsolidation pressures. In the sample from the depth of 6.0 m shells were found and that explains probably the low value of σ'_c. Furthermore, the compression moduli and permeability are shown in Figure 5.36.

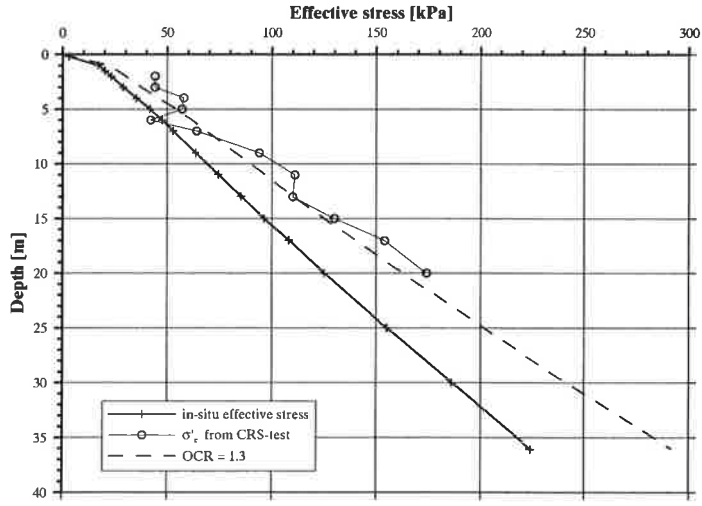

Figure 5.35 Evaluated in-situ effective stress with depth and preconsolidation pressures of borehole CTHA1, at the Hanhals test site. Assumed pore pressures corresponding to a ground water table 1.0 m below the ground surface.

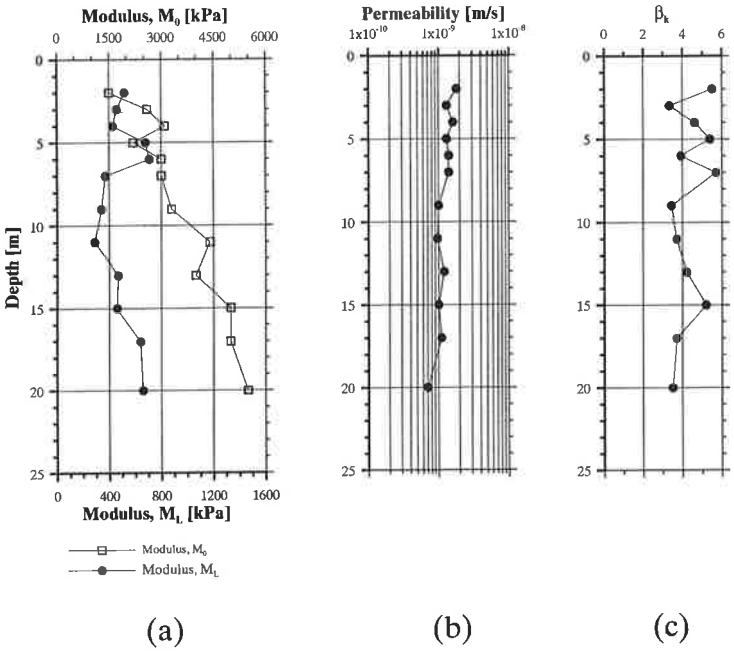

Figure 5.36 Compression characteristics of borehole CTHA1 at the Hanhals test site.

5.5.2.3 Results from incremental loading tests

In order to examine the creep behaviour of the clay at the Hanhals test site, a number of incremental loading (IL) tests were conducted. The test method was generally to reconsolidate the sample for a vertical effective stress of about $0.95 \cdot \sigma_c'$, before the sample was unloaded to a stress of about the in-situ stress and then loaded again. In Figure 5.37 the results are shown from determination of the creep parameter α_s versus normalised effective stress.

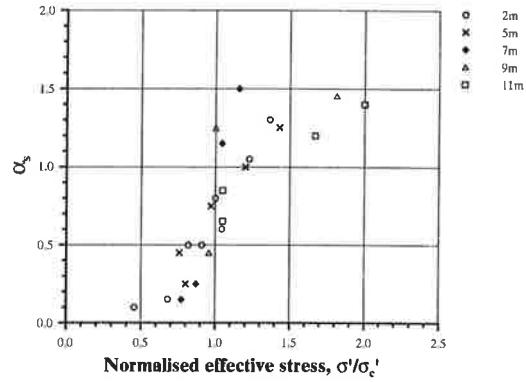

Figure 5.37 *Results of determination of α_s from IL-tests at the Hanhals test site, borehole CTHA1.*

Corresponding values of the creep parameter but in terms of time resistance number are presented in Figure 5.38.

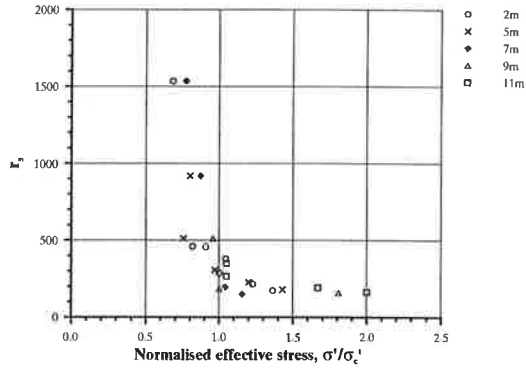

Figure 5.38 *Results of determination of the creep parameter in terms of time resistance number, r_s, at the Hanhals test site, borehole CTHA1.*

5.5.3 Measured settlements

The levelling of the embankment surface started in November 1994. Thus the monitored settlements also include compressions that have occurred in the embankment, which should be considered. The compression of the EPS fill can be estimated to about 1%

of its height, i.e. about 0.03 to 0.05 m. At the north side of the bridge, levelling of the embankment surface started directly after completion in June 1995.

The measured settlements, up to August 2002, are about 0.25 m at section 0/345 and about 0.50 m at section 0/453 (Ekström, 2002). The location of each section is illustrated in Figure 5.31 and the change in measured settlements over time for the studied stretch of the road is given in Figure 5.39

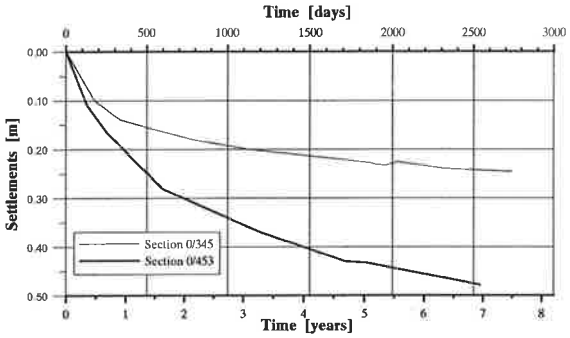

Figure 5.39 *Measured settlements in section 0/345 and 0/453 at the Hanhals test site.*

5.6 The Lundby Strand test site

For the future exploitation of Lundby Strand and also other areas in central Göteborg it is of great interest to investigate the deep deposits of soft clay in the area with respect to their geotechnical properties and with emphasis on the deformation behaviour. The test site was part of a larger area for geotechnical investigation. The investigation formed the base for the design of foundations for future buildings in the area.

The Lundby Strand test site is situated in the southern part of the island of Hisingen, near the Göta River, not far from the central part of Göteborg, see Figure 5.40.

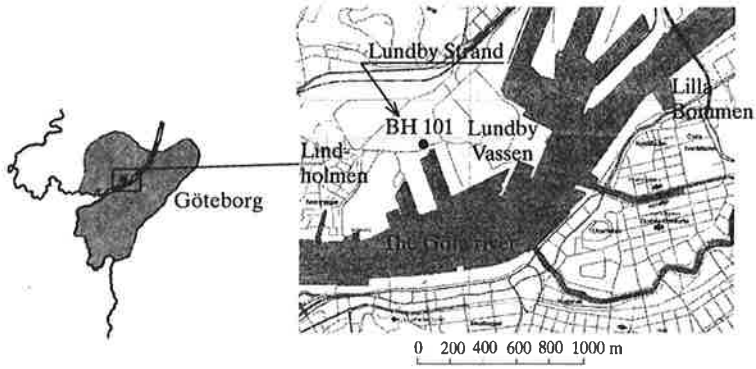

Figure 5.40 The location of the Lundby Strand test site on the island of Hisingen, Göteborg.

Before 1855, the Lundby Strand area was a part of the Göta River called Lundby Vassen. At that time the average water depth was estimated to 0.5-1.0 m. At the end of the 1850s and during the 1860s, the area was filled up with dredged materials from the bottom of the Göta River. Later, layers of crushed rock were placed in the area and covered with a fill of soft, fine-grained soil up to a level corresponding to more or less the ground level of today.

In 1865 a new quay was constructed, with almost the same outline as today, and with a level at about +12.0. Figure 5.41 shows the area and the outline of the quay in the year 1865. From 1865 up to 1940, trade increased rapidly and the harbour at Lindholmen was enlarged on several occasions, and new harbour basins were constructed. Figure 5.40 shows the Lindholmen harbour today and the location of borehole 101 is also shown.

The purpose of the investigation was to evaluate and describe the compression behaviour, with special emphasis on the creep effects of the clay at great depths, i.e. a depth of 20 m or more. The clay samples were taken from borehole 101 at every 5 m, to a depth of 70 m.

Figure 5.41 *A map of Lindholmen and Lundby Vassen from the year 1855. The 1865 quay-line is also shown (map from Kungliga General Lantmäteri Kontoret, 1855).*

The results from the above investigation have also been compared with the results from an investigation carried out at Lilla Bommen (Alte et al., 1989), where the consolidation conditions were evaluated to a depth of about 70 m below the ground surface. Lilla Bommen is situated about 1.7 km east of Lundby Strand on the south side of the Göta River, see Figure 5.40.

5.6.1 Site investigation

This investigation included one borehole, designated 101 (Jacobsson & Widmark AB el al., 2001). Borehole 101 is located about 70 m northwest of the inner part of the harbour basin, see Figure 5.40

The natural deposit at the test site consists of approximately 100 m of soft clay. The clay deposit is covered by fill material, mainly crushed rock and coarse

soil and sediments obtained from dredging work on the Göta River.

A cone penetration test (CPT) to a depth of 50 m was also conducted. The low point resistance and the logged pore pressure indicated very homogeneous clay, see Figure 5.42.

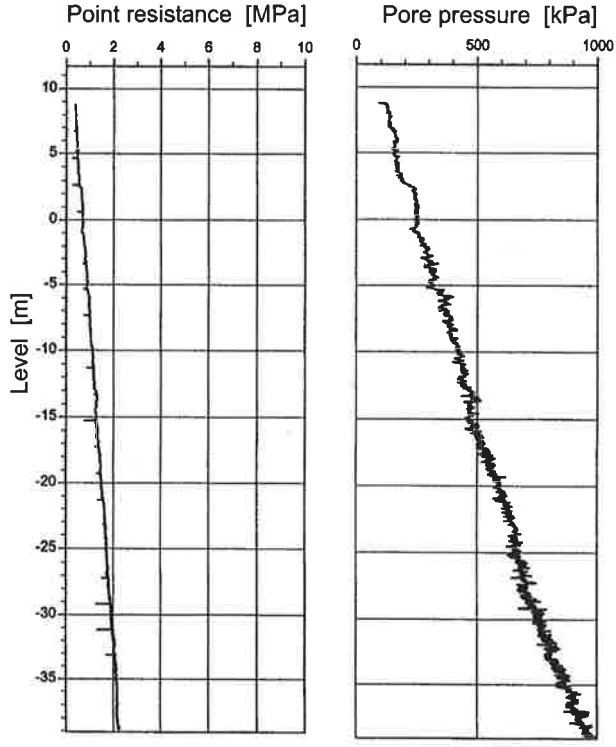

Figure 5.42 Results from the CPT-test borehole 101, point resistance and pore pressure respectively versus level.

Moreover, field vane tests were carried out to a depth of 70 m below the ground level. The results are presented in Figure 5.44 together with the result from the fall-cone test.

In order to determine the pore pressure distribution through the clay profile, five piezometers were installed, about every 10 m to a depth of 60 m below the ground surface, see Figure 5.43. The pore pressures were measured at two occasions, in June and December 2000.

Since the area is close to the Göta River, the sea level is expected to affect the ground water level in the upper aquifer. Therefore the groundwater table was assumed to be close to the mean sea level, i.e. +10.1.

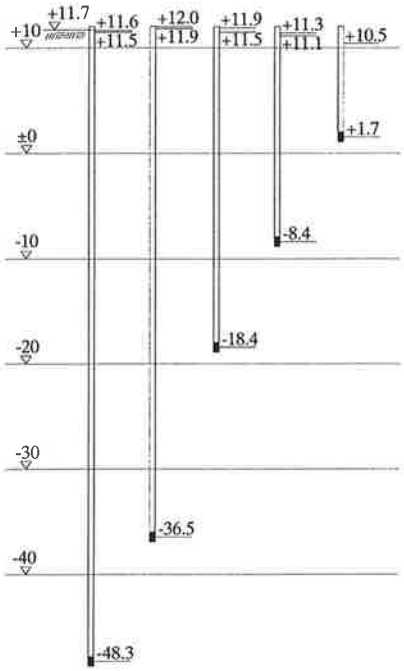

Figure 5.43 Installed piezometers and monitored pore pressure levels.

As can be seen in Figure 5.43, the measured pore pressure levels increase with depth down to level –36.5, i.e. at a depth of 48.2 m. But further 12 m below, at level –48.3, the pore pressure level decreased somewhat.

5.6.2 Geotechnical properties

5.6.2.1 Routine laboratory tests

The geotechnical properties were determined by standard routine tests, CRS tests, incremental loading tests and K_0-

consolidated undrained triaxial tests. The test results reveal that the deposit was remarkably homogeneous and that the clay properties were typical of the so-called Göteborg-clay and very similar to the Lilla Bommen clay (Alte et al., 1989).

The bulk density of the clay varied from about 1.6 t/m^3, near the top of the natural deposit, to about 1.75 t/m^3 at a depth of 70 m below the ground surface. The water content was about 80 % in the top stratum of the soft clay and decreased with depth to about 50%. The parameters are given in Figure 5.44.

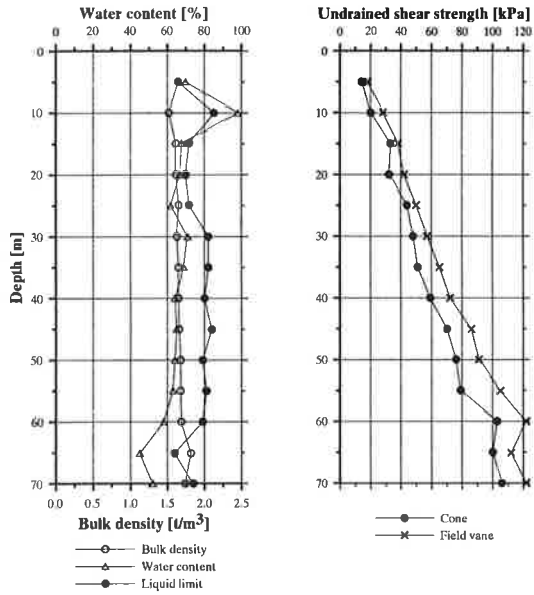

Figure 5.44 Soil characteristics of borehole 101.

5.6.2.2 CRS and triaxial tests

The evaluated results from the conducted CRS tests and triaxial tests reveal that the overconsolidation ratio, OCR, was remarkably constant in the entire clay deposit. The agreement between the evaluated magnitude of the

preconsolidation pressure from CRS tests and the triaxial tests was noticeably consistent. The magnitude of the overconsolidation was about 30-35 % higher than the in-situ effective stress, i.e. an overconsolidation ratio, OCR, of about 1.30-1.35, see Figure 5.45. The procedure of the CRS test has mainly been tested for clays down to depths of about 20-25 m, which should be considered when the test results are evaluated. However, the results appeared to be very in very good agreement with conducted triaxial tests and what might be expected concerning OCR. A note is that the specimens from 60-70 m depths were conducted with a reduced strain rate, 0.0012 mm/min (0.36 %/h), i.e. the half standard strain rate.

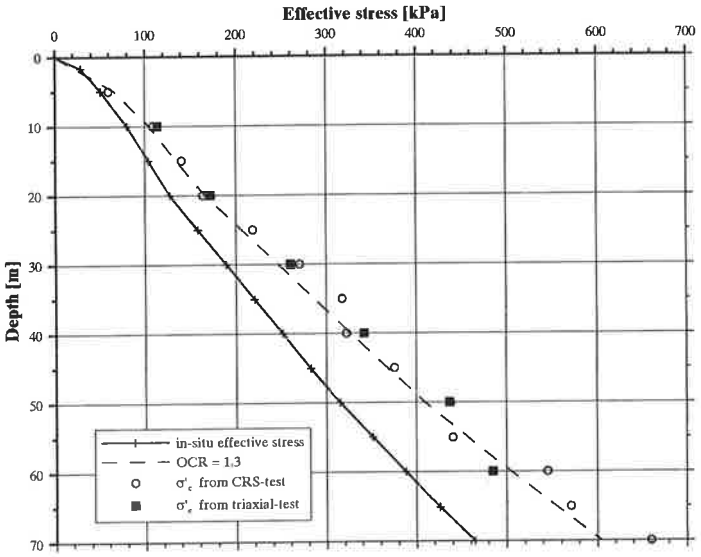

Figure 5.45 *Evaluated in situ effective stress and the determined preconsolidation pressure from CRS and triaxial tests conducted at borehole 101.*

The determined compression characteristics are shown in Figure 5.46.

In addition, a comparison with the determined consolidation properties at Lilla Bommen shows a remarkable similarity with respect to the preconsolidation

pressure at the same depths (Alte et al., 1989). The result is given in Appendix C.

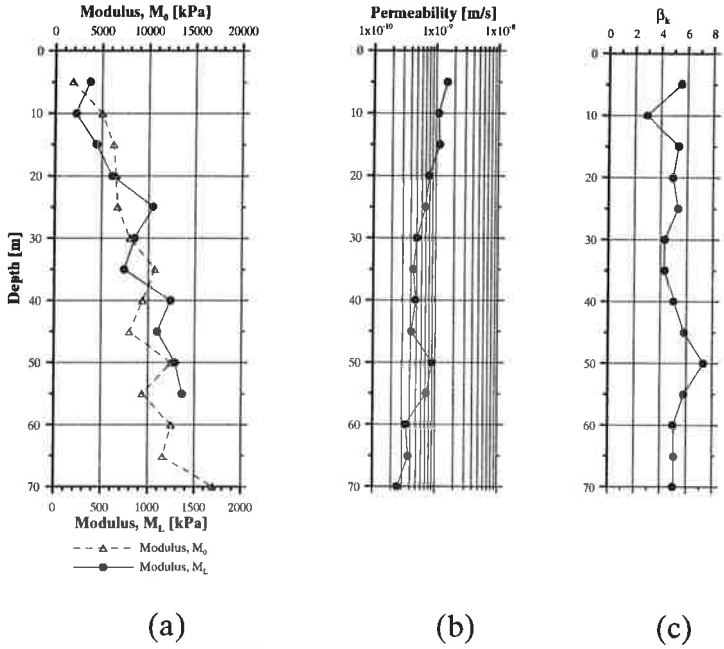

Figure 5.46 Compression characteristics of borehole 101.

5.6.2.3 Results from incremental loading tests

In order to evaluate the creep behaviour of the clay, incremental loading tests were conducted. Two different test procedures, in terms of the load increment, were used. One procedure was carried out in the usual way by increasing the load step-wise. The other procedure meant that the clay specimen was reconsolidated for in-situ effective stresses. Further loads were then applied in a step-wise manner. The purpose of the alternative tests was to obtain a load increment that simulated an in-situ loading with moderate load increment corresponding to effective stresses around the preconsolidation pressure. Figure 5.47 gives an example of both test procedures.

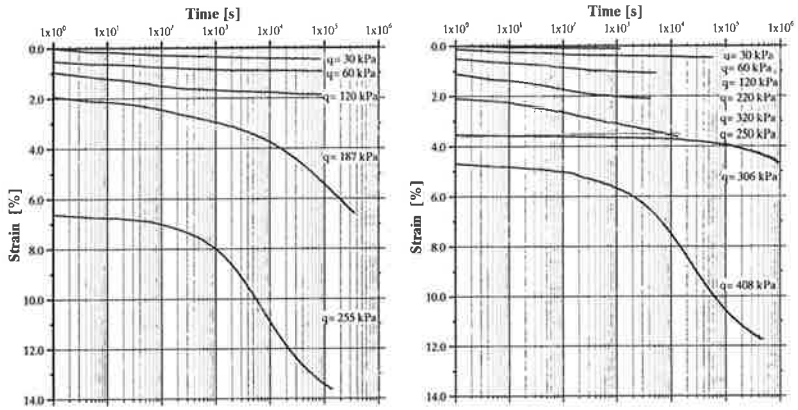

(a) Lundby Strand, depth 20 m. IL test with normal procedure under two-sided drainage conditions. σ'_c=170 kPa.

(b) Lundby Strand, depth 40 m. IL test with reconsolidation of the specimen. σ'_c =325 kPa.

Figure 5.47 Results from incremental loading tests performed with different procedures, (a) normal procedure and (b) with reconsolidation of the specimen.

The IL tests were evaluated with respect to the creep parameter coefficient of secondary compression, α_s. The results are shown in Figure 5.48.

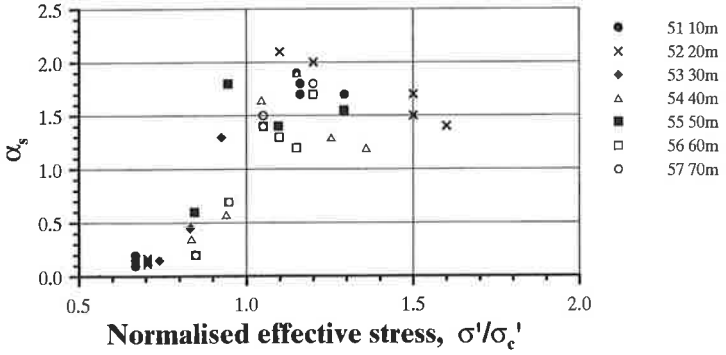

Figure 5.48 Values of α_s plotted versus normalised effective stress at Lundby Strand tests site.

The creep behaviour was also described by the parameter time resistance number, r_s. In terms of time resistance number the results from the incremental loading tests are given in Figure 5.49

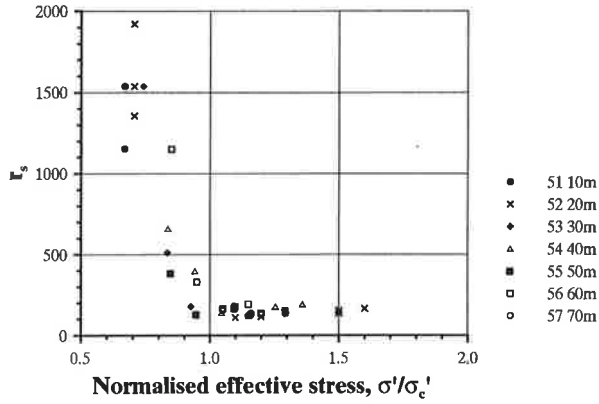

Figure 5.49 *Values of r_s plotted versus normalised effective stress at Lundby Strand tests site.*

The results from the IL tests are analysed in Chapter 6.

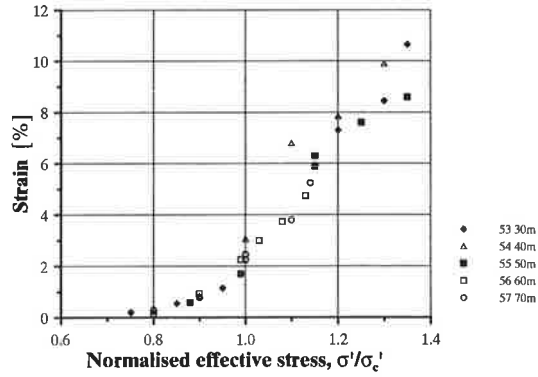

Figure 5.50 *Normalised effective stress versus strain, duration for each load increment was 5 days. The specimens were reconsolidated before the first presented load was applied.*

The result from the oedometer tests can also be presented in a diagram with the normalised effective stress as a

function of measured total strains, following reconsolidation of the samples. This is shown in Figure 5.50. The duration for each load increment was 5 days. For a normalised effective stress of about 0.9, the monitored strains were about 1% or less after 5 days. For stress ratios above $0.95 \cdot \sigma_c'$ the strains increased almost linearly with an increase in the normalised effective stress.

In laboratory tests, the compression behaviour of samples from deep deposits of clay, seem to be in accordance with that of clay from more normal depth, i.e. about 2-20 m.

5.7 The Lilla Mellösa test site

The Lilla Mellösa test site is an old full-scale loading test site with soft clay deposits and it has consolidated for the load of the test fill over a long period of time. It was constructed by SGI in 1945 and is situated in a flat area about 30 km north of the city of Stockholm, near the village of Upplands Väsby, see Figure 5.1. The reason for the construction of the test site was the search for a suitable site for a new airport. The airport project at Lilla Mellösa was abandoned but measurements at the test site have continued regularly since then. The data thus obtained is unique in terms of long-term monitoring and continuous records stretching back over a period of almost 60 years. A comprehensive description of the background and history of the test site is given by Chang (1981).

The layers of soft clay were about 14 m at this site, and not as deep as at the other test sites presented in this work. However, the site is of great interest due to the long term monitoring of settlements and pore pressures.

5.7.1 Soil conditions

Comprehensive investigations of the site and evaluation of soil parameters and conditions are presented by e.g.

Chang (1969) and Larsson (1986). The parameters used for the computations presented in this section are those evaluated by Larsson (1986), see Figure 5.51. Note that the natural deposit of soft clay contains about 2 % or more of organic material in the uppermost 7 m of the profile.

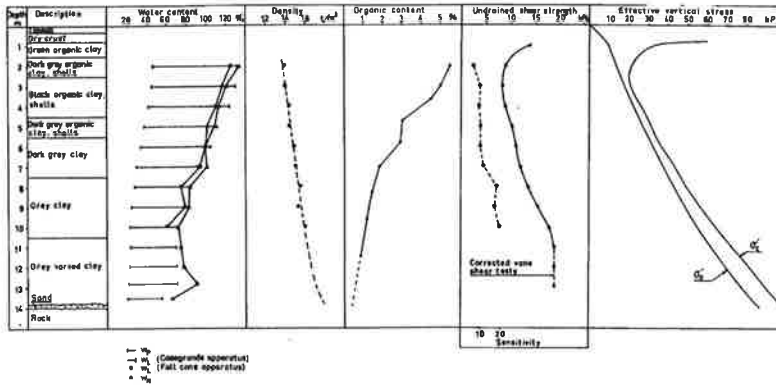

Figure 5.51 Evaluated soil parameters at the Lilla Mellösa test site (Larsson, 1986).

The deposit of soft clay is highly compressible and hence the value of the compression modulus and the time resistance number were quite small. Figure 5.52 presents the interpreted compression- and permeability parameters.

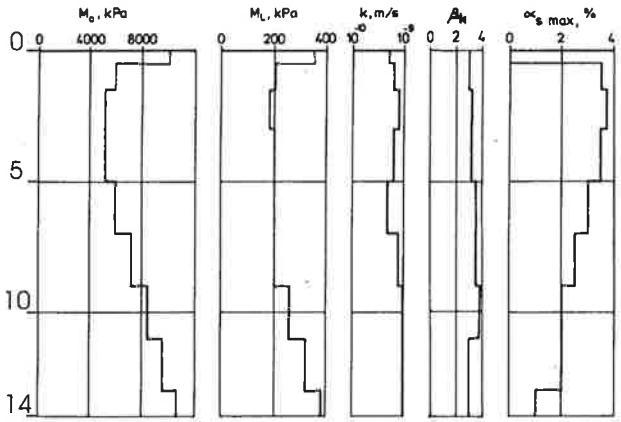

Figure 5.52 Evaluated parameters of compression modulus, permeability and coefficient of secondary consolidation (Larsson, 1986).

The fill was placed in an area measuring 30x30 m^2 and corresponded at the start to a load of about 40 kPa. After 20 years, i.e. in year 1965, the overburden load was estimated to be about 27 kPa (Chang 1981), due to hydraulic up-lift, as the fill had settled beneath the groundwater table.

5.7.2 Measured settlements and pore pressures

Measurements of settlements and pore pressures have been conducted since the fill was placed in 1945. The latest available data is from August 2002 (Larsson, 2002). The data thereby covers a period of 57 years. The data series was made available for this project by SGI. Measured settlements and excess pore pressure are shown in Figure 5.53.

The groundwater table was determined 0.8 m below the ground surface with a hydrostatic distribution in the soil profile.

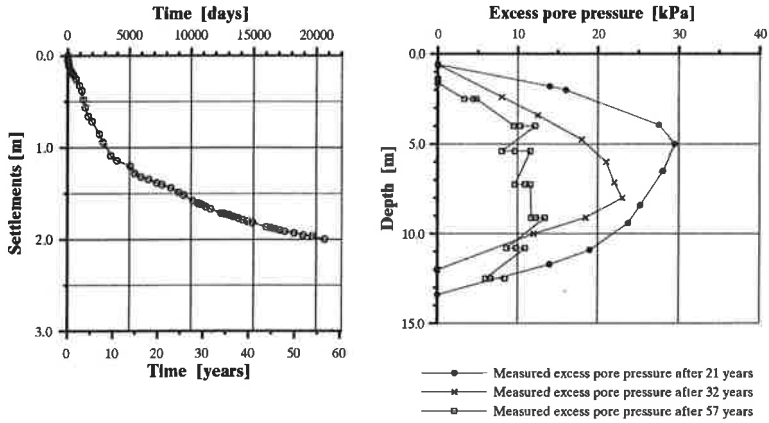

Figure 5.53 Measured settlements and excess pore pressures at the Lilla Mellösa test site.

6. ANALYSIS OF RESULTS FROM LABORATORY TESTS

6.1 Introduction

In order to obtain well-defined soil models the properties related to compression of the clays were thoroughly determined at the different test sites. This was of great importance because the soil models are the foundation for verifying the proposed computation model. The general properties such as bulk density, water content, liquid limit, shear strength and sensitivity were also determined for the clay in accordance with Swedish standard but the details of that will not be discussed.

The purpose was also to develop new and hopefully more efficient test procedures, in terms of determining an appropriate creep parameter. The factors, which were of special interest were; load increment ratio, duration and laboratory equipment.

6.2 Variation of the coefficient of secondary compression, α_s

6.2.1 Introduction

In order to determine the coefficient of secondary compression or the time resistance number, an extensive series of oedometer tests were carried out. Different test procedures were used under different boundary conditions, one-sided or two-sided drainage, load increment ratio (LIR) and duration of each load step. The purpose of the study was to determine how different conditions influence the compression behaviour of soft clays and also to obtain a more extensive database for the creep parameter. The clay samples from the Lundby Strand test site, taken from depths of 25 to 70 m, are of

special interest and unique, due to the limited testing experience of clay from such large depths.

To evaluate the results from IL tests the standard method is to plot the result in a semi-logarithmic diagram with log time versus strain. Using time in a logarithmic scale is necessary for the interpretation of the creep parameter because of the expected linear behaviour after EOP. Figure 6.1 illustrates the great difference in the shape of the curves between the diagrams for the same test in linear scale and in semi-logarithmic scale respectively.

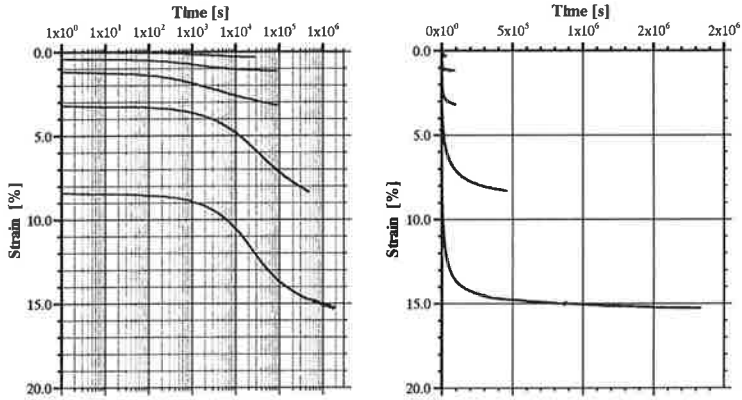

(a) (b)

Figure 6.1 Results from an IL test presented in (a) semi-logarithmic and (b) linear scale, Änggården CTH12-5.

6.2.2 Incremental loading test, traditional procedure

Traditionally, an IL-test is carried out under two-sided drainage conditions, and the load is doubled for each load step. Depending on the magnitude of the effective stress, in relation to the preconsolidation pressure, the curve of each load step follows a significant pattern. Figure 6.2 presents the results from a test sequence including all the load increments. For load increments resulting in stresses of a magnitude less than about $0.9 \cdot \sigma_c'$ the strains are small and occur within a short period of time, often within 1 hour. In Figure 6.2 the described case corresponds to the two upper curves.

When the load was increased and the effective stress was about equal to the preconsolidation pressure the obtained curve dropped and levelled out to describe an almost linear shape from about $6 \cdot 10^3$ s, as illustrated by the curve for load step 3, q= σ'_c, in Figure 6.2.

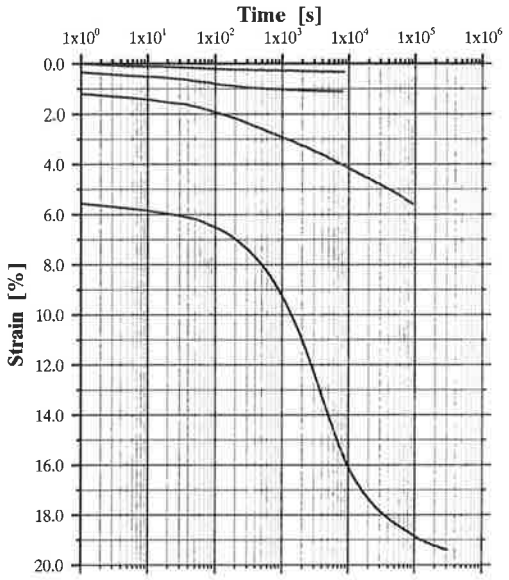

Figure 6.2 An example of results from an IL-test with the characteristic shape of the obtained stress – strain curves. Test sample Änggården CTH11-7m, one-sided drainage and doubling of each load step. The loads correspond to an effective stress of 0.25, 0.50, 1.0 and 2.0· σ'_c respectively.

Finally, for an applied load that corresponded to an effective stress greater than 1.2· σ'_c the typical reversed S-shape was obtained.

However, the shape of the curve partly depends on the magnitude of the load increment. How this affects the stress – strain curve and how some other conditions and test procedures influence the behaviour will be further discussed in the following paragraphs.

6.2.3 A study of the excess pore pressure dissipation

There are two commonly used methods for the determination of EOP and the coefficient of consolidation c_v. The first of these methods was proposed by Casagrande (1936) and the second was developed by Taylor (1948). In Figure 6.3 the EOP is determined according to Casagrande and the classical method of determining the coefficient of secondary consolidation is also shown.

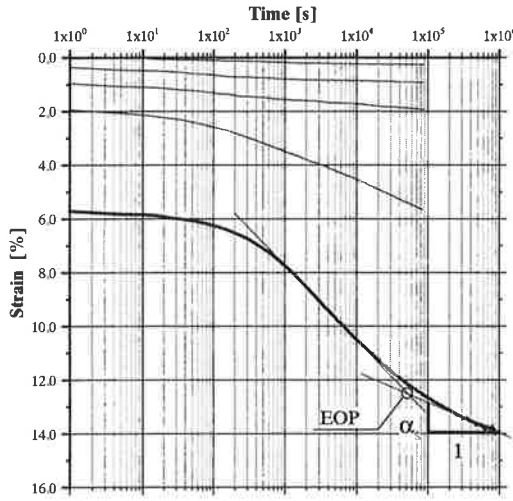

Figure 6.3 Determination of the end of primary consolidation, EOP, according to Casagrande and the coefficient of secondary consolidation for load step 5, Änggården CTH11-7m (S20:2), two-sided drainage conditions.

However, for IL tests where a load increment results in a stress of about $0.9\text{-}1.2 \cdot \sigma_c'$, the curvature of the obtained stress - strain curves was usually not the typical reversed S-shape, see Figure 6.3, load increment 4, and Figure 6.4. Hence it is not possible to use the method described above to determine the point of EOP.

A number of IL tests carried out under one-sided drainage conditions were studied, which led to the observation that EOP, interpreted as when the excess pore pressure was less than 1 % of the applied load

increment, had occurred when the strain curve had levelled out and became a straight line. This is shown in Figure 6.4, q= 45 → 80 kPa, where the monitored excess pore pressure also is plotted. The monitored excess pore pressure had dissipated before the point of time when the curve can be interpreted as a straight line.

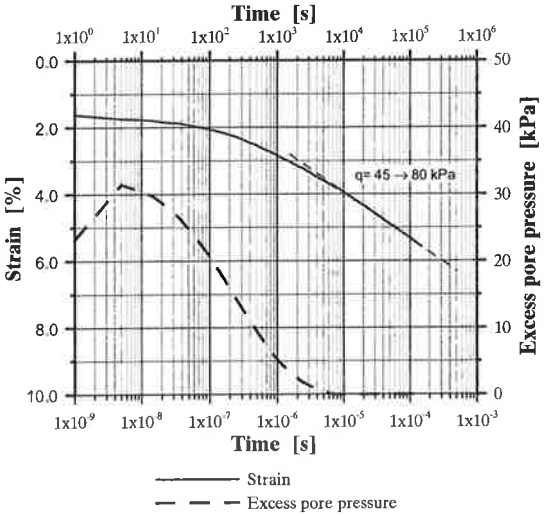

Figure 6.4 *Results from an IL test, Änggården CTH11-7m (S20b), σ'_c=68 kPa, q=45 → 80 kPa. A study of when the strain curve becomes a straight line in comparison with monitored excess pore pressure.*

6.2.4 Drainage conditions

Many of the IL tests were run under one-sided drainage conditions, with the intention of monitoring the excess pore pressure at the undrained boundary. The reason for this was that the dissipation of the excess pore pressure was of interest for the analysis of the consolidation process. Therefore it was important to study how length of drainage path affects the results and hence the determination of the creep parameter. Figure 6.5 presents results from two tests performed under the same conditions, except that one test had one-sided drainage and the other had a two-sided drainage conditions.

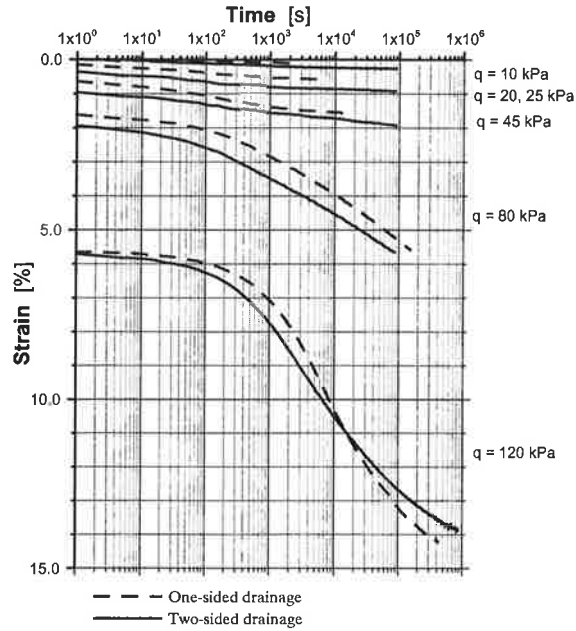

Figure 6.5 *Änggården CTH11-7m (S20:2 and S20b), σ'_c = 68 kPa. IL-tests conducted with the same applied load steps (except load step 2), but under two- and one-sided drainage respectively.*

When comparing the two sets of curves, the differences were not as large as might be expected according to Terzaghi's theory of consolidation. The time to the evaluated EOP should be about four times longer for the one-sided drainage condition, according to the time factor T_v in equation (6.1), due to the difference of drainage lengths of the sample, if no creep occurs.

$$T_v = c_v \cdot \frac{t}{H^2} \tag{6.1}$$

where t = time

H= drainage length

c_v = the coefficient of consolidation, given as:

$$c_v = \frac{M \cdot k}{\gamma_w} \qquad (6.2)$$

The differences between the curves vary somewhat during the consolidation process and the curves for load step 5 cross each other, which is probably caused by different modulus.

Therefore, one-sided drainage conditions affected the consolidation process in a less significant way than expected compared to two-sided drainage condition, considering classical one-dimensional consolidation theory. The value of α_s does not appear to be significantly influenced by the drainage conditions, as illustrated by Figure 6.5. Neither should it be according to theory.

6.2.5 Load increment ratio (LIR), Δq/q

The main purpose of conducting a great number of IL tests was to increase the empirical base pertaining the creep behaviour and determination of the creep parameter for clays from the western part of Sweden. In addition, it was important to investigate whether or not the magnitude of the load increment ratio (LIR) influenced the evaluation of α_s, and hence r_s, and, if so, how this would affect the evaluated creep parameter.

As mentioned before the traditional way of running an oedometer test involved that the load was doubled for each applied load increment. A number of researchers, e.g. Mesri and Godlewski (1977), Graham et al. (1983) Leroueil et al. (1985) carried out tests with a reduced magnitude of LIR, e.g. a ratio of 0.5 was commonly used. The intention was to make a more accurate evaluation of the stress – strain curve. It was also possible to determine more than one value for the creep parameter, in the range $0.8\text{-}1.3 \cdot \sigma_c'$, from one test sequence if a load ratio of about 0.5 or slightly less was used.

The oedometer tests conducted with different LIR were analysed and it was found that different LIR, which were

greater than 0.2, seemed to have a negligible influence on the magnitude of the coefficient of secondary consolidation α_s. Figure 6.6 presents three tests on clay from CTH12-16m performed with different LIR, 0.25, 0.5 and 1.0 respectively, but with the same applied total load. As can be seen, the inclinations of the plotted curves agree very well in the stress region where α_s is evaluated.

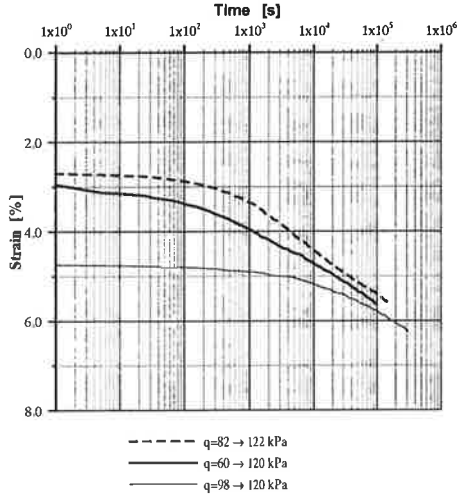

Figure 6.6 *Three tests with q=120-122 kPa, but with LIR 0.25, 0.5 and 1.0 respectively. The test samples are from borehole CTH12-16m (S3 and S4) and the tests were conducted under one-sided drainage condition. Note that the strain curves are adjusted in vertical direction so the curves fall together in the end to facilitate the comparison.*

Further, in Figure 6.7 stress-strain curves for different LIR are presented for two different loads greater than σ_c'. It can be observed that the interpretation of α_s gives about the same value independent of LIR for the loads (a) 200 kPa and (b) 190 kPa.

The conclusion based on a large number of tests is that the magnitude of α_s for a given stress level is independent of the LIR. That is in agreement with Mesri and Godlewski (1977) and Graham et al. (1983).

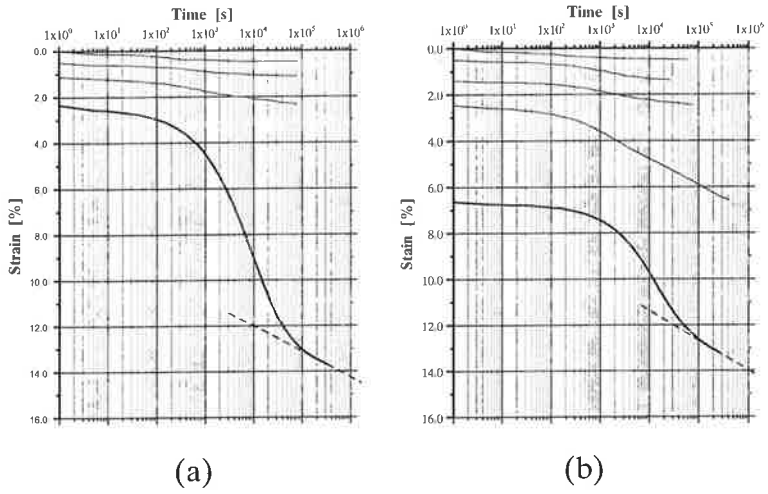

Figure 6.7 *Results of interpreted value of α_s from conducted IL-test, one-sided drainage condition, Änggården CTH12-16, with different LIR. (a) α_s=1.25 % with LIR= 1.0 and q= 200 kPa (S4:2). (b) α_s=1.15 % with LIR= 0.5 and q= 190 kPa, (S15:1)*

However, if the LIR was less than 1.0, and particularly less than 0.5, it was essential to take the duration into account when evaluating the α_s. In general a longer duration than 24 hours (86 400 s) was required before a reliable interpretation of α_s could be done. For an applied load corresponding to an effective stress around the preconsolidation pressure the evaluation of α_s could be underestimated. When the applied load was about $1.1 \cdot \sigma_c'$ or greater and the load ratio of the same magnitude as described above the consequence could on the other hand be an overestimation of the value of α_s. As shown in Figure 6.8 an interpretation of α_s after 24 hours duration of a test may grossly overestimates the true α_s.

For LIR of about 0.3 or less, the required duration was in general more than 3 days. Particularly loads corresponding to stresses close to the preconsolidation pressure might require even longer durations, see Figure 6.9.

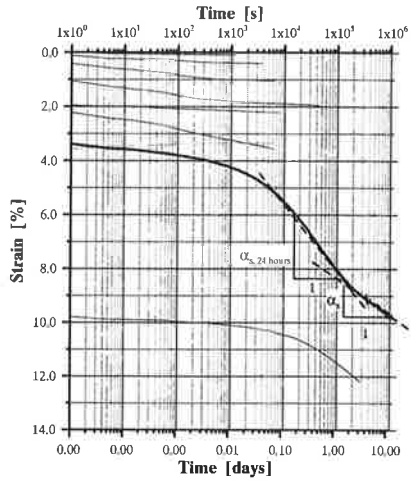

Figure 6.8 *Result from evaluating α_s at two different point of times, t= 24 hours and t=4-11 days, for a load ratio of 0.5 (q=482 kPa or $1.1 \cdot \sigma'_c$), the Lundby Strand test site depth 50 m (S50:3).*

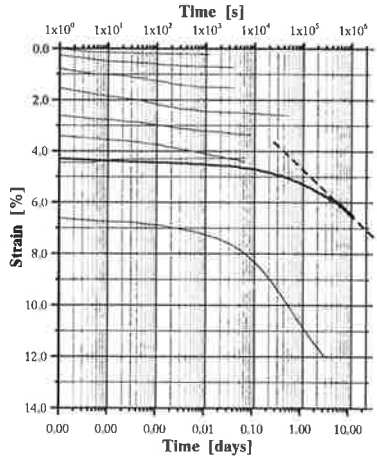

Figure 6.9 *Evaluation of α_s for load step 8 q=416 kPa, i.e. $0.95 \cdot \sigma'_c$, at the Lundby Strand test site depth 50 m (S50:2).*

In general, the smaller the load increment the longer the required time to obtain a reliable determination of α_s from tests with a load corresponding to an effective stress

of about σ_c' or greater. Also when the strains were large, about 7-10 % or larger, it usually requires a longer duration of the load step than 24 hours.

6.2.6 Long term incremental loading tests

It was recognised that the duration of a load step could have a significant impact on the determination of α_s. To investigate as to whether α_s was constant over a longer time period, a number of long-term tests were carried out. According to e.g. Larsson (1981), the assumption is that α_s is constant for a certain effective stress is a simplification. Figure 6.10 shows a test of 34 days duration for load step 3, q=80 kPa.

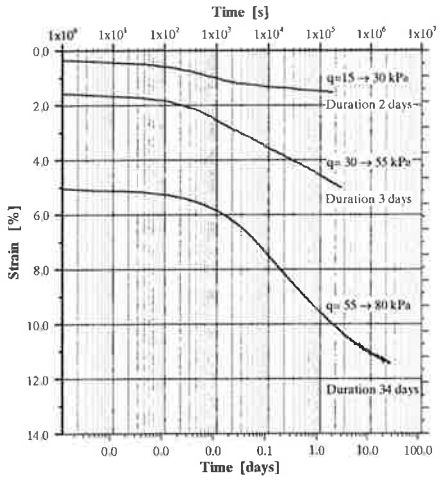

Figure 6.10 Long term IL-test, duration 34 days for q=80 kPa. Änggården test site, CTH11-5m (S21:2), $\sigma_c' = 50$ kPa.

The inclination of the curve clearly decreases from the 1-day point (86 400 s), to the end of the curve. The creep strains from about the 10-days mark to the completion time of 34 days seemed to correspond to a fairly straight line.

6.2.7 The magnitude of coefficient of secondary compression, α_s

So far, different test procedures and test conditions have been studied to analyse whether or not these factors have effects on determining the coefficient of consolidation. A great number of incremental loading tests have been evaluated and analysed. In the following text the magnitude and variation of the coefficient of secondary consolidation, α_s, will be studied.

One way of describing α_s is as a function of strain. Another way is description of the variation of α_s, as a function of the effective stress, normalised with respect to the preconsolidation pressure. The latter definition may probably simplify the calculation model, described in Chapter 7. The determined values of α_s for the Änggården site are presented in Figure 6.11.

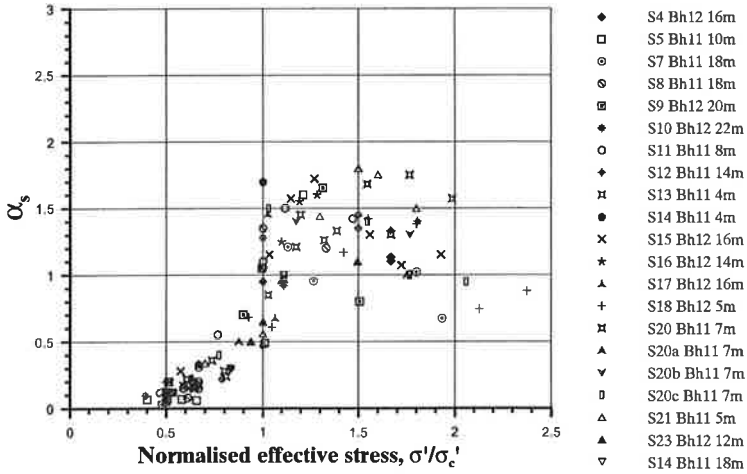

Figure 6.11 Determined values of coefficient of secondary compression, α_s, versus normalised effective stress for the Änggården site.

As can be seen in Figure 6.11, the value of α_s depends strongly on the magnitude of the effective stress. For an effective stress below approximately $0.7 \cdot \sigma_c'$, the value of α_s was very low, less than about 0.2 %. For an increase in

the effective stress from about $0.8 \cdot \sigma_c'$, α_s increased gradually up to a maximum value about $1.1\text{-}1.2 \cdot \sigma_c'$. The maximum magnitude of α_s was about 1.2-1.7 % for the Änggården clay. For additional loads α_s appeared fairly constant within a certain range or decreased slightly. At a high magnitude of stresses, corresponding to a strain of about 12-15%, α_s decreased linearly with increasing effective stresses.

In comparison with the recommended values of $\alpha_{s,max}$ from Larsson et. al. (1994), the difference, in general, was that obtained values of $\alpha_{s,max}$ from the Änggården test site did not vary as much with respect to the natural water content as suggested in computer program manual. As described above, the maximum value of α_s varied between 1.2 to 1.7 % when the natural water content mainly varied between 50 and 90 %. For corresponding value of w_N, Embankco suggested $\alpha_{s,max}$= 1.0-2.5 %, which is a notably wider range.

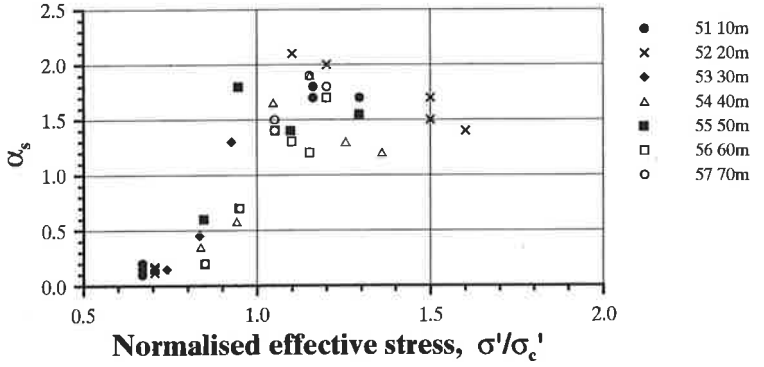

Figure 6.12 Determined values of α_s obtained from IL tests of clay from the Lundby Strand test site.

For the Lundby Strand test site, where clay from very deep layers, down to 70 m, was examined, the evaluated maximum value for α_s was about 1.4-1.9 %, which is of a similar magnitude as the values for clay taken from more moderate depths, i.e. down to about 20 to 30 m. Also the variation of α_s with the effective stress has the same

pattern as the result from the Änggården site. In Figure 6.12 the evaluated values of α_s from Lundby Strand are presented as a function of normalised effective stress.

A study of recommended values of $\alpha_{s,max}$ by Larsson et. al. (1994) gave $\alpha_{s,max}$= 1.4-1.8 %, for the Lundby Strand clay. This was in very good agreement with the determined values of $\alpha_{s,max}$ for the Lundby Strand test site.

In some tests the determined value of α_s was greater than 2.0 %. However, that can probably be explained by a too short duration of the test considering the load increment ratio.

Also for the clays from larger depths the same general behaviour regarding α_s was observed.

For the modified test procedure conducted on the clay from Lundby Strand test site (with the exception of clay from a depth of 10 and 20 m), and also used for the Hanhals test site, the significances were the reconsolidation procedure, a small magnitude of the load increment ratio (LIR) and a long duration, which was in excess of 24 hours, for each load step. For the obtained time-stress curves from tests with a load corresponding to 0.8-1.2$\cdot\sigma_c'$, the shape was similar to normal tests, even though the monitored strains were smaller. In Figure 6.13 two examples are shown of tests where the specimens were reconsolidated. Note the small value of LIR after reconsolidation, between 0.22 and 0.36, and the required time for the determination of a reliable value of α_s.

When the test results were analysed, it was observed how remarkably homogeneous the very deep deposit of clay is and how consistent the results from the incremental loading tests are. It thus appears that slightly overconsolidated soft clays at great depths have, in principle, the same behaviour, as clays at depths down to about 20-25 m, which constitute the bulk of the experience.

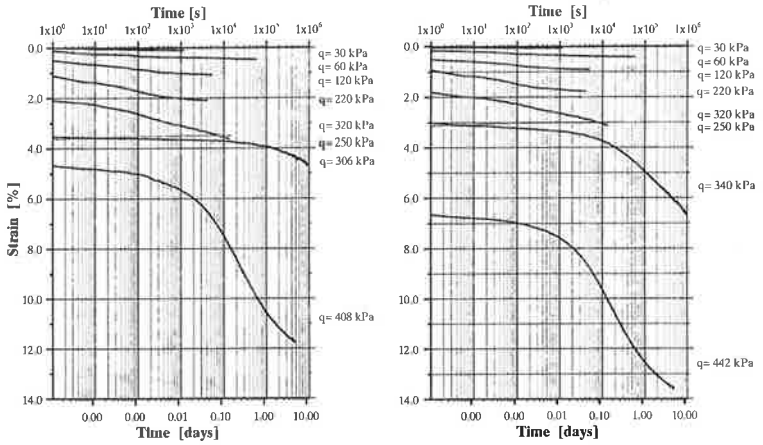

Figure 6.13 Lundby Strand depth 40m (S4:2, S4:3), σ'_c = 340 kPa. Examples of different sequences of IL tests with reconsolidated specimens.

6.3 Relationship between effective stress, strain and strain rate

6.3.1 Relationship between effective stress, strain and strain rate in general

It is widely accepted that there is a unique relationship between the effective stress, strain and strain rate for one-dimensional consolidation. In 1957 Šuklje presented a model that was built on this relationship by means of a set of isotaches. Leroueil et al. (1985) confirmed the unique relationship by an extensive investigation of different types of clay. The strain rate behaviour of soft, lightly overconsolidated natural clays has also been investigated by researchers such as Sällfors (1975), Larsson (1981, 1986), Graham et al. (1983) and Länsivaara (1999), to mention just a few. The strain rate effect is often explained in terms of viscous effects. According to

Leroueil et al. (1985) the viscosity of clay is closely related to creep property.

The viscous behaviour and the relationship between effective stress, strain and strain rate were also studied within this project.

6.3.2 Analysis of CRS tests and CRS tests with different strain rates

The viscous effects or rate dependency for the consolidation of soft clay is a characteristic and a very important property. Hence one-dimensional stress – strain behaviour can be illustrated by the results from CRS tests. By running a number of CRS tests with different strain rates, each test produces a unique stress – strain curve.

Tests conducted of Bäckebol clay (Sällfors 1975) provides an example of such behaviour, which is illustrated in Figure 2.10. The higher the strain rate the higher the effective stress for a given strain. Leroueil et al. (1985) normalised the stress – strain curves presented in Figure 2.10 with respect to the preconsolidation pressure and the results are given in Figure 6.14.

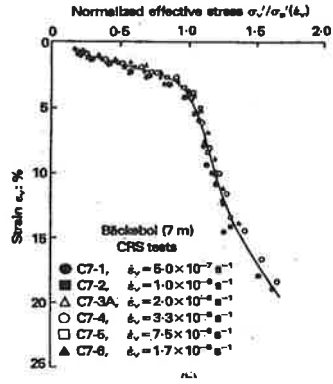

Figure 6.14 Bäckebol, depth 7m. The plotted results are the stress-strain curves shown in Figure 2.10 normalised with respect to the preconsolidation pressure (Leroueil et al. 1985).

The results fall in a very narrow range and are an effect of the unique relation between effective stress, strain and strain rate, which is described in this Section. The strain rate dependency for the stress–strain behaviour can also be observed by changing the strain rate during a CRS test, see Figure 6.15

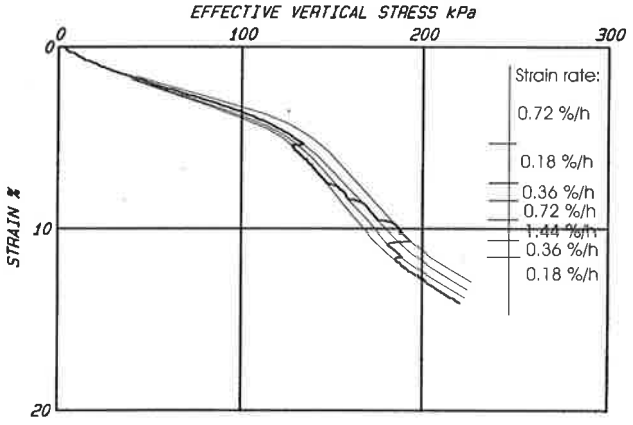

Figure 6.15 Änggården CTH12-16m (NOL12_16y), with different strain rates. Interpreted stress-strain curves for different strain rates are also plotted.

By means of comprehensive investigations of clays from different locations, Leroueil et al. (1985) showed that a unique relationship exists between effective stress, strain and strain rate and they expressed the rheological behaviour of natural clays by the two equations:

$$\sigma_c' = f(\dot{\varepsilon}) \tag{6.3}$$

$$\frac{\sigma'}{\sigma_c'}(\dot{\varepsilon}) = g(\varepsilon) \tag{6.4}$$

This is described in detail in Chapter 2.

Instead of running a number of CRS tests, each test with a different strain rate, a test procedure was adopted where the strain rate was altered during the CRS test. The intention was to obtain corresponding results by running just one test. The advantage with such a test is also that

the deviations in the results from different specimens from the same sample, due to the natural variation in soils, is avoided. A CRS-curve from such a test is shown in Figure 6.16. Note the almost instant changes in effective stress when the strain rate was altered. Such a test makes it possible to interpret the unique stress – strain curve for each strain rate with a good degree of reliability.

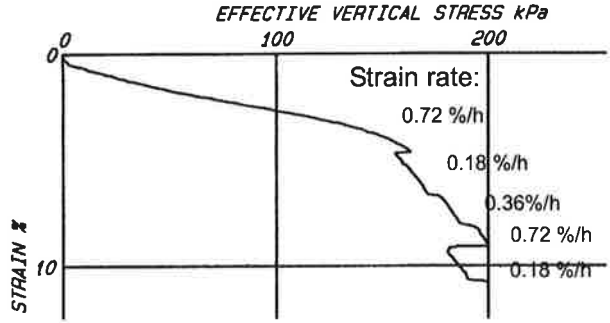

Figure 6.16 CRS test with different strain rates, Änggården CTH11-18m.

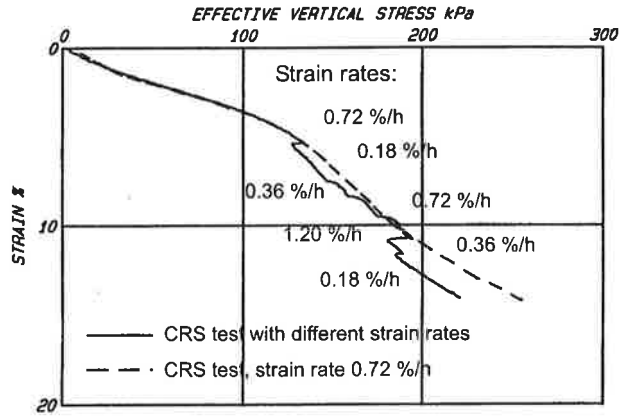

Figure 6.17 Änggården CTH12-16m. CRS tests with different strain rates and also one test with constant strain rate.

When the results from CRS tests with different strain rates were studied some details could be observed. When

the strain rate was changed, regardless of whether it was increased or decreased, the curve distinctly changed position and the new position corresponded fairly well to the curve obtained from a test performed with a constant identical strain rate, as can be seen in Figure 6.17.

In order to study the relationship between the apparent preconsolidation pressure and the strain rate a number of tests were evaluated. In Figure 6.18 CRS tests from Änggården, CTH11-7m, are presented.

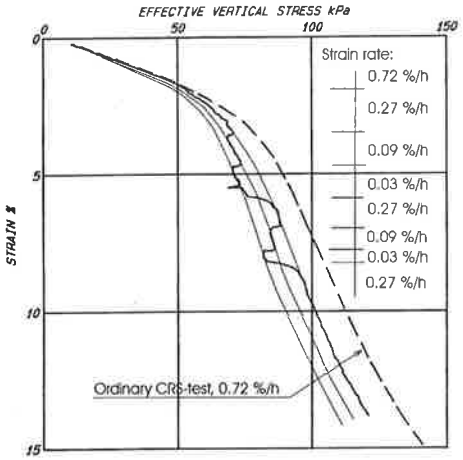

Figure 6.18 Änggården, CTH11-7m. CRS test with different strain rates and a conventional CRS test. The plot of stress – strain curves for each strain rate is interpreted from the obtained curve.

For two curves with $\dot{\varepsilon} = \dot{\varepsilon}_1$ and $\dot{\varepsilon} = \dot{\varepsilon}_2$, showing the preconsolidation pressure σ'_{c1} and σ'_{c2} respectively for a certain strain, the effective stress can be given by the equation (6.5), (Leroueil et al., 1985):

$$\frac{\sigma'_{v1}}{\sigma'_{cv1}} = \frac{\sigma'_{v2}}{\sigma'_{cv2}} \qquad (6.5)$$

This relationship agreed very well with the clays examined in this project. Thus it was possible to evaluate a preconsolidation pressure for different strain rates from

CRS tests. For the CTH11-7 m clay, presented in Figure 6.18, the evaluated preconsolidation pressures, according to Swedish practice (Sällfors 1975), for each strain rate are:

$$\sigma'_{c1}(\dot{\varepsilon}_1 = 0.72\%/h) = 66kPa$$

$$\sigma'_{c2}(\dot{\varepsilon}_2 = 0.27\%/h) = 59kPa$$

$$\sigma'_{c3}(\dot{\varepsilon}_3 = 0.09\%/h) = 55kPa$$

and $$\sigma'_{c4}(\dot{\varepsilon}_4 = 0.03\%/h) = 52kPa.$$

For the CRS test with $\dot{\varepsilon}_1 = 0.72$ %/h the evaluated value of the preconsolidation pressure appears to be somewhat higher compared to the other tests with respect to the strain rate. However, considering that two different specimens were used it is within normal variation of clays and the shape of the curves was fairly similar.

Furthermore, a study of how the evaluated preconsolidation pressure depends on the strain rate was carried out. With respect to the test, CTH11-7m shown in Figure 6.18, and a number of other conducted tests, it appeared that when the strain rate was doubled, the preconsolidation pressure increased by about 4-5%. The corresponding effect was obtained if the strain rate was halved. The results are consistent with what other researchers have observed. Graham et al. (1983) concluded that if the strain rate was increased tenfold, the resulting preconsolidation pressure showed an increase of 10-20% for slightly overconsolidated clays. The corresponding value is 5-15% according to Leroueil and Marques (1996).

In Figure 6.19 the normalised preconsolidation pressure is plotted against the logarithm of strain rate. The scatter is very small, and the pattern is similar to previous studies performed by Leroueil et al. (1985) and Länsivaara (1999). The relationship is almost linear. Graham et al. (1983) suggested a linear relationship in a semi-logarithmic diagram.

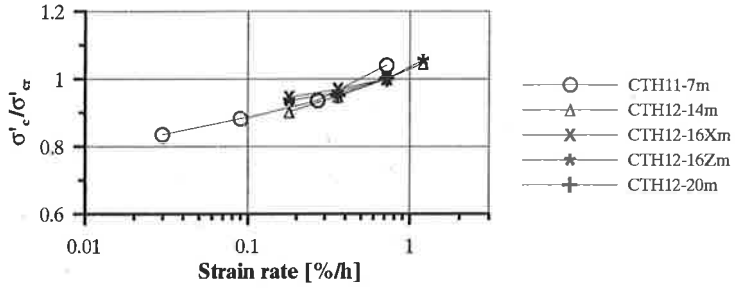

Figure 6.19 Normalised preconsolidation pressure versus the strain rate in logarithmic scale. $\sigma'_{cr}=\sigma'_c$ for the strain rate 0.72 %/h. The preconsolidation pressure for each strain rate is interpreted from CRS tests with different strain rates.

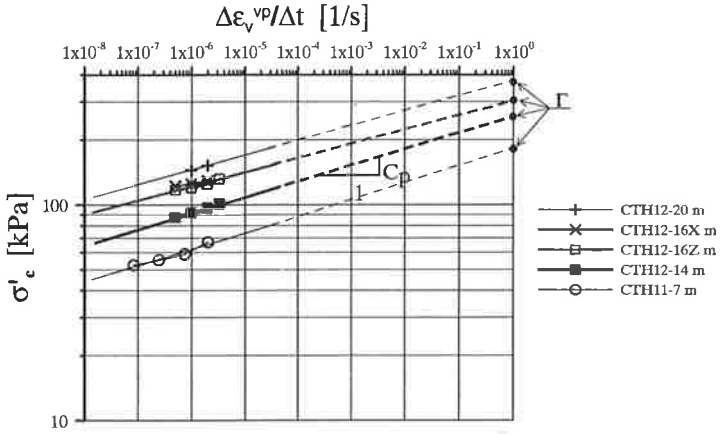

Figure 6.20 Preconsolidation pressure versus strain rate in a double logarithmic diagram. The preconsolidation pressure for each strain rate was interpreted from conducted CRS tests with different strain rates as illustrated in Figure 6.19.

In their proposed elastic-viscoplastic model (EVP-model) Leroueil and Kim (2001) utilised the relationship between the preconsolidation pressure and strain rate to describe the viscous behaviour. The equation describes the relation between preconsolidation pressure and strain rate $\sigma'_p = f(\dot{\varepsilon}_v^{vp})$, and can be expressed as a linear function in a $\log\sigma'_c$—$\log\dot{\varepsilon}_v^{vp}$ diagram as:

$$\log \sigma'_p = \Gamma + C_p \cdot \log \dot{\varepsilon}_v^{vp} \tag{6.6}$$

The parameters and the expression for the rate of viscoplastic strain are described in Chapter 2. In Figure 6.20 the same data are given as in Figure 6.19, but in a $\log \sigma'_c - \log \dot{\varepsilon}_v^{vp}$ diagram. Hence it was possible to observe an almost linear relationship and to determine the value of Γ and C_p at various depths for tests on clays at the Änggården site. The determined values of C_p varied between 0.06 and 0.08.

According to Leroueil and Marques (1996) the value of C_p is equal to the ratio C_α / C_c, as proposed by Mesri and Godlewski (1977). Further Janbu (1985) defined the relation between modulus number m and time resistance number r_s as:

$$\frac{C_\alpha}{C_c} = \frac{m}{r_s} \tag{6.7}$$

when the stiffness of the clay increases linearly with stress in the normally consolidated domain, i.e. $M = m \cdot \sigma'$.

Mesri and Castro (1987) found the relationship C_α / C_c to be 0.04±0.01 for inorganic soft clays, see Chapter 2.

For the presented results, in Figure 6.20, at the Änggården test site, the values of C_p were larger than suggested by Mesri and Castro, but agreed very well with results presented by Länsivaara (1999), B= C_α / C_c =0.073.

Länsivaara (1995, 1999) proposed a model for determination of the creep parameter *time resistance number,* r_s. The first step was to evaluate the factor *B,* based on results from CRS tests with different strain rates, according to equation (6.8):

$$\frac{\sigma'_{v1}}{\sigma'_{v2}} = \frac{\sigma'_{cv1}}{\sigma'_{cv2}} = \left(\frac{\dot{\varepsilon}_1}{\dot{\varepsilon}_2} \right)^B \tag{6.8}$$

where: σ'_{v1} = the effective stress for strain rate $\dot{\varepsilon}_1$

σ'_{v2} = the effective stress for strain rate $\dot{\varepsilon}_2$

σ'_{cv1} = the σ'_c for strain rate $\dot{\varepsilon}_1$

σ'_{cv2} = the σ'_c for strain rate $\dot{\varepsilon}_2$

By using the relation, according to equation (6.7) the value of r_s was obtained by the proposed equation:

$$r_s = \frac{M(\sigma')}{\sigma' \cdot B} \tag{6.9}$$

The concept of this model is described in Chapter 2. However, as pointed out previously, the model required that the compression modulus increased linearly with increasing effective stress. For Swedish clay the compression modulus is evaluated as constant from σ'_c to σ'_L. This implies that the relation becomes more complicated and hence more difficult to solve.

6.3.3 Normalising of stress-strain curves from CRS-tests

A study was carried out where comparisons were made between stress - strain curves, normalised with respect to the preconsolidation pressure, obtained from conducted CRS tests from the Lundby Strand test site. In Figure 6.21 the results from conducted CRS tests, from depths of 10-35 m, are plotted in an effective stress – strain diagram.

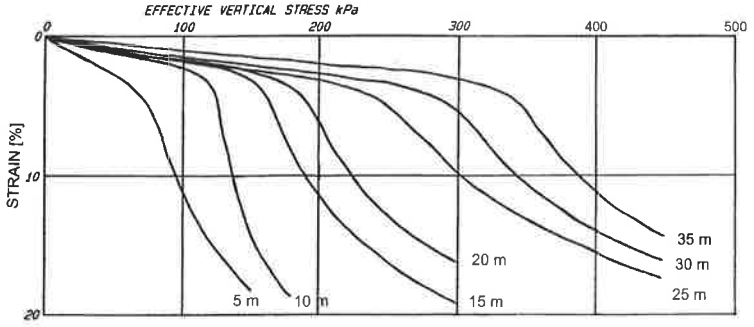

Figure 6.21 Results in linear scale from CRS tests, depths 5-35 m, the Lundy Strand test site.

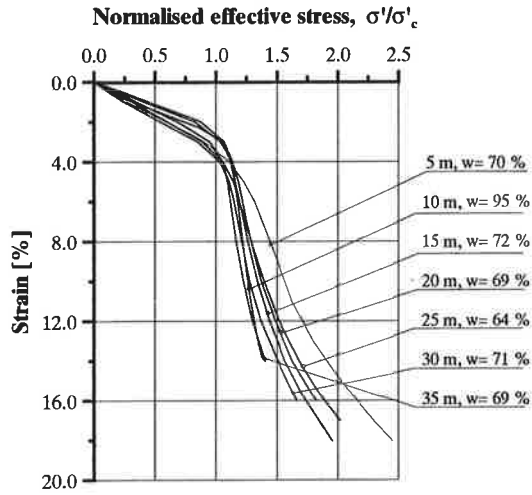

Figure 6.22 CRS-curves normalised with respect to the preconsolidation pressure, depths 5-35 m, i.e. the same stress-strain curves shown in Figure 6.21.

By normalising the curves with respect to the preconsolidation pressure, the curves fell within a remarkably narrow range, which is shown in Figure 6.22, despite the large difference in depth.

A corresponding study was made for the clay from Kv Guldet, Lilla Bommen, Göteborg (Alte et al. 1989), see Figure 6.23. The location of the test site is given in Figure 5.40.

From the study it appears that the stress-strain curve for the same type of clays, normalised with respect to the preconsolidation pressure, show noticeable similarity. The concordance in the result is probably related to the equivalence in the sedimentation conditions and the type of clay minerals.

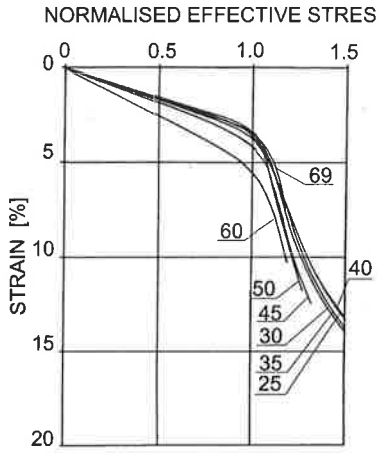

Figure 6.23 Result from conducted CRS test, depths 25-69 m, from Kv Guldet, Lilla Bommen, Göteborg. The effective stress is normalised with respect to the σ'_c (after Alte et. al., 1989).

6.3.4 Analyses of CRS test comparing to IL tests

Further analyses have been made to confirm that the behaviour of soft clay during one-dimensional consolidation is controlled by a unique $\sigma' - \varepsilon - \dot{\varepsilon}$ relationship. Results from CRS tests were compared with results from IL tests carried out on the same clay.

The study was performed according to the following procedure: the strain rate from an incremental loading test was continuously determined for each load step. Figure 6.24 shows the results from the Änggården site, CTH11-18m, for an incremental load test with one-sided drainage.

Then the strain was determined for each load step for a specific strain rate, i.e. in this case the strain rate of the CRS test, $2 \cdot 10^{-6}\, 1/s$ (0,72%/h). The current effective stress was evaluated for the so determined strain. The effective stress, for one-sided drainage conditions, was obtained by:

$$\sigma' = q - \frac{2}{3}u_b \tag{6.10}$$

where u_b is the measured pore pressure at the base of the specimen and $\frac{2}{3}u_b$ is the average value of the pore pressure, assuming a parabolic pore pressure distribution in the sample (Smith and Wahls, 1969 and Wissa, 1969).

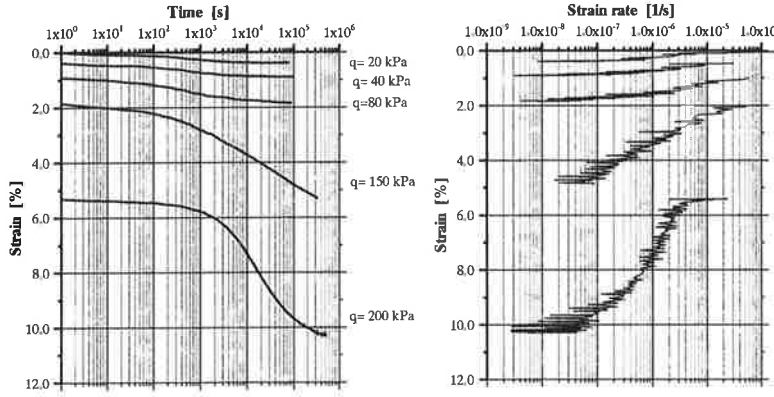

Figure 6.24 The Änggården test site, CTH11-18m (S8:1). IL test under one-sided drainage conditions. (a) log time versus strain and (b) evaluated strain rate in logarithmic scale versus strain.

The data thus obtained could finally be plotted in a diagram showing effective stress on the abscissa and strain on the ordinate, see Figure 6.25. As can be seen, the evaluated results from the IL test agree well with the CRS-curve.

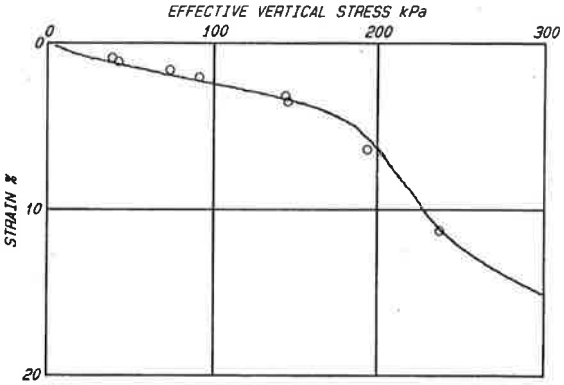

Figure 6.25 Änggården CTH11-18m. Results from CRS test. The dots are evaluated stress-strain points from the IL-test (S8:1 and 3) where the strain rate is 0.72 %/h.

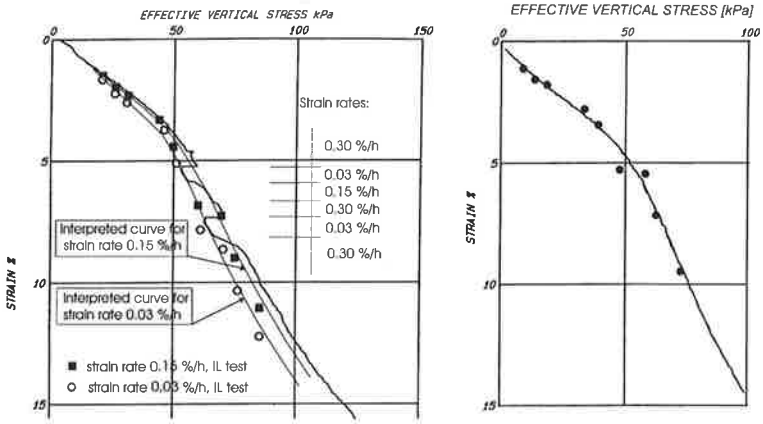

Figure 6.26 Änggården CTH11-5m, (a) evaluated stress – strain coordinates for strain rates 0.03 %/h and 0.15 %/h from IL-tests compared to the results from a CRS test with different strain rates. The interpreted curves for the corresponding strain rates are also plotted. (b) evaluated stress – strain coordinates for strain rates 0.72 %/h compared to CRS test with corresponding strain rate 0.72 %/h.

A comparison between an IL-test and a CRS test with both different and constant strain rates was also performed with CTH11-5m clay from the Änggården site. The result is presented in Figure 6.26.

The comparison shows that the same results were obtained when CRS test was conducted with a constant strain rate, with different strain rates and when incremental load tests were carried out under one- or two-sided drainage conditions. The proposed unique relationship between effective stress, strain and strain rate thus appears to be valid for the examined clays.

6.4 Discussion

The findings from laboratory tests can briefly be summarised as follows. Firstly, the creep behaviour is strongly dependent on the effective stress. From an effective stress about $0.7 \cdot \sigma_c'$ up to approximately $1.1 \cdot \sigma_c'$ the coefficient of secondary compression, α_s , gradually increased to a maximum value. With a further increase in the effective stress, α_s, remained fairly constant within a certain range or showed a slight decrease. The same general behaviour regarding α_s was also observed in clays from deep layers down to about 70 m below the ground surface,

Secondly, the drainage conditions or the LIR for IL tests appears to have no or very limited effect on the value of α_s . However, the duration of each load step should be taken into consideration, otherwise the consequence could be an misjudging of the value of α_s .

From the CRS tests conducted with various strain rates, it can be concluded that clay shows viscous effects. The stress-strain curve is unique due to the strain rate, which confirms that there is a unique relationship between effective stress, strain and strain rate for clays under one-dimensional consolidation.

Furthermore, the described relationship can also be proved by evaluating the effective stress and strain of a certain strain rate from each load step of IL tests and by plotting the data obtained. The plotted data agree very well with the obtained curve from a CRS test on the same clay and with a corresponding stain rate.

7. A MODEL FOR SETTLEMENT CALCULATION INCLUDING CREEP EFFECTS

7.1 Introduction

The one-dimensional consolidation model for settlement calculation described in this chapter was presented by Alén (1998). The model was intended as a tool in engineering practice. It is based on a hypothesis that the time dependent settlement in clay can be adequately described by three different physical phenomena; consolidation, elastic-plastic strains and creep strain.

In this work the model has been applied in a newly developed computer code, providing improved parameter models. The program is able to model both laboratory tests, such as incremental loading (IL) tests, and the full-scale behaviour of soft clays. Furthermore, the models of the input parameters compression modulus and time resistance number have been thoroughly studied and modified.

The computer program was, in a first step, verified against analytical calculations excluding creep effects. Secondly, the computer program was tested and verified by the simulation of previously conducted incremental loading tests. Under such well-defined conditions it was possible to conduct reliable studies of each parameter and to analyse the simulation of each parameter and in addition the consolidation process including creep effects.

The next stage, and the most interesting one, was to verify the computer model for full-scale settlement calculations. For this purpose the test sites previously described were of vital importance and constituted the base of the verification.

7.2 Description of the computer model

The theory of the model for settlement calculation is based on the classical theory of one-dimensional consolidation presented by Terzaghi (1923), which is described in Chapter 2. However, the creep effects are not accounted for in the basic differential equation (2.1). Also the present model is limited to one-dimensional consolidation.

In the model, it is assumed that the time dependent strains are described by three different phenomena, which are in detail described by Alén (1998):

- Consolidation — the process of dissipation of excess pore pressure, which restricts the strain rate in the model.
- Elastic/plastic strains — strains caused by an increase in the effective stress.
- Creep strains — strains occurring over time at a constant effective stress level.

The interaction between these three phenomena is described by a rheological model, see Figure 7.1

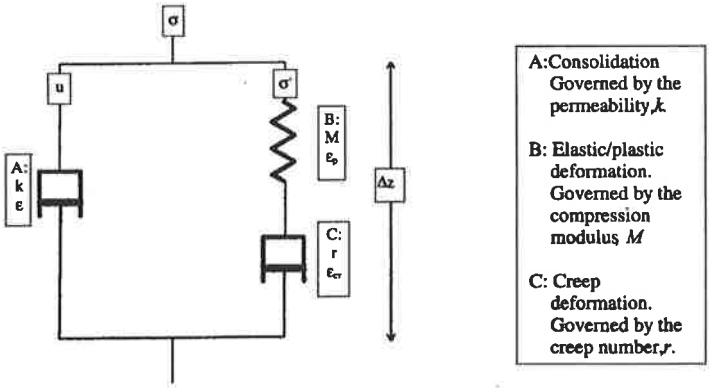

Figure 7.1 *Rheological soil model describing long term strain in clay (Alén, 1998).*

7.3 Theory and differential equations

In the rheological model (Alén, 1998) in Figure 7.1 is described in this section:

A: The strain rate is equal to the relative change in height of a volume during a time increment using the equation for one-dimensional consolidation:

$$\frac{\partial \varepsilon_z}{\partial t} = -\frac{\partial}{\partial z}\left[\frac{k_z}{\gamma_w}\cdot\left(\frac{\partial u}{\partial z}\right)\right] \tag{7.1}$$

where ε_z = total vertical strains

k_z = vertical permeability [m/s]

u = *pore pressure [kPa]*

z = *depth [m]*

t = *time [s]*

γ_w = *unit weight of water [kN/m^3]*

B: The total stress is assumed to be constant. The change in effective stress is equal to the change in pore pressure:

$$\Delta\varepsilon_z^{ep} = \frac{\Delta\sigma_z'}{M(\sigma_z')} \tag{7.2}$$

where ε_z^{ep} = the vertical elastic and plastic strains

and

$$\dot{\varepsilon}_z^{ep} = -\frac{1}{M(\sigma_z')}\cdot\frac{\partial u}{\partial t} \tag{7.3}$$

C: The creep behaviour is defined by the time resistance parameter, R, and is defined as:

$$R = \frac{\partial t}{\partial \varepsilon_z^{cr}} \tag{7.4}$$

From Figure 2.8 we obtain:

$$R = r_s \cdot (t - t_r) \tag{7.5}$$

where r_s is the time resistance number and the creep strain rate is:

$$\frac{\partial \varepsilon_z^{cr}}{\partial t} = \dot{\varepsilon}_z^{cr} = \frac{1}{R} = \frac{1}{r_s \cdot (t - t_r)} \tag{7.6}$$

where ε_z^{cr} = the vertical creep strain

t_r = the reference time

The total vertical strain must be equal to the sum of elastic-plastic strain and creep strain:

$$\varepsilon_z = \varepsilon_z^{ep} + \varepsilon_z^{cr} \tag{7.7}$$

By deriving with respect to time (t) the equation can be expressed as:

$$\frac{\partial \varepsilon_z}{\partial t} = \dot{\varepsilon}_z = \dot{\varepsilon}_z^{ep} + \dot{\varepsilon}_z^{cr} \tag{7.8}$$

where $\dot{\varepsilon}_z^{ep}$ = elastic plastic strain rate

$\dot{\varepsilon}_z^{cr}$ = creep strain rate

By substituting equation (7.3) and (7.6) into (7.8) and then combining equation (7.1) and (7.8) it becomes:

$$-\frac{\partial}{\partial z}\left[\frac{k_z}{\gamma_w} \cdot \left(\frac{\partial u}{\partial z}\right)\right] = -\frac{1}{M} \cdot \frac{\partial u}{\partial t} + \frac{1}{R} \tag{7.9}$$

or

$$\frac{\partial}{\partial z}\left[\frac{k_z}{\gamma_w} \cdot \left(\frac{\partial u}{\partial z}\right)\right] = \frac{1}{M} \cdot \frac{\partial u}{\partial t} - \frac{1}{R} \tag{7.10}$$

Equation (7.10) is used to calculate the strain by means of the finite difference technique. To calculate the change in excess pore water pressure over time, equation (7.10) is rewritten as:

$$\frac{\partial u}{\partial t} = M \cdot \left[\frac{\partial}{\partial z}\left[\frac{k_z}{\gamma_w} \cdot \left(\frac{\partial u}{\partial z}\right)\right] + \frac{1}{R}\right] \tag{7.11}$$

The term $\left[\frac{\partial}{\partial z}\left[\frac{k_z}{\gamma_w}\cdot\left(\frac{\partial}{\partial z}\cdot u\right)\right]+\frac{1}{R}\right]$ must obviously be less than zero, in order to cause a decrease in the pore pressure. If not, it will be assumed that $\frac{\partial u}{\partial t}=0$. In other words, the creep strain rate $\dot{\varepsilon}_z^{cr}$ cannot be greater than the total strain rate, $\dot{\varepsilon}_z$.

Before solving equation (7.11), the variable R will be expressed in such way so the total time parameter, t, can be replaced by other terms as shows in the following equation:

$$R=-r_s\cdot t_r\cdot e^{r_s\cdot\varepsilon_{cr}}=-r_s\cdot t_r\cdot e^{r_s\left(\varepsilon_z+\frac{\Delta u}{M}\right)} \tag{7.12}$$

Equation (7.11) can now be written as:

$$\frac{\partial u}{\partial t}=M\cdot\left[\frac{\partial}{\partial z}\left[\frac{k_z}{\gamma_w}\cdot\left(\frac{\partial}{\partial z}\cdot u\right)\right]+\frac{1}{-r_s\cdot t_r\cdot e^{r_s\left(\varepsilon_z+\frac{\Delta u}{M}\right)}}\right] \tag{7.13}$$

Equation (7.13) can now be written in finite difference form.

In order to avoid stability problem concerning the selection of time step, the differential equation was solved by using the Crank-Nicholson finite difference method. A detailed description of the calculation model is given by Baker and Claesson (2003).

7.4 General description of the computer program

The features of the newly developed computer program will be discussed in general terms in this Section. It assumes one-dimensional consolidation and the input parameters can be varied with depth. The permeability also changes with strain and the change is described by the parameter β_k. The improved models for the

compression modulus and the time resistance number are, however, functions of the effective stress, which is described in greater detail in Section 7.5.

The load can be defined as two general cases for a distributed load, one with unlimited distribution and one with a given width. The load is restricted to one load increment, constant with time.

A ground water table and a hydrostatic distribution can be used to describe the pore pressure profile. It is also possible to define a hydrodynamic pore pressure profile.

With the present version of the computer program it is not possible to simulate internal drainage layers in the clay deposit. However, by combining two cases this will also be possible to simulate.

7.5 Parameter models

As mentioned before, one important object of this research project was to improve the model for describing the compression modulus and the creep parameter. The intention was to describe and model the natural behaviour of soft clay in a fairly simple but still relevant manner.

The compression modulus varies with the effective stress and the most interesting stress range for improving the model is for stresses close to the preconsolidation pressure. The time resistance number, r_s, and thus the coefficient of secondary consolidation, α_s, also vary significantly with the current level of effective stress. According to results from laboratory tests, r_s appears to describe the behaviour of natural clays as a bi-linear function of the effective stress in a more adequate way compared to α_s, see Section 7.5.2. The creep property is therefore defined by the time resistance number, r_s. A more comprehensive description of the results from verifying of the calculation model is given in Baker and Claesson (2003).

7.5.1 The compression modulus

The compression modulus, M=$d\sigma'/d\varepsilon$, is with great change around the σ_c' a function of the effective stress, where the preconsolidation pressure has a significant influence. According to Swedish practice, the compression moduli M_0 and M_L are each assumed to be constant for a given clay layer. For an effective stress that exceeds the σ'_L, the modulus is assumed to increase linearly with effective stress, see Figure 7.2.

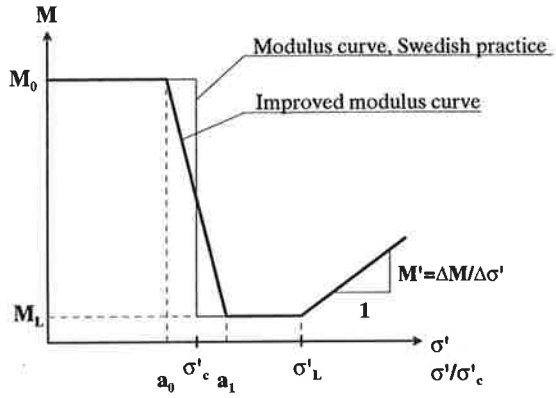

Figure 7.2 *Swedish practice for interpretation of the variation of the compression modulus from a CRS-test and the proposed model for the compression modulus. The factors a_0 and a_1 are given as values with respect to the normalised effective stress.*

In order to improve the description, a modification was proposed, which assumes that the modulus decreases linearly from M_0 to M_L in a stress interval around the preconsolidation pressure, see Figure 7.2.

The result of a linear change in the modulus over a given interval is that the stress – strain curve takes on a parabolic shape between a_0 and a_1, which may be a more relevant description of the behaviour of natural soft clay, see Figure 7.3.

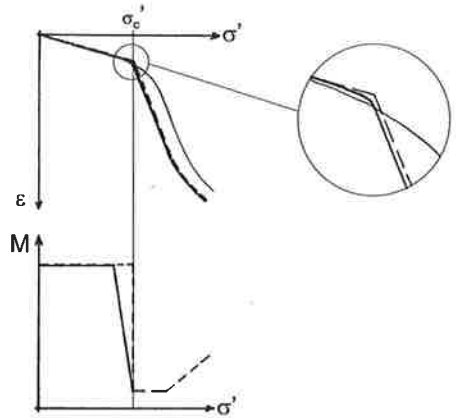

Figure 7.3 *Illustration of how M varies with σ' in the proposed model and the corresponding principal strain-curve compared to Swedish practice when the factors a_0 and a_1 are set to 0.8 and 1.0.*

The factors a_0 and a_1, which are part of the definition of the modulus curve, will be given as input data in the computer program.

7.5.2 The time resistance number, r_s

From the results obtained from incremental loading tests, it appears that the time resistance number, r_s, is a better linear approximation of the variation of the creep parameter than the coefficient of secondary compression, α_s. This is illustrated in Figure 7.4. As can be seen a linear interpretation of r_s, particularly in the stress range between say 0.7 and $1.0 \cdot \sigma'/\sigma'_c$, is more appropriate than that obtained from α_s from the same stress interval. Results from extensive tests also showed good agreement between simulated and measured time-strain curves when using r_s as the creep parameter, as will be presented in Chapter 8.

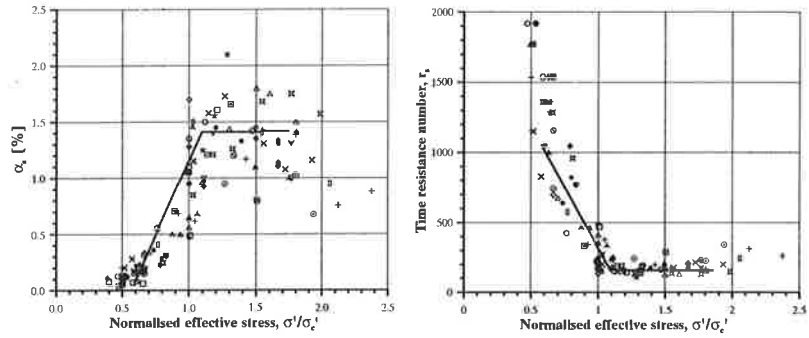

(a) (b)

Figure 7.4 *An example of linear interpretation of the creep parameters (a) α_s and (b) r_s from IL tests, results from the Änggården test site.*

In the proposed parameter model, the creep property is defined by the time resistance number parameters r_0, and r_1 and the factors b_0 and b_1, see Figure 7.5.

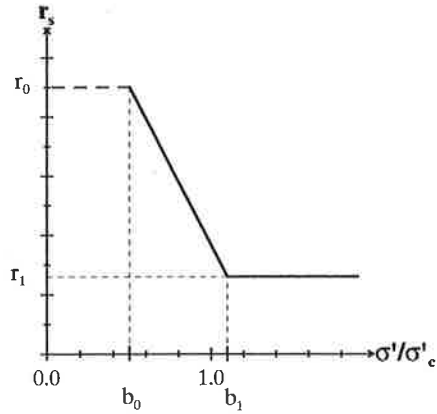

Figure 7.5 *Definition of the time resistance number model, including the factors b_0 and b_1 as a function of the normalised effective stress.*

A necessary parameter for defining the time resistance, R, see Figure 2.8, is the reference time, t_r, which governs the point of time, t_0, when creep will be involved in the consolidation simulation. A definition of t_r is given in

Figure 2.8. For full-scale computations, the influence of t_r appears to be of minor importance, due to the period of time, often 1-50 years. An appropriate value of t_r for full scale calculations seems to be -1 day. If t_r is allocated a value numerical less than -0.1 day, the consequence can be an unreasonably high rate of creep strain in the initial part of the consolidation process, due to the procedure for determining r_s.

When modelling incremental loading tests a recommended value for t_r is between -0.1 and -0.2 day in order to obtain an appropriate creep strain rate value, when the effective stress after dissipation of excess pore pressure is about $0.9 \cdot \sigma_c'$ or greater. When the current effective stress is less than $0.9 \cdot \sigma_c'$ a greater absolute value of t_r should be chosen due to the lower rate of creep strains or, in other words, the greater time resistance of the clay, which is in concordance with the Bjerrum model (1967) and Graham and Yin (1994). Examples of modelled IL test and the t_r value are given in Chapter 8.

Thus, when the input value of t_r is chosen for the model, it is important to take account of the history and starting point of the effective stress. This will be further discussed in Chapter 8.

7.6 Modelling of applied load

When modelling loads there are two different conditions that should be taken into consideration. First, the modelling of laboratory tests and second, the modelling of test sites. With respect to laboratory tests, such as incremental loading tests, the frictional forces between the specimen and the oedometer ring have to be considered, unlike full-scale modelling.

For oedometer tests with incremental loading, the loads are applied stepwise. The load increment ratio (LIR), $\Delta q_i/q_{i-1}$ was varied between 0.17 and 1.0. LIR equal to 1.0

is in accordance to the traditional Swedish IL tests procedure.

Berre and Iversen (1972) and Sällfors (1975) have studied the effect of friction between the clay sample and the oedometer ring during the test. The results obtained by Berre and Iversen (1972) measured a total frictional force of about 10% of the total applied load when the outer steel ring was lubricated with silicon grease. The tests were carried out with different height specimens.

Furthermore, Sällfors (1975) examined the frictional force by means of standard oedometer tests carried out with a stainless steel oedometer ring, the inside of which was lubricated with silicon grease. The height of the samples was 20 mm. The measured frictional loss was about 15 % of the applied load when the load was doubled for each load step.

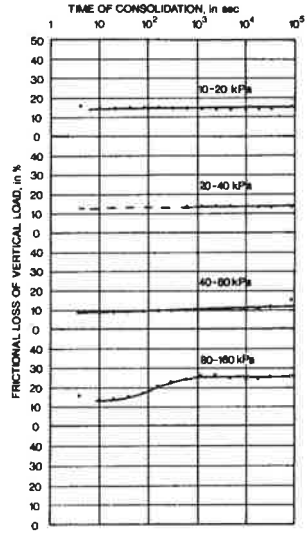

Figure 7.6 *Measured frictional force for a standard incremental loading test. Stainless steel oedometer ring lubricated with silicon grease (Sällfors, 1975).*

The average effective stress will thus be reduced by half the percentage mentioned above, assuming that the

frictional stress is distributed equally over the oedometer ring.

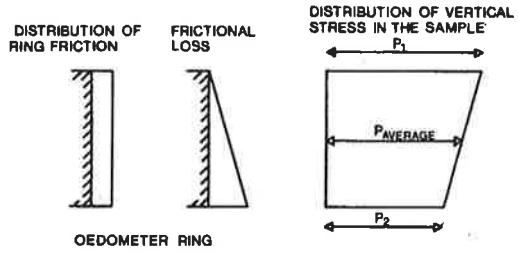

Figure 7.7 Assumed distribution of frictional loss in the oedometer ring (Sällfors, 1975).

Within this research project, the incremental loading tests, were conducted with a polished teflon oedometer ring, see section 4.2, which was lubricated with silicon grease on the inside in order to minimise the frictional loss. A 10 % reduction of the applied load increment was assumed for the calculation program input data, which is about the same range as the results described in the paragraphs above.

7.7 Discussion

By searching in the literature for the best, yet simple model for settlement calculation, including creep effects, a study of different models was conducted. The purpose of developing the computer code for settlement calculations presented in this thesis was to enable a prediction of settlements with a satisfactory degree of accuracy by means of a fairly simple rheological model (Alén, 1998). Furthermore, in order to facilitate future implementation of the model as a tool for practicing geotechnical engineers compression parameters in accordance with standard Swedish practice was used. The work also included a modification of the way of describing the governing parameters.

In order to obtain a more satisfactory description of the natural compression behaviour of clay, the models of compression modulus and the creep parameter have been improved.

A linear changeover from M_0 to M_L is suggested for the compression modulus to obtain an improved description of the compression model.

The evaluated results from creep tests (IL tests) indicate that, when r_s is given as a bi-linear function of the effective stress, r_s appears to provide an adequate description of the creep behaviour.

In the suggested model the preconsolidation pressure, σ_c', is independent of the strain rate. However, as described in previous chapters, this is a simplification. But the standard procedure of the CRS test and the subsequent interpretation procedure appear to provide an adequate value of σ_c' for in-situ conditions.

Results from conducted settlement calculations are presented in Chapter 8.

8. COMPARISON OF CALCULATED AND MEASURED SETTLEMENTS

8.1 Introduction

Settlement in soft clays, where creep plays an important role, is a very complicated process and the verification of a constitutive model and a computer code is a delicate task. As the number of parameters influencing the results for full-scale behaviour is large and the evaluation of parameter values is far from simple and unambiguous, the following procedure was chosen.

Results from a number of incremental loading tests in the laboratory and measurements of settlements at a handful of well-documented test sites have been compared with results from numerical calculations using the newly developed computer code. In addition, the modelling and calculations increased the understanding of the consolidation process and also illustrated how the different parameters affect the result. Moreover, the modelling of some of the parameters was studied more thoroughly, e.g. how the compression modulus and the time resistance number vary with the magnitude of the effective stress.

In the following Sections results from calculations using the newly developed computer code will be shown. The calculations were performed for a number of different loading sequences such as stress-level relative to the preconsolidation pressure, ratio of load increment and duration of load increments. Another important condition was analysed, one- and two-sided drainage conditions. The case of one-side drainage condition made it possible to study and compare the dissipation of the excess pore pressure, which is an important and decisive process. However, a particular condition to pay attention to when the laboratory tests were modelled, compared to modelling of full scale behaviour, was that the stress

situation in the specimen was not governed by the existing effective stresses caused by overlaying soil layers. In the laboratory tests, it was the previous load and prevailing excess pore pressure that governed the effective stresses and thus the initial conditions for the calculation.

The next step in the evaluation of the proposed model and computer code was to analyse full-scale behaviour. This was done for all the test sites described in Chapter 5, with exception of the Lundby Strand test site.

8.2 Modelling of incremental loading tests

This Section will present the results from modelling of IL tests and is divided into three parts with respect to the effective stress level in relation to the preconsolidation pressure. The reason is that in the three ranges of stresses, there are certain aspects that should be considered due to loading history for the clay sample because of previous load step and also due to rate effects.

There are some particular circumstances that have to be considered when modelling laboratory tests compared to full-scale modelling. The present computer program has not the feature to model several increments of loading or unloading, so it is necessary to evaluate the start parameters and condition for the present load step. It is also necessary to consider high strain rates close to the preconsolidation pressure.

The input data are in concordance with the evaluated parameter given in Chapter 5. The factors a_0, and a_1 were set to 0.9 and 1.1 respectively. These values are related to the high strain rate during the course of consolidation for laboratory tests and due to the method of evaluating the preconsolidation pressure. The creep factor b_0 and b_1 were set to values corresponding to the initial effective stress and to 1.1 respectively.

When modelling IL test the load increment is reduced by 10% due to frictional loss between the clay specimen and

the oedometer ring made of teflon. This is discussed in Chapter 7.6.

8.2.1. Modelling of stresses up to the preconsolidation pressure

When modelling incremental loading (IL) tests where load increments represent effective stresses up to the preconsolidation pressure, the choice of parameters is fairly uncomplicated and straightforward. The compression modulus is quite large and hence, small strains are obtained. The excess pore pressure dissipated after a short time, in about 1-2 hours, in case of one-sided drainage conditions in the laboratory test as well as for the model calculation.

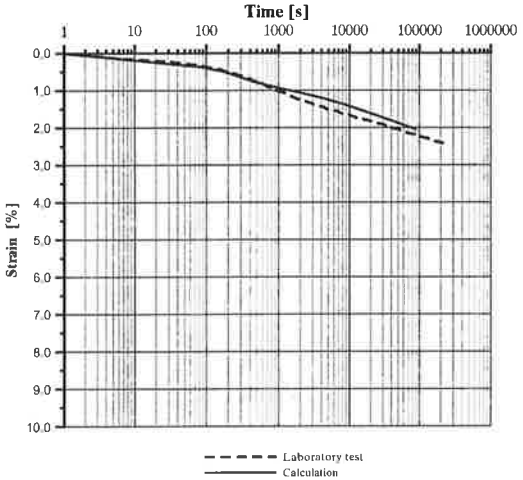

Figure 8.1 *The Änggården test site, CTH11-5 m (S21), applied load from 25 to 50 kPa and σ'_c=50 kPa. Results from the calculation and the laboratory test.*

When evaluating input values for the modulus M_0, it is necessary to consider the previous load step. The modulus of the sample had increased to some extent in relation to the corresponding $M_{0,CRS}$. The increase in the modulus is an effect of the stress level and creep strains occurred in the previous load step. In the calculations conducted, an input value of $M_0=2 \cdot M_{0,CRS}$, generally produced results

comparable to incremental loading tests. When the clay specimen was reconsolidated in the IL test, it was obvious that the existing modulus was even larger. Therefore, the selected input value of the modulus was about $4 \cdot M_{0,CRS}$.

Figure 8.1 and Figure 8.2 are examples of modelling of a load step for incremental loading tests under different conditions.

The test illustrated in Figure 8.1 was performed according to traditional IL test, with a clay sample from the Änggården test site, bore hole CTH11, depth 5 m. The input data is given in Section 8.3. The reference time, t_r, was set to -0.2 day.

The calculated stress - strain-curve is quite consistent with the stress - strain-curve obtained from the laboratory test.

The second example comes from the Lundby Strand test site and the sample was taken from a depth of 30 m. As was mentioned in Chapter 5, it was of particular interest to study the behaviour of clay from such deep layers as in the Lundby Strand test site. The specific condition in this test, was that the specimen was reconsolidated for an effective stress of 250 kPa, about $0.95 \cdot \sigma_c'$, and then unloaded to 185 kPa, before the load increment was applied, as illustrated in Figure 8.2. The reconsolidation of the specimen led to a value of $M_0 = 4 \cdot M_{0,CRS} = 30000$ kPa. The obtained results, both from the modelling and the laboratory test are shown in Figure 8.2.

From these two tests it can, first of all, be observed that with the chosen values of the parameters the agreement between results from the calculated time – strain relation and the laboratory test is very good. It is interesting to note the difference in time when the strains appear. For the clay specimen from the Änggården test the curve in the log-time – strain plot started to bend after about 300-400 s, while this occurred after about $3x10^4$- $4x10^4$ s for the clay sample from the Lundby Strand test site. The time difference was approximately a factor 100.

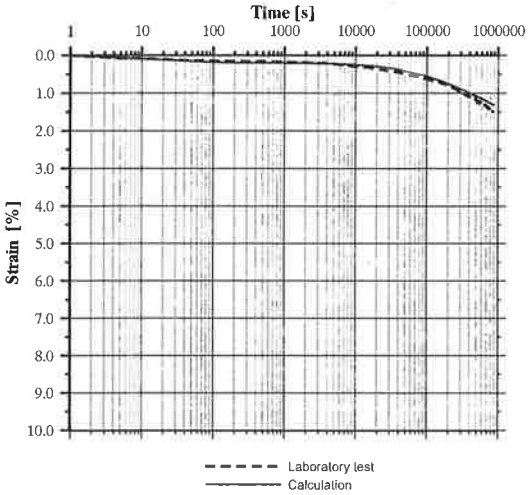

Figure 8.2 *The Lundby Strand test site, depth 30 m, load increment from 185 to 250 kPa and σ'_c=270 kPa. The result from the calculation and the result from the corresponding IL test.*

The differences in the two tests mainly depend on two conditions. Firstly, the Lundby Strand clay sample was reconsolidated and unloaded before the load step studied was applied. Secondly, the two samples had quite different compression modulus, 2500 and 30000 kPa respectively. It could also be observed that the duration of the applied load had to be more than a week to enable a fairly relevant interpretation of the time – settlement process for the Lundby Strand clay specimen.

Furthermore, it was important to consider that the rate of creep strain is much lower at stresses less than $0.95 \cdot \sigma'_c$, than for stresses in the normally consolidated range, in particular for a reconsolidated clay specimen. Hence the parameter reference time, t_r, in the model had to be adjusted to describe the prevailing conditions i.e. the very low creep strain rate. In the case of the Lundby Strand clay, the value of t_r was therefore set to –1.0 day.

8.2.2. Modelling in the stress range σ_c'-1.3$\cdot\sigma_c'$

Within the 1.0-1.3$\cdot\sigma_c'$ range of effective stresses, the input values of σ_c' and the modulus M_L affect the result and are thus of great importance. The calculations conducted demonstrate that the proposed parameter model for the compression modulus showed a very good agreement with the corresponding laboratory tests. A description of the proposed model is given in Figure 8.3

Clay samples taken from Änggården, bore hole CTH12, at a depth of 16 m were used as examples of modelling and calculation of incremental loading tests, in the range of effective stresses 1.0-1.3$\cdot\sigma_c'$. The evaluated parameter model of the compression modulus and the time resistance number, r_s, are given in Figure 8.3. The reason to the value of b_0 was set to 0.5 is due to the range of the stress interval for the present cases. The load increments from the laboratory tests are q=63→126 kPa, 70→140 kPa and 77→155 kPa respectively. The tests were conducted under one-sided drainage conditions, in which it was possible to measure the dissipation of the excess pore water pressure. Hence a better verification could be made of the calculated consolidation process.

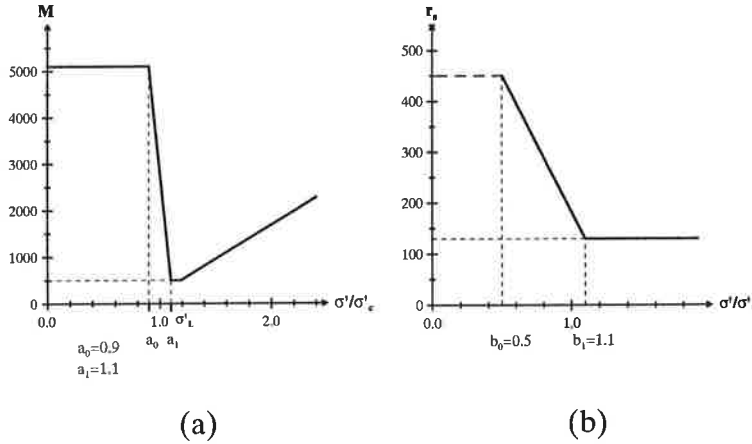

Figure 8.3 *Evaluated parameters for the modulus and the time resistance number for Änggården, CTH12-16m (S15).*

The results from the calculations and the obtained test results are presented in Figure 8.4. Also the excess pore pressures, both calculated and monitored, are given in the Figure 8.4.

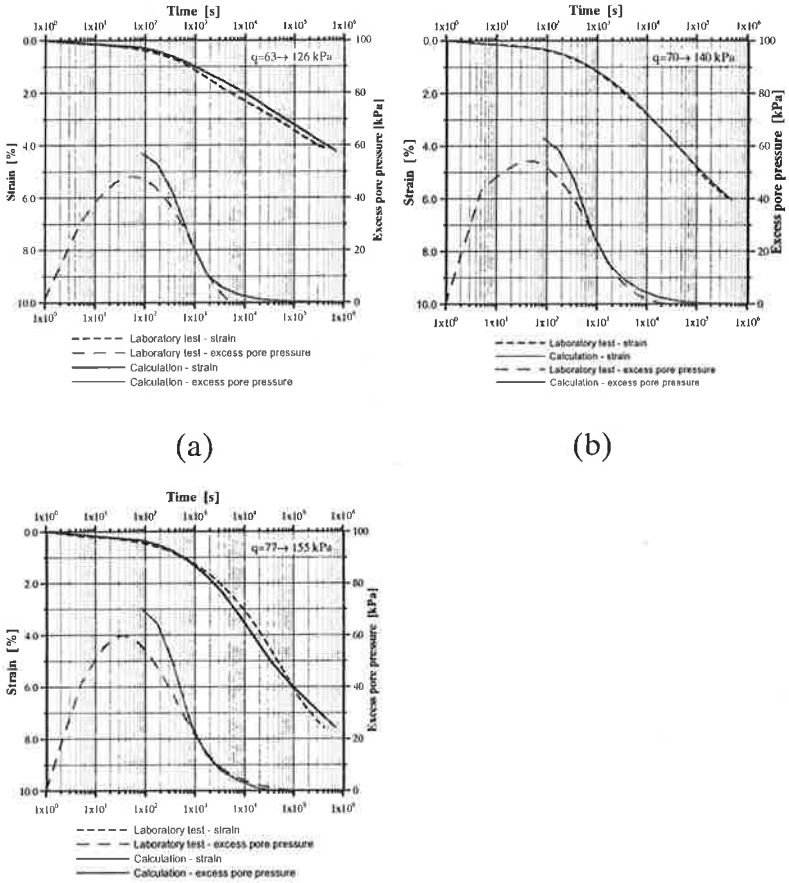

Figure 8.4 *Results from three different load cases conducted with clay specimens from a depth of 16 m. The total load for each load case corresponds to an effective stress, after EOP, of (a) $1.0 \cdot \sigma'_c$, (b) $1.15 \cdot \sigma'_c$ and (c) $1.3 \cdot \sigma'_c$. Änggården, CTH12-16m, σ'_c=122 kPa.*

As can be seen, the change in strain over time for the calculated and measured strains agrees very well.

For case (c) an interesting aspect of the behaviour of the clay appeared. At the point where the average effective stress for the clay was about 122 kPa, equal to $\sigma'_{c,CRS}$, the strain rate in the specimen was higher than the standard CRS-test strain rate (0.72 %/h). As pointed out in Chapter 4, the apparent preconsolidation pressure is dependent on the strain rate and thus the apparent preconsolidation pressure in this case should be higher than $\sigma'_{c,CRS}$.

In order to analyse the existing preconsolidation pressure, with regard to the strain rates in combination with the increasing effective stress, the effective stress–strain curve for load step 4 was plotted together with the result from the CRS-test with different strain rates, see Figure 8.5. The stress–strain curves agree fairly well for the tests when the different strain rates are taken into account. The starting point of the curve for the load step 4 in the diagram is adjusted in the y-direction with respect to the existing strain rate for the IL test, in relation to $\dot{\varepsilon}_{CRS}$, just before the load step 4 was applied.

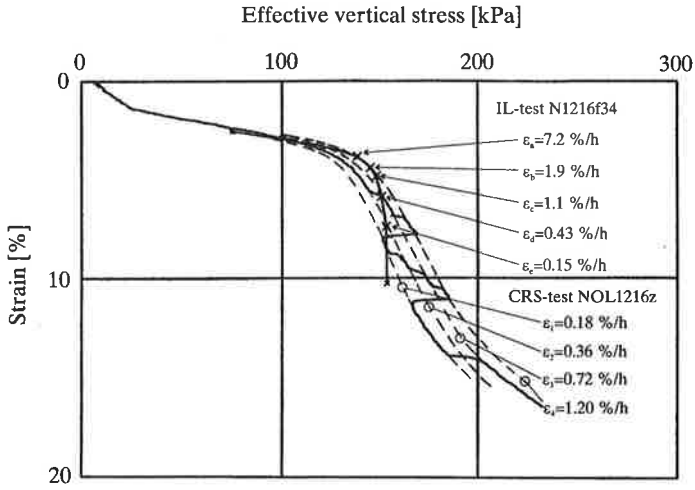

Figure 8.5 *IL test load step 4, q=77→155 kPa, the same load step as shown in Figure 7.4c, plotted with the result from CRS-test with different strain rates, Änggården, CTH12-16m.*

It is obvious that strain rate is an important factor to consider when modelling laboratory tests. It can be seen from Figure 8.5 that the stress-strain curve for the applied load bends off at about 145 kPa, which will correspond to the point $1.1 \cdot \sigma_c'$, in the parameter model for the compression modulus in the computer program, where the modulus change to M_L. Hence the interpreted value of the σ_c', considering the existing conditions, was assessed to 130 kPa. With this input, the modelling of the laboratory test gave fairly good agreement with the test result, as shown in Figure 8.4c.

In addition, it was of great interest to study the dissipation of the excess pore water pressure. This is a sensitive indicator of how well the model describes the consolidation process. The outcome of all these three cases was that the model gave calculated pore pressures that agreed very well with the measured excess pore pressure. However, a certain deviation was observed during approximately the first 400 s. This is related to the assumption in the model that the pore pressure build up is instantaneous at load application, whereas, in the tests it is a time-bound process. It can thus be noted from the monitoring of the excess pore pressure that there is a time lag in the system. This may be related to both the apparatus and the measuring system and also to the simplifications in the description of the parameters and the assumption of incompressibility of soil and pore water

Strain rate effects can be significant when modelling laboratory tests on small specimens and evaluation of parameters to be used in predictions of behaviour in full-scale field conditions. However, the low strain rates normally existing for field conditions are considered in the method of determining the preconsolidation pressure from CRS-test.

8.2.3. Modelling of stresses over $1.3 \cdot \sigma_c'$

In order to model IL tests with a total load corresponding to an effective stress after EOP of about $1.3 \cdot \sigma_c'$ or higher,

a particular consideration is the value of the preconsolidation pressure. As already mentioned, the value of σ_c' is a function of the strain rate. There is also another aspect that must be taken into account and that is the creep strains obtained during the previous load increment. A consequence of the creep strains is that the stiffness of the clay will increase. These effects are in accordance with the conceptual model proposed by Bjerrum (1967). Other researchers e.g. Berre and Iversen (1972) Sällfors (1975), Leroueil et al (1985), Graham et al (1983) and Länsivaara (1999) have also shown that σ'_c exhibit significant dependency on the strain rate and the history of stresses.

As an example of how the increased stiffness of clay affects the properties, an IL test with a load increment from 80 kPa to 120 kPa (Änggården bore hole 11, depth 7 m) will be used. Figure 8.6, presents the test with all the load steps.

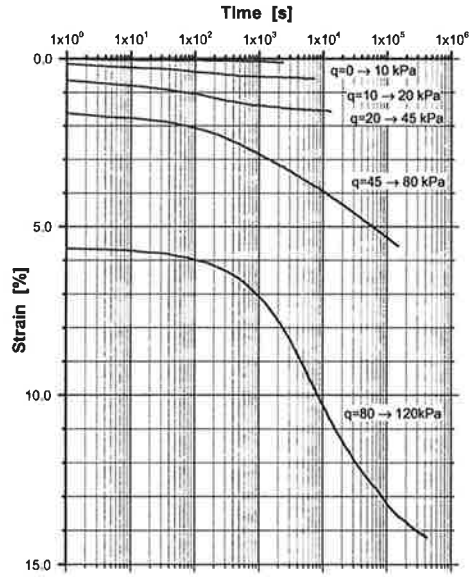

Figure 8.6 *Änggården CTH11-7 m (S20b). Incremental loading test with 5 load steps. The preconsolidation pressure interpreted from a CRS-test was about 68 kPa.*

For this IL test, the effective stress of load step 4 was larger than $\sigma'_{c,CRS}$, i.e. the effective stress is within the normally consolidated range. The apparent value of σ'_c after this step is larger than the applied 80 kPa, because of the creep strains, which occurred during the load increment. In order to evaluate the σ'_c at this state, the first step was to estimate the creep strain effects. In Figure 8.7 the stress-strain curve from the CRS-test CTH11-7m is plotted together with the evaluated stress-strain curves from the IL test presented in Figure 8.6. It was possible to plot the average effective stress change as a function of strain, as the pore pressure was measured at the undrained side of the specimen.

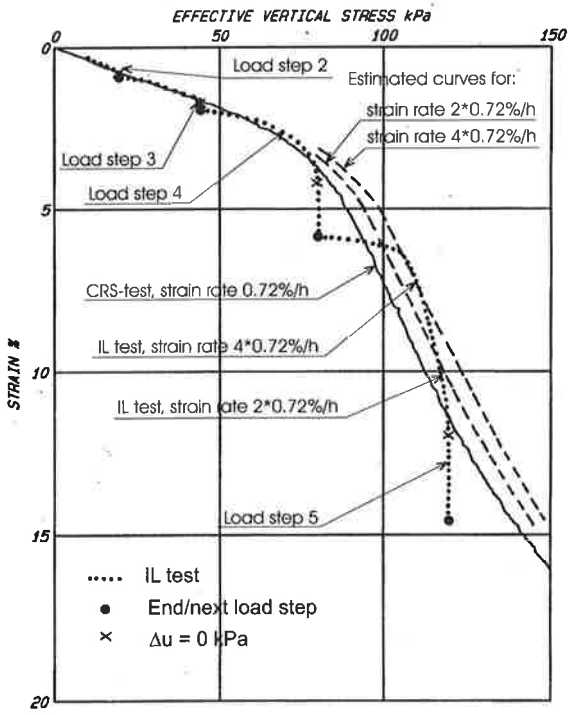

Figure 8.7 *Änggården 11-7 m, CRS-tests and stress – strain curves from the incremental loading test (S20b). In the diagram the estimated stress-strain curves are also plotted for the strain rates 1.4 %/h* $(2 \cdot \dot{\varepsilon}_{CRS})$ *and 2.8 %/h* $(4 \cdot \dot{\varepsilon}_{CRS})$ *with the assumption that a doubling of the strain rate will give an increase in* σ'_c *of about 5 %.*

As can been seen in Figure 8.7, the creep strain of load step 4 has a significant influence on the behaviour of the clay in the next load step. As a result, both the apparent σ_c' and modulus M_0, up to this pressure, increase.

The next condition to consider was the strain rate. Because of the relatively high strain rate in the initial part, greater than $\dot{\varepsilon}_{CRS}=2\cdot10^{-6}$ 1/s, in load step 5, the clay specimen exhibited an even higher value of σ_c'. The effective stress was about 104 kPa before the stress – strain curve started to bend off, i.e. exceeded the apparent σ_c' and the compression modulus changed to M_L. To model this load case with respect to the stress – strain behaviour the value of $a_1\cdot\sigma_c'$ was thus determined to 104 kPa. Assuming the parameter a_1 equal to 1.1, the input value of $\cdot\sigma_c'$ became 95 kPa.

As shown in Figure 8.8 the results of calculated strains and the dissipation of excess pore pressure are in quite good agreement with the result from the laboratory test. It is clear that an adjustment of σ_c' was necessary in relation to the existing strain rate and stress when the load was applied. In particular, the excess pore pressures clearly differ when the input data do not match the prevailing conditions, as illustrated in Figure 8.8.

Hence, when predicting settlements it is of great importance to evaluate the "apparent" σ'_c with respect to previous load history, strain and strain rate. In this particular case, σ_c' increased from the actual preconsolidation stress 80 to 95 kPa because of creep and rate effects. This change in σ_c' was of great importance for understanding the consolidation process.

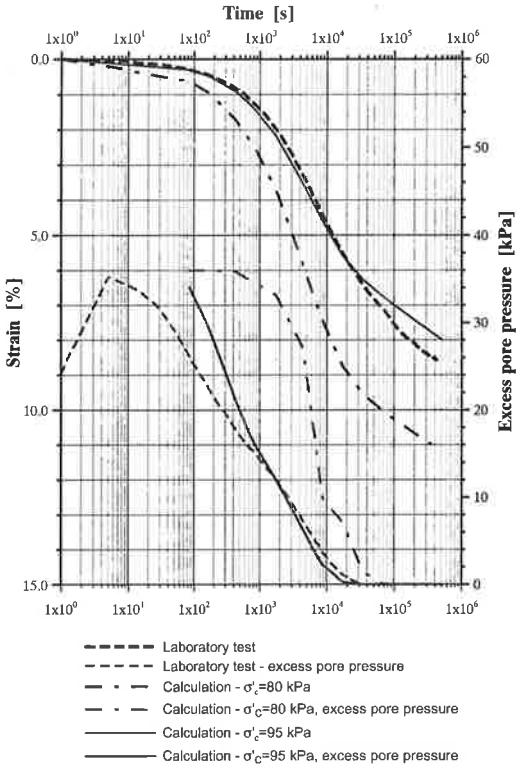

Figure 8.8 *The calculated strains and excess pore pressures, assuming σ'_c=80 and 95 kPa respectively, compared to the results from the laboratory test, Änggården CTH11-7 m, load step 5 with q=80 → 120 kPa.*

8.3 Settlement analysis for the different test sites

In the following Sections results from settlement calculations for the Änggården, Bratteröd, Hanhals and Lilla Mellösa test sites will be presented. The test site conditions were described in detail in Chapter 5. The purpose of this study is to verify the improved calculation method for full-scale behaviour of settlements including creep effects. Many models have been presented in the literature, which predict the stress-strain behaviour for laboratory tests, whereas case studies of full-scale behaviour are relative rare.

For the compression modulus model the factors a_0 and a_1 were set to 0.8 and 1.0 respectively. The factors b_0 and b_1 related to the time resistance number model were set to 0.70 and 1.1 respectively. The reference time, t_r, was in all calculations given the value –1.0 day.

8.3.1. The Änggården test site

At the Änggården test site settlement calculations were made in one section of the eastern part of the building where the largest settlements occurred, see Figure 8.9.

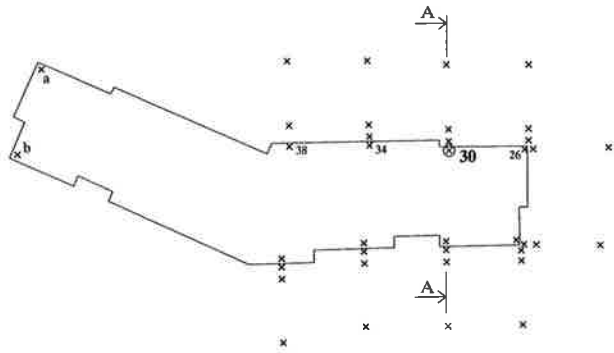

Figure 8.9 *Levelling point 30, in section A-A, of the Änggården test site where calculated and measured settlements are compared.*

The calculated settlements and the measured settlements were compared at levelling point 30, which is shown in Figure 8.9. In the section A-A, the natural clay layers were about 24 m deep and the height of the fill was estimated at about 0.6 m. There were thin layers of sand and silt in the clay deposits, as illustrated in section C-C, Figure 5.9.

The parameters were evaluated based on investigations at borehole CTH01. When evaluating the preconsolidation pressure, the conditions prior to construction were taken into consideration and the parameters used in the settlement calculations are given in Figure 8.10.

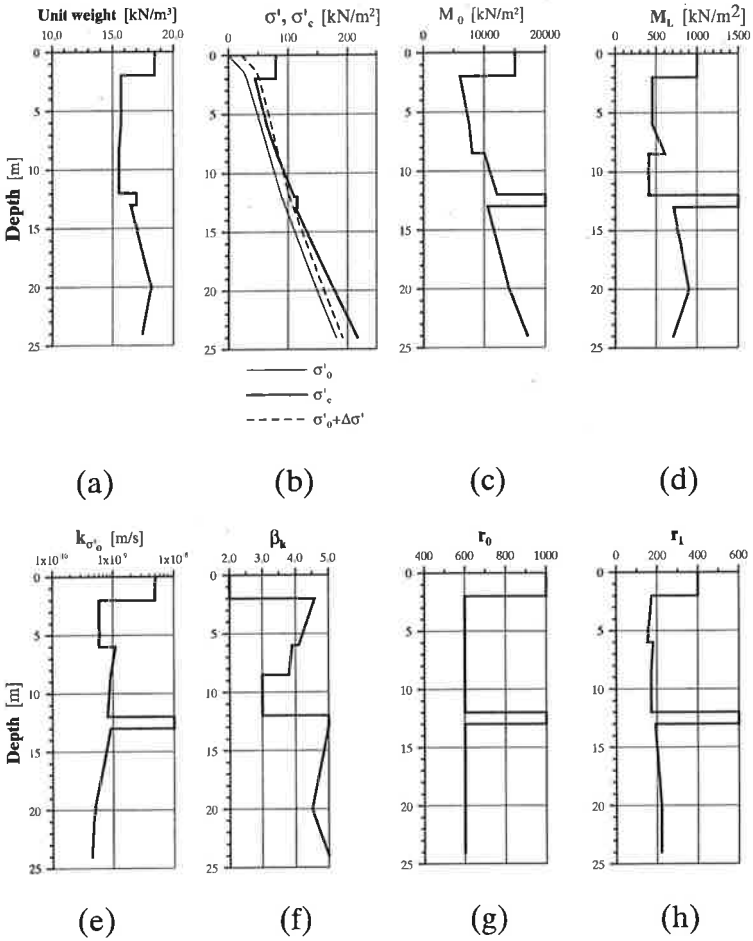

Figure 8.10 *Evaluated parameters for settlement calculations at the Änggården test site.*

The estimated pore pressure distribution corresponded to a hydrostatic pore pressure with a ground water table at a depth of 1.4 m below ground surface. Free drainage conditions were assumed at ground surface, in the sand layer at a depth of 12-13 m and at the bottom of the clay deposit.

The load was determined from the fill and the weight of the building. Because of the limited extension of the loaded area the increase in effective stress changed with depth, see Figure 8.10.

The initial overburden load was determined to about 24 kPa at the original ground level and decreased with time, due to settlement into the ground water. After about 6 years the load was estimated to be approximately 20 kPa.

In order to simulate a free drainage layer at a depth of 12 to 13 m below ground surface, the settlement calculations were made in two steps due to limitation in the present version of the computer program.

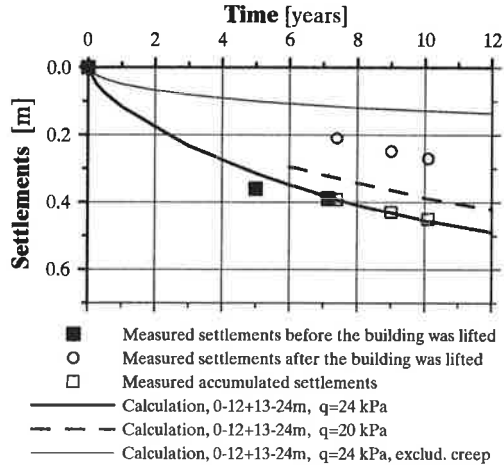

Figure 8.11 Calculated and measured settlements for levelling point 30 at the Änggården test site.

Figure 8.11 shows the calculated settlements over time together with the measured settlements. The calculated rate of settlement at the site is initially perhaps somewhat lower than the actual settlement rate. However, after 5-6 years the rates of the calculated and measured settlements agree very well. It should be noted that the occurred settlements during the first 5 years after completion are estimated.

8.3.2. The Bratteröd test site

The calculated settlements at the Bratteröd test site were compared to the settlements measured in two sections, 0/920 and 0/950, see Figure 8.12. The deposit of natural

clay is about 35 m deep in both sections. There were thin layers of sandy silt and/or shell deposits in the clay strata, which somewhat complicated the modelling of the soil profile.

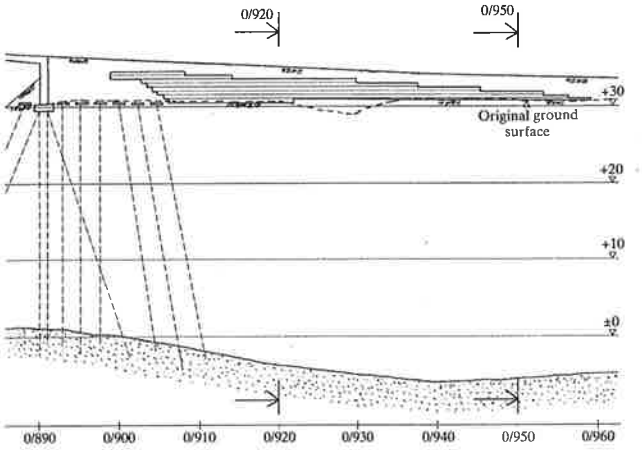

Figure 8.12 The two sections, 0/920 and 0/950, where settlement calculations were performed at the Bratteröd test site.

The OCR was another condition that was difficult to determine with great accuracy, due to the variation of the OCR in the area. In the north-western part (borehole CTH01) the interpreted OCR was on average about 1.25. Further east, at borehole CTH02, the OCR was between 1.5 and 2.5. Along the main road alignment, at boreholes 0/860 and 1/020, the evaluated OCR was approximately 1.7 at a depth of 5 m and generally decreased with depth to approximately 1.3 at the bottom of the profile. The applied value of OCR for the profile was according to boreholes 0/860 and 1/020, see Figure 5.27, which also means an average value of the OCR with respect to boreholes CTH01 and CTH02. The compression moduli also exhibited higher values than those normally found for soft clays in the region. The assumed compression moduli and the preconsolidation pressures are presented in Figure 8.13.

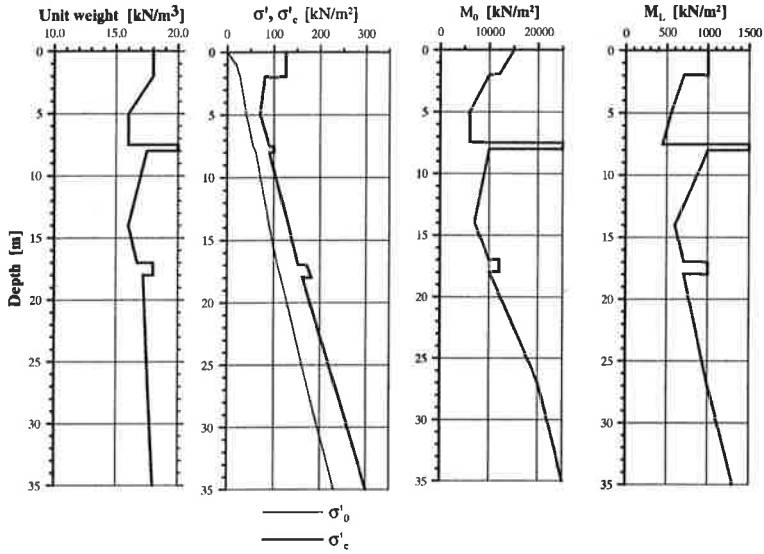

Figure 8.13 Evaluated values of unit weight, preconsolidation pressure and compression moduli for settlement calculation at section 0/920 and 0/950 of the Bratteröd test site. Note the layer of sand/silt at about 8 m depth.

The creep parameter of the clay at this test site was not investigated. However, the interpretation of the creep parameter was based on water content, bulk density, OCR and the compression modulus of the soil strata and then compared to the evaluated creep parameter for the Änggården, Hanhals and Lundby Strand test sites. Figure 8.14 shows the evaluated values of the time resistance number and a simple model was chosen. The reference time t_r was given the value –1.0 day.

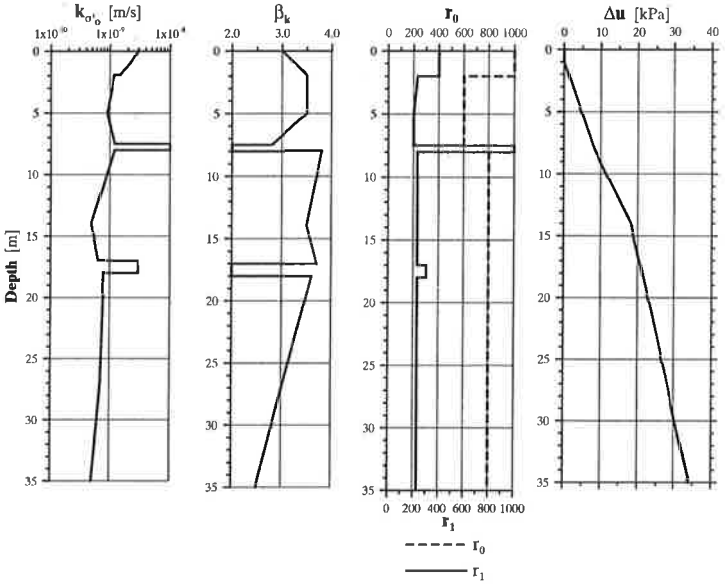

Figure 8.14 *Evaluated values of permeability (for in-situ stress), decrease in permeability with compression, time resistance number and excess pore pressure distribution compared to a hydrostatic pore pressure distribution for a ground water table 1.0 m below the ground surface, for the settlement calculations for section 0/920 and 0/950 at the Bratteröd test site.*

The interpreted ground water table was about 1.0 m below the ground surface. The measured pore pressure distribution was artesian, increasing with depth. In Figure 8.14d the pore pressure profile is shown as the excess pore pressure relative to a hydrostatic pore pressure distribution with a ground water table 1.0 m below the ground surface. Free drainage is assumed at the ground surface and at the bottom and also in the sand/silt layer at 7.5 m depth.

The soil profile for both studied sections were assumed to be identical. The significant difference in the two sections was the surcharge load. The loads from the road

the value of r_1 was changed ± 20 %. The obtained result revealed that the difference in the additional calculations was about 0.05 m over 18 years duration. Hence, under the given conditions, a moderate variation of the time resistance number had minor effect on the calculated settlements for the studied range of r_1.

Section 0/950: There is a fairly good agreement between calculated and measured settlements also for section 0/950, see Figure 8.18. After 18 years the calculated settlement is about 0.55–0.60 m, and there is only about 0.05 m discrepancy between the calculated and the measured settlement. The most significant difference between calculated and measured settlements is in the first 3-4 years. During this period of time the calculated settlement is about 0.1 m less than the measured values. A possible reason for the difference in settlement rate in the first part of the period is an underestimation in the simulation of the drainage conditions in the thin layers of sandy silt/shells deposits.

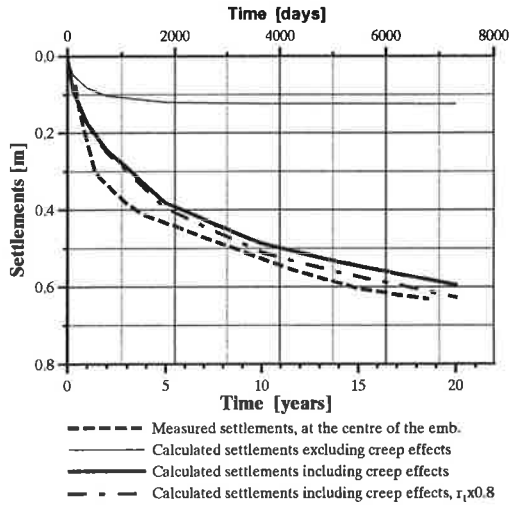

Figure 8.18 Calculated and measured settlements for section 0/950 at the Bratteröd test site.

Thereafter the rates of calculated and measured settlement are fairly similar. Also for this studied section,

a change in r_1 with ±20 %, had only a minor significant effect on the calculated settlements, see Figure 8.18.

When the creep effect was excluded, the total calculated settlement was about 0.15 m, see Figure 8.18.

The conclusion from the results obtained from the calculations is that the proposed parameter models seem to simulate the occurred settlements very well. The calculation results were also less sensitive for a moderate variation of the creep parameter than expected. Nevertheless, the creep effects appear to be most significant for the settlements. Also the thin layers of high permeable soil seem to have a great impact on the time-settlement curve, especially during the first 2-3 years after the load was applied.

8.3.3. The Hanhals test site

At the Hanhals test site two sections of the road embankment were studied. The two sections were chosen because of their different conditions in respect of the thickness of the soft clay layer and the size of overburden load.

The first section, 0/345, is situated south of the bridge where the natural clay deposit is about 11 m deep and the road embankment is 6 m high. Figure 8.19 shows a section of the embankment and the natural soil deposit. The second studied section is situated north of the bridge in section 0/453, where the layer of soft clay is considerably deeper, about 36 m, and the height of the road embankment is about 4.0 m, see Figure 8.19. The settlements of the embankments have been measured periodically since 1994-95. As settlement measurements were conducted on the road surface the deformations in the embankments were also included in the measured settlements. Also the deformation in the EPS fill should be considered. The estimated deformation in the EPS fill can be expected to 1.0-1.5 % of the height, which gives a settlement of about 0.03-0.07 m in the embankment.

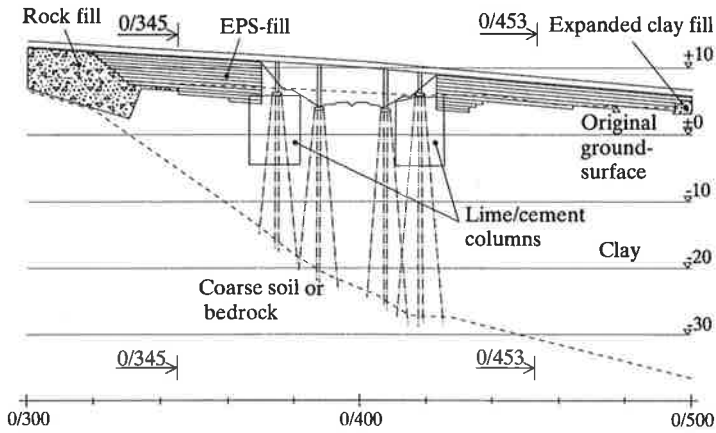

Figure 8.19 The Hanhals test site, sections 0/345 and 0/453 where settlement calculations were conducted.

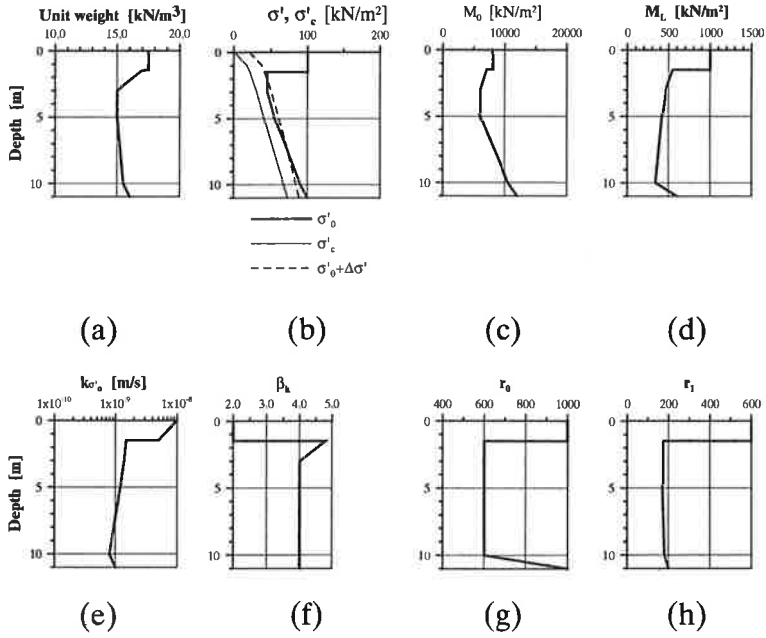

Figure 8.20 Evaluated parameters for settlement calculation in section 0/345 at the Hanhals test site.

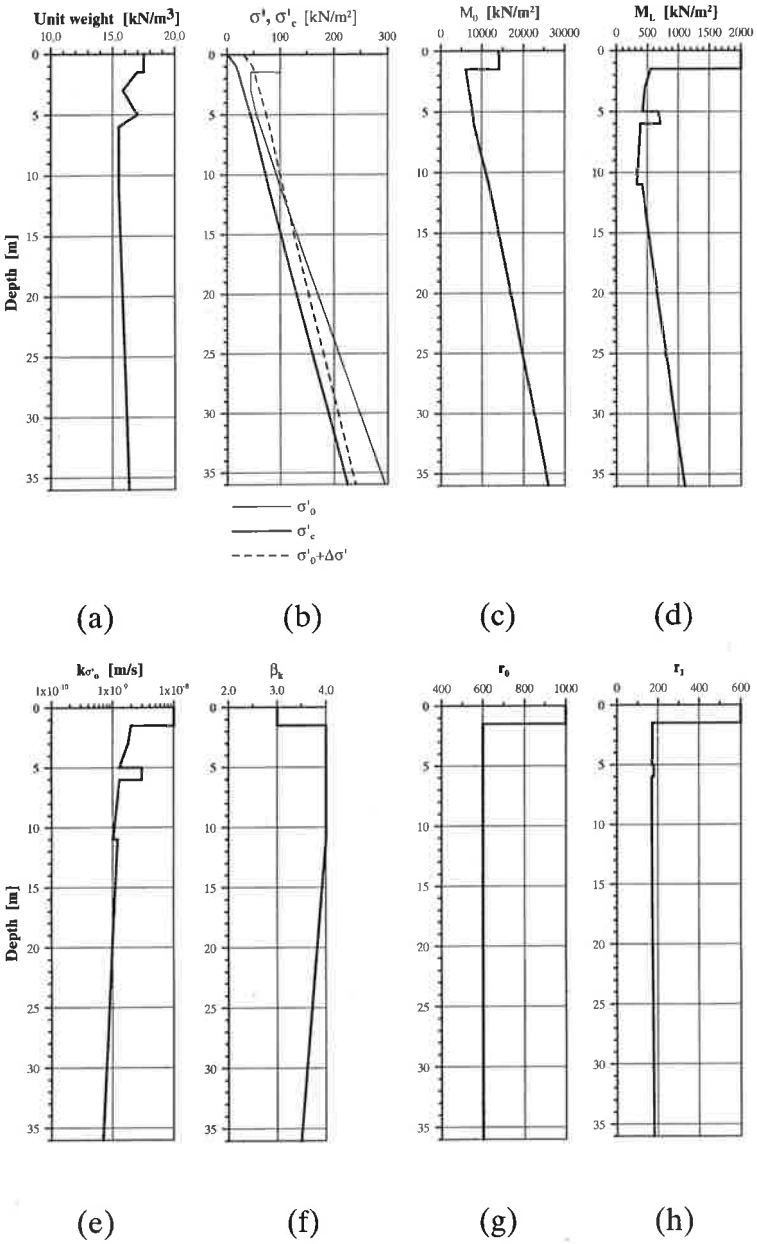

Figure 8.21 Evaluated parameters for settlement calculation in section 0/453 at the Hanhals test site.

In general, the parameters for the settlement calculation were determined from conducted investigations at

borehole CTHA1, but results from other investigations at the test site were also studied (Kjessler &Mannerstråle AB 1993, 1999). The evaluated soil parameters are presented in Figure 8.20. The reference time value was set to –1.0 day. The ground water table was assumed to be 1.0 m below the ground surface and with a hydrostatic pore pressure distribution. Free drainage was assumed at the ground surface and at the bottom of the soft clay deposit.

Section 0/345: The results from the calculations are presented in Figure 8.22. The calculated and measured settlements agree fairly well, about 0.20 m after about 7 years. The measured settlement rate was somewhat higher during the first two years. A corresponding difference was also obtained for section 0/453, see Figure 8.23, and a more comprehensive study was made of that section, which is described in the following paragraph. When creep effects were excluded in the calculation, less than half of the measured settlements were obtained.

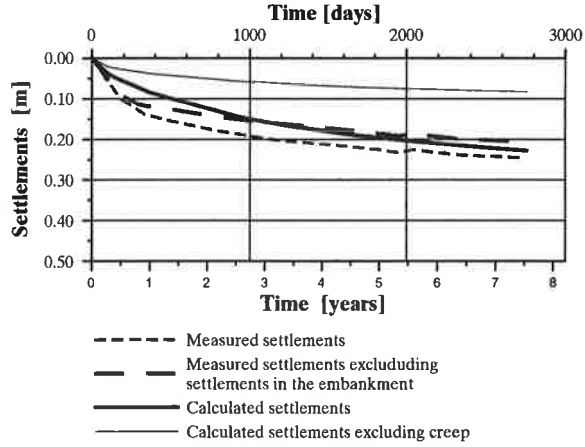

Figure 8.22 Calculated and measured settlements for section 0/345 at the Hanhals test site.

Section 0/453: In section 0/453 the measured settlements are larger than those in section 0/345 by almost 0.5 m, including settlements in the embankment fill. The result of the calculation seems to be in good agreement with the

measured settlements, which is shown in Figure 8.23. The settlement-time curve, excluding calculated settlements in the EPS-fill, is also plotted.

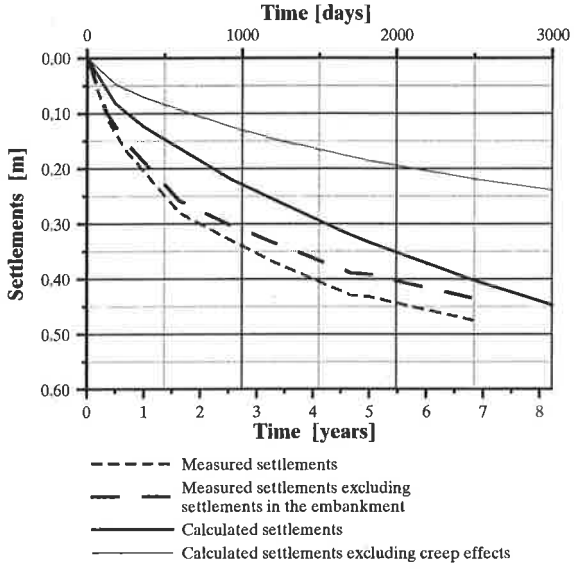

Figure 8.23 Calculated and measured settlements for section 0/453 at the Hanhals test site.

As illustrated in Figure 8.23 the measured settlement rate in this section is also higher than the calculated settlement rate for the first 2-3 years. After that there is a fairly good agreement between the calculated and measured settlement rate. One reason for the difference could be the presence of a thin layer with higher permeability and two-dimensional effects in terms of water flow. Unfortunately, no CPT test was carried out in the area of the road embankment. However, from the CPT test and the undisturbed sampling at borehole CTHA1 there is an indication of a layer of clay with shells at a depth of about 6 m depth.

A study was conducted on the effect of a assumed drainage layer on the course of settlement for the uppermost 5 m clay layer, with two-sided drainage conditions. Both one- and two-sided drainage conditions

were calculated for comparison, see Figure 8.24. The one-sided drainage condition corresponded to the uppermost 5 m of the soil profile in the ordinary calculation presented above. Figure 8.24 shows that the settlement rate is noticeably higher in the first two years for the two-sided drainage conditions was. A layer with greater horizontal permeability at a depth of 5 à 6 m could thus explain the higher settlement rate during the first two years.

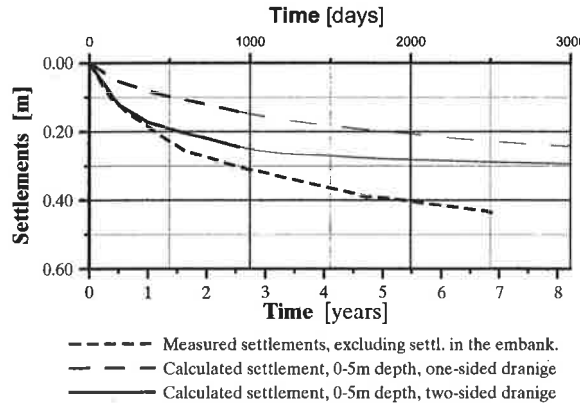

Figure 8.24 *Calculated settlement for the uppermost 5 m of the soil profile at section 0/453, with one- and two-sided drainage conditions respectively.*

In order to illustrate of how a layer with higher permeability might affect the time-settlement curve for the section, the difference between the calculated settlements for one- and two-sided drainage conditions were added to the first presented settlement calculation for the section (Figure 8.23). The result is presented in Figure 8.25. It is apparent that in this case such drainage layer increases the settlement rate, particularly during the first 1-2 years and results in better agreement with the observed settlements. However, the intention behind this particular study was not to adjust the calculated settlement to correspond to the measured values, but rather to illustrate the effects of a layer with higher permeability on the settlement rate.

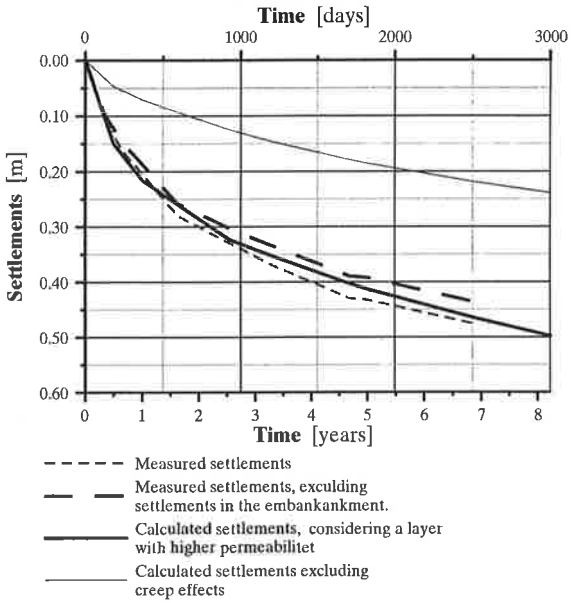

Figure 8.25 *The result of a calculation where a drainage layer was modelled at a depth of 5 m below the ground surface in section 0/453 at the Hanhals test site.*

The calculated settlements agree quite well with the measured settlements, especially in section 0/345 where the thickness of the layer of soft clay was limited. In both sections the predicted settlement rate was somewhat less than the measured settlement rate for the first 3-4 years. However, as shown above, one possible reason can be the existence of a layer (or layers) with relatively high permeability and with a significant horizontal water flow. A study of such conditions showed a calculated time-settlement curve that well matches the measured settlement, see Figure 8.25.

8.3.4. The Lilla Mellösa test site

The Lilla Mellösa test site (Chang 1981) is unique in terms of the long period of time during which occurred settlements and pore pressure distributions have been measured. Measurement began in 1945 and is still on-going, a total of 57 years so far. In this section both

calculated settlements and excess pore pressures are compared to measured data.

The parameters for the calculations presented in this section are the same as the parameters presented by Larsson (1986), see Figure 8.26. Only a minor change has been made for the permeability near the ground surface for the dry crust. The given value of permeability is assumed to be somewhat higher than the original data due to cracks and roots in the dry crust, which is common. Note that the natural clay was highly compressible, due to its high water content, of over 100 %, and organic content, especially in the uppermost 7 m of the clay profile. Hence the value of the compression modulus and the time resistance number are fairly low.

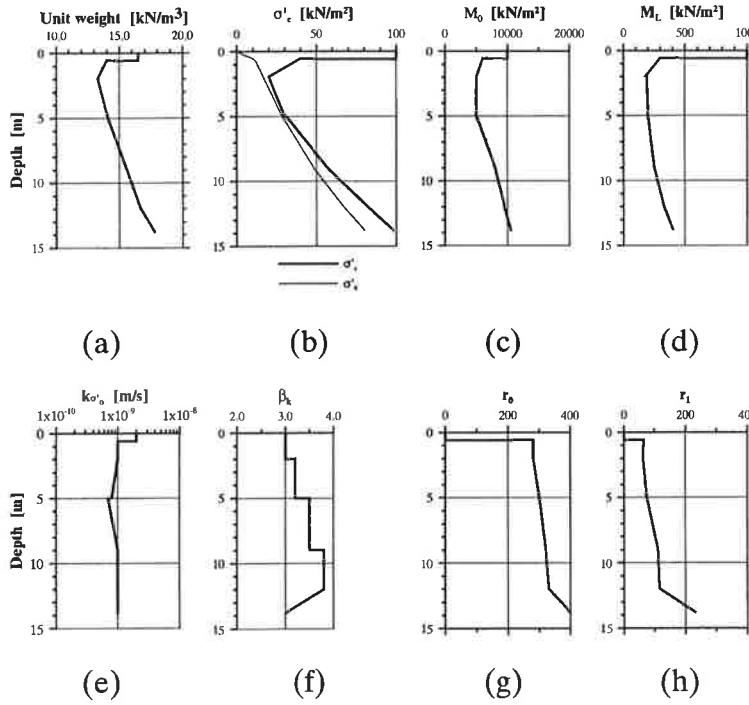

Figure 8.26 Parameters evaluated for settlement calculations.

For the model of compression modulus and time resistance number, the factors a_0, a_1, b_0 and b_1 were set at 0.8, 1.0, 0.70 and 1.1 respectively, i.e. the same values as

used for all the test sites. The reference time was set at –1.0 day.

The groundwater table was determined to 0.8 m below the ground level and the pore pressure distribution was hydrostatic with depth. The fill corresponded to an initial load of about 40 kPa. However, the load decreased over time due to hydraulic up-lift, when the fill settles beneath the groundwater table. According to Chang (1981) the overburden load was estimated to 27 kPa after 20 years, i.e. in 1965.

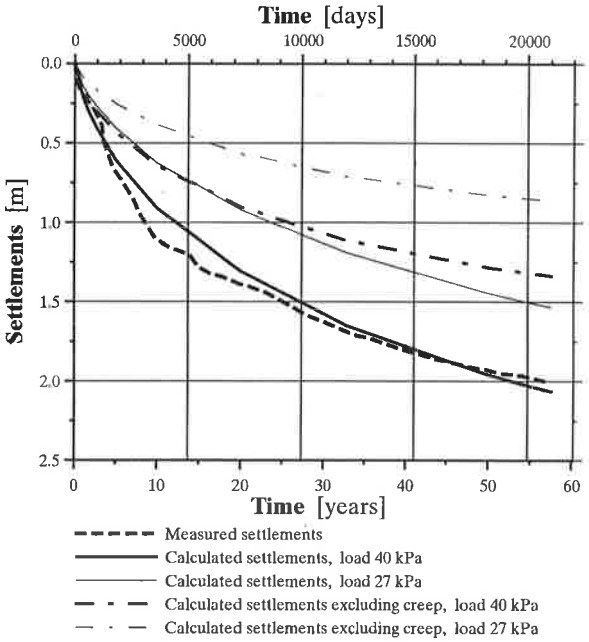

Figure 8.27 Measured and calculated settlements for the Lilla Mellösa test site.

In order to model the conditions with change of overburden load with time as accurately as possible, a simple modification was made. The calculation was divided in two parts. First, the settlement and excess pore pressure were calculated for a load of 40 kPa, which corresponded to the initial conditions. The results are presented in Figure 8.27 and Figure 8.28. The calculated settlements agree remarkably well with the measured

settlements considering the long period of time and the highly compressible clay.

The second step was to calculate the settlement and the excess pore pressure with a load of 27 kPa, the estimated load after 20 years (Chang 1981), in order to obtain conditions, which take the decrease in the overburden load over time into account. The results are shown in Figure 8.27 to Figure 8.29.

From the two calculations a simple construction of the time-settlement curve was made by using the calculated settlement for 40 kPa over a period of 20 years, and then link it to the 27 kPa settlement curve for the time from 20 to 57 years, see Figure 8.28. The resulting time – settlement curve then agrees notably well with the measured settlement rate. After 57 years, the difference in the settlement is less than 0.05 m for a total settlement of about 2.0 m.

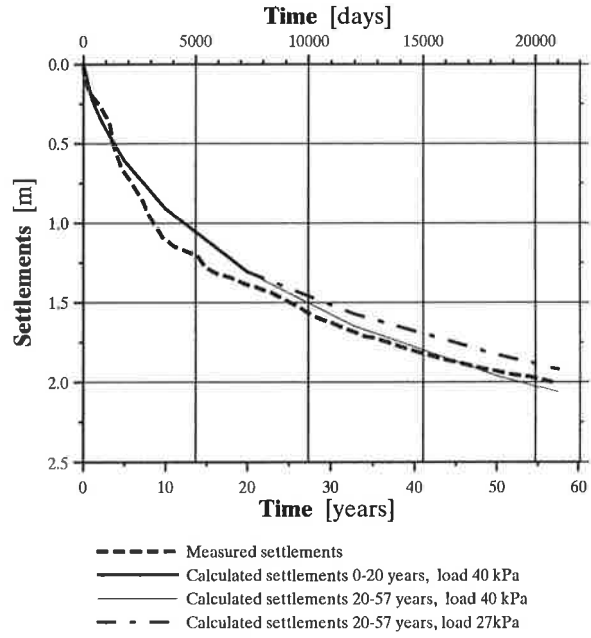

Figure 8.28 *Settlement curve based on settlement calculations with the 40 and 27 kPa loads for the Lilla Mellösa test site.*

In order to study the influence of creep effects, calculations were conducted excluding creep effects. The obtained settlements were about half of the calculated settlements which included creep effects, see Figure 8.27.

The obtained results from the settlement calculations agree well with what Larsson (1986) found.

A study of calculated and measured excess pore pressure was also performed. Figure 8.29 shows the results after 21, 32 and 57 years. Due to the decrease in the effective overburden load with time, the excess pore pressure was calculated at 21 years for both 40 and 27 kPa loads for the purpose of comparison as described earlier. At 57 years, a calculation for an estimated effective load of 20 kPa was carried out, taking further settlement into account. The simulated and measured excess pore pressures show fairly good agreement. The results are surprisingly good in view of the given conditions.

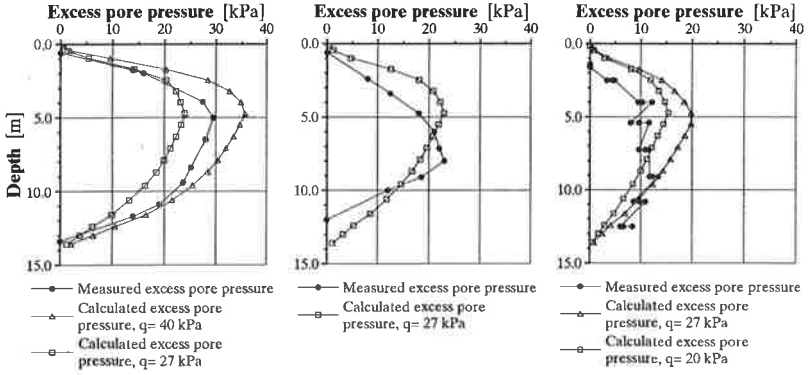

(a) after 21 years (b) after 32 years (c) after 57 years

Figure 8.29 Measured and calculated excess pore pressure at 21, 32 and 57 years at the Lilla Mellösa test site.

8.4 Discussion

For simulation of IL tests with the newly developed computer code the results of calculated and measured strains and pore pressures agree very well, for a variety of

drainage conditions, load ratio or stress level in respect to the preconsolidation pressure. However, it is essential to consider the loading history of the clay specimens and the strain rate when estimating the preconsolidation pressure for the present conditions. Berre and Iversen (1972) reported corresponding observations This is of critical importance when simulating load steps, with initially comparatively high strain rates, resulting in stress – strain relations that are partly to the right of the normal oedometer curve, i.e. higher effective stress at corresponding strains.

Moreover, the calculations indicate that the use of the creep parameter time resistance number simulated the creep behaviour well. The proposed models for time resistance number and for the compression modulus also appear to provide a good simulation of the time-strain behaviour. A study of the result calculations conducted on the modelling of IL tests showed that when the factors a_0 and a_1 , related to the modulus model, were set to 0.9 and 1.1 respectively, the calculated strain curves were often in very good agreement with strain curves obtained from laboratory tests. Modelling was made for different stress levels, load increment ratios (LIR) and clay specimens taken from different depths.

In addition, the modulus M_0, determined from CRS-test, had to be modified considering stiffening effects in the clay caused by creep effects during the previous load step in incrementally loaded tests. A suitable M_0 value for modelling an IL test appeared to be $2 \cdot M_{0,crs}$.

However, the situation changed when the specimens were "reconsolidated". In these cases the clay had been recompressed for stress situation fairly close to assumed in-situ conditions. As a consequence the input value for the M_0 modulus should be modified to about $4 \cdot M_{0,crs}$. This can be attributed to disturbance effects when taking the sample and the stress relief.

In order to model full-scale conditions the factors a_0 and a_1 were set at 0.8 and 1.0 respectively. The reason for the

lower values is that, during the consolidation process, strain rates are considerably lower in field conditions compared to laboratory conditions.

When modelling full-scale conditions, an assumption of M_0 equal to about $4 \cdot M_{0,crs}$ seems to give relevant calculated settlements.

In the creep model, the value of the factor b_1, set to 1.1 appears to adequately describe the creep behaviour when modelling both IL tests and full-scale conditions. The factor b_0 input value should be chosen corresponding to the present value of σ'_0.

The soil models used in the full-scale calculations are always a simplification of real site conditions. One of the most important consolidation parameters, with the exception of the preconsolidation pressure, is the permeability. Unfortunately, permeability is perhaps the parameter showing the greatest scatter. Furthermore, the computer model assumes one-dimensional water flow, which at some occasions can be a very rough simplification, particularly when a drainage layer exists in the clay profile.

The most significant result of the calculations performed was the great influence of creep on the calculated settlement as earlier illustrated by several researchers. The contribution of creep effects to settlements could be equal to or larger than calculated settlement without considering the creep effects. Creep could, under certain conditions, be a major cause of settlement. An example of such conditions is the studied sections at the Bratteröd test site. In particular, section 0/920 provides conditions with effective stresses up to about the preconsolidation pressure. This implies that the compression modulus value was relatively large, which results in small consolidation settlements, whereas the time resistance number close to the minimum value, r_1, results in large creep effects. These conditions, combined with a deep layer of soft clay of about 36 m, were the probable reasons for the very large

creep settlement in relation to the calculated settlements excluding creep effects.

A study of the sensitivity of the parameter r_s was conducted for sections 0/920 and 0/950 at the Bratteröd test site. One reason for the study was that the creep properties at the Bratteröd test site were not explicitly determined. When the value of r_1 was changed ±20 % of the determined value, the calculated total settlement after 18 years altered by less than 10 % for both of the studied sections.

Furthermore, it could be observed that a thin layer of highly permeable soil has a great influence on the settlement rate, particularly in the early part of the consolidation process. This effect was obvious at the Bratteröd test site

Some general comments concerning settlement calculations will be given. When carrying out settlement calculations for a soil profile consisting of deep layers of soft clay, at depths in excess of 20-25 m, and with a wide load, minor changes in the parameters could cause differences in the calculated settlements. Hence, in order to make a reliable assessment of the predicted settlements, it is of great importance to study how a moderate variation in the input parameters affects the calculated settlements, normally with focus on the preconsolidation pressure, σ_c'; permeability, k; compression modulus, M_L; and the time resistance number, r_s.

9. CONCLUSIONS AND PRACTICAL ASPECTS

The conclusions drawn from this work have resulted in an improvement and understanding of the methods of modelling soil compressibility and settlement calculation and a new computer code employing this results. The purpose of the research was to extend the empirical base and to increase the understanding of the compression behaviour of clays due to creep. For the most part, the conclusions are presented in the order in which the work was carried out. In the concluding section some practical aspects of settlement calculations have been noted.

9.1 The creep parameter

Based on the performance and analysis of incremental loading (IL) tests, this study has substantially extended the empirical base for the creep behaviour of soft clays as well as established that the creep behaviour of clay layers at large depths, from around 25 to 70 m below the ground surface, is similar to that of clays from depths of 20 m and above. This provides essential knowledge for the accurate prediction of settlements, particularly in areas where the clay profile involves deep deposits of soft, lightly overconsolidated clays.

The value of the interpreted creep parameter, α_s or r_s, determined by means of IL tests appears to be independent of the load increment ratio (LIR) in the investigated range of 0.3 to 1.0. However, it is often necessary to prolong the duration of each load step for LIR < 1.0, as otherwise there is a risk of miss interpreting the creep parameter. From a practical point of view a reduction of the LIR from the common standard ratio of 1.0, means that the creep parameter can be determined two or three times in the stress interval of 0.8 – $1.3 \cdot \sigma'_c$ during a series of load steps in a test.

9.2 The relationship between effective stress, strain and strain rate

The study has emphasised that the stress - strain behaviour is governed by the effective stress, strain and strain rate $(\sigma' - \varepsilon - \dot{\varepsilon})$, which confirms that there is a unique relationship between these parameters for one-dimensional consolidation.

A consequence of the unique relationship is, for example, that the stress – strain curve is dependent on the strain rate. By changing the strain rate during CRS tests this characteristic has been clearly demonstrated. The conducted tests have shown that a doubling of the strain rate, compared to the standard rate, led to an increase of about 4-6 % in the apparent preconsolidation pressure. The corresponding pattern was obtained for a decrease in the strain rate.

Another condition that affects the stress – strain behaviour is the temperature. However, the temperature is almost constant in natural clay deposits and will therefore have little bearing on the behaviour in the field. In this project, the temperature during laboratory testing has been kept constant at +8°C. However, the usual test conditions in commercial geotechnical laboratories are about +20°C, which to a limited extent will influence the interpretation of the test result.

9.3 A model for settlement calculations

The extensive work of analysing results from laboratory tests conducted under varying conditions has contributed to the understanding of the compressibility behaviour of clays. The aim of this study was to further develop the calculation model proposed by Alén (1998) for one–dimensional consolidation. The model is able to predict the stress–strain behaviour and the excess pore pressure dissipation with respect to time for both IL tests and full-scale modelling with satisfactory degree of accuracy.

The first step was to verify the model excluding creep effects. The second step was to improve the parameter models and to verify the calculation model by the modelling of IL tests, conducted under very well defined conditions.

The model of the compression modulus was improved by a gradual change of the modulus from M_0 to M_L. In this way the calculated results will hence be less abruptly affected by moderate variations of the applied load when the final effective stress is close to the preconsolidation pressure.

Furthermore, it has been concluded that if the creep parameter time resistance number, r_s, is expressed as a bi-linear function of the effective stress, the creep property of soft clays is adequately described.

The next step was to compare the results from full-scale settlement calculations with measured settlements from a number of case records.

The calculation model has thus been tested both under laboratory conditions (IL tests) and against a number of full-scale records under varying conditions. The used parameters are well known and are in accordance with Swedish practice. It can thus be concluded that the computer code with the suggested models for the compression modulus and time resistance number is a useful tool for describing the time – settlement behaviour under various conditions, including the dissipation of the excess pore pressure, with a satisfactory degree of accuracy.

9.4 Practical aspects

During this work the complexity of the compression behaviour of natural clays has become even more evident. The parameters σ'_c, M_L, k and r_s, all can have a great influence on the calculated settlements. Calculations of the settlement behaviour, including creep effects, requires

calculation with a computer program, including an advanced numerical method. The consolidation process is too complicated to be solved with reliable result using a simple model and a hand calculator.

The description of the clay characteristics by means of models is always a simplification of the natural conditions. Moreover, the properties of the soil layers vary, not only with depth but also horizontally. In particular, the permeability, k, can exhibit a great variation. Furthermore, the horizontal permeability often significantly deviates from the vertical permeability, which can greatly affect the field behaviour.

The presence of layers with high permeability in a clay profile can obviously influence the settlement behaviour of the clay profile. Therefore, it is of vital importance to identify existing layers with high permeability in the clay at geotechnical site investigations, in order to enable accurate settlement predictions.

A basic requirement is that geotechnical investigations are conducted with great care and sufficient extent in order to create an acceptable base for relevant evaluations and predictions of the clay behaviour.

In many cases, the results from both settlement observations in the field and of the modelling of full-scale conditions showed very large settlements due to creep effects compared to calculated settlements excluding creep.

A useful and fairly simple, but often forgotten method to be aware of the margin of errors is to complement with calculations in which each essential parameter is varied in order to observe how it affects the result. This should provide a sound base for the geotechnical engineer to arrive at a more reliable decision, when dealing with the natural variations in the clay layers, in the field.

Finally, nature always has a more or less significant three-dimensional natural variation. This should be considered

in the light of the fact that compression parameters are often interpreted based on one-dimensional conditions and that settlements are normally calculated from a one-dimensional consolidation theory. It is important to keep these facts in mind when evaluating results of settlement calculations.

10. FUTURE RESEARCH

As previously mentioned, the consolidation process is very complex. Comprehensive research has been carried out all over the world, and efforts are repeatedly being made, to improve the knowledge and understanding of the compressibility of soft clays.

The present thesis is a contribution to the understanding of the compression behaviour of deep deposits of soft, lightly overconsolidated clay, although the key to this behaviour still remains to be found. The task of describing the physical model is an even greater challenge.

One step towards the further improvement of the proposed calculation model could be a study of the model of preconsolidation pressure, σ_c'. Today σ_c' is often treated as a constant independent of the strain rate. However, it has been shown that σ_c' dependent on the strain rate. To develop the σ_c' model in which σ_c' is a function of strain rate will almost certainly improve the modelling of IL tests, due to the relatively high strain rates, particularly in the initial phase of each load step. However, although the effect is not as obvious with full-scale modelling, it will probably lead to a refinement of the results also here.

For determination of the creep parameter on a more frequent or regular basis in relevant projects, an important research area would also be to develop a more convenient procedure for determining the creep parameter. It would be preferable to make use of existing laboratory equipment, such as CRS oedometer. For this purpose it would be appropriate to establish a procedure by which the results obtained in a modified CRS test procedure are used to determine the creep properties.

Finally, it would be desirable to develop a tool to assist geotechnical engineers in making rough estimates to determine whether or not more extensive settlement calculations due to creep effects are to be expected.

REFERENCES

Alén, C. (1998). On probability in geotechnics. Volume 1, 2, Ph.D. Thesis, Department of Geotechnical Engineering, Chalmers University of Technology, Göteborg.

Alte, B., Olsson, T., Sällfors, G., & Bergsten, H. (1989). Djupdykning i Göteborgsleran, Bo Alte AB & Chalmers tekniska högskola, Report Göteborg.

Andersson, H., & Åhnberg, H. (1996). Settlements of lightweight road embankments. *XII Nordiska Geoteknikermötet*, Reykjavik, pp. 347-352.

Baker, S., & Claesson, P. (2003). Internal report - A computer program for settlements calculations including creep effects, Dep. of Geotechnical Engineering, Chalmers University of Technology, Göteborg.

Bengtsson, P. E., & Larsson, R. (1994). Användarhandbok Program Embankco, version 1.02, Statens Geotekniska Institut och Vägverket, Linköping.

Bergsten, H. (1989). Stratigraphy of a late weichselian-holocene clay sequence at Göteborg, south-west Sweden, Ph.D. Thesis, Department of Geologi, University of Göteborg and Chalmers University of Technologi, Göteborg.

Berre, T., & Iversen, K. (1972). Oedometer tests with different specimen heights on a clay exhibiting large secondary compression *Géotechnique* Vol. 22, No. 1, pp. 53-70.

Bjerrum, L. (1967). Engineering geology of Norwegian normally- consolidated marine clays as related to settlements of buildings, The 7th Rankine Lecture *Géotechnique* Vol. 17, No. 2, pp. 81-118.

Bjerrum, L. (1972). Embankments on soft ground. *Performance of earth and earth-supported structures*, Purdue University, Lafayette, Indiana, pp. 1-46.

Boudali, M., Leroueil, S., & Murthy, B. R. S. (1994). Viscous behaviour of natural soft clays. *Proc. 13th ICSMFE*, New Delhi, pp. 411-416.

Brinkgreve, R. B. J., & Vermeer P.A. (1998). Soft-Soil-Creep model. Plaxis, Material Models Manual, Rhoon, A.A. Balkema, Rotterdam, pp. 5-1 - 5-14

Buisman, A. S. K. (1936). Results of long duration settlement tests. *Proc. 1st Int. Conf. on Soil Mechanics and Foundation Engineering*, Cambridge, Massachusetts, pp. 103-106.

Casagrande, A. (1936). The determination of the Preconsolidation Load and its Practical Significance. *Proc. 1st Int. Conf. on Soil Mechanics and Foundation Engineering*, Cambridge, Massachusetts.

Chang, Y. C. E. (1981). Long term consolidation beneath the test fills at Väsby, Sweden, SGI, Report Linköping,.

Claesson, P. (2003). Internal report - The Änggården Test Site, Dep. of Geotechnical Engineering, Chalmers University of Technology, Göteborg.

Ekström, J. (2002). Personal communication - Measured settlements at Hanhals test site, Claesson, P, Göteborg.

Emdal, A. (2000). Computational Geotechnics - Plaxis, Soft Soil Creep model, NTNU, Trondheim.

Fredén, C. (1994). Berg och jord, Bra Böcker, Höganäs.

GF Konsult AB (1997). Nol, Änggården Förskola, Sättningsskador, Geoteknisk utredning, Report 655 02323, Göteborg.

Graham, J., Crooks, J. H. A & Bell, A. L. (1983). Time effects on the stress-strain behaviour of natural soft clays *Géotechnique* Vol. 33, No. 3, pp. 327-340.

Jacobson & Widmark AB, Geosenior Bo Alte & Chalmers tekniska högskola (2001). Lindholmen / Lundby Strand, Norra Älvstranden, Rapport Rgeo, Göteborg.

Janbu, N. (1963). Soil compressibility as determined by oedometer and triaxial tests. *Proc. 3rd European Conf. Soil Mechanics*, Wisebaden, pp. 19-25.

Janbu, N. (1969). The resistance concept applied to deformations of soils. *The 7th Int. conference on soil*

mechanics and foundation engineering, Mexico, pp. 191-196.

Janbu, N. (1985). Soil models in offsore engineering, The 25th Rankine Lecture *Géotechnique* Vol. 35, No. 3, pp. 241-281.

Kabbaj, M., Tavenas, F., Leroueil, S. (1988). In situ and laboratory stress-strain relationships *Géotechnique* Vol. 38, No. 1, pp. 83 - 100.

Kim, Y. T. & Leroueil, S. (2001). Modelling the viscoplastic behaviour of clays during consolidation: application to Berthierville clay in booth laboratory and field conditions *Canadian Geotechnical Journal* Vol. 38, No. 3, pp. 484 - 497.

Kjessler & Mannerstråle AB (1993). Byggnadsteknisk beskrivning, geoteknik (BGEO), Väg 927/928, Report Göteborg.

Kjessler & Mannerstråle AB (1999). Väg 927/928 och bro N804 över Västkustbanan vid Hanhals, Rapport Geoteknisk undersökning (RGEO), Göteborg.

Larsson, R. (1981). Drained behaviour of Swedish clays, Swedish Geotechnical Institute, Report Linköping.

Larsson, R. (1986). Consolidation of soft soils, Swedish Geotechnical Institute, Report Linköping.

Larsson, R. (2002). Personal communication - Measured settlements and pore pressures at Lilla Mellösa test site, Claesson P., Linköping.

Larsson, R., Bengtsson, P.-E. & Eriksson, L. (1994). Sättningsprognoser för bankar på lösa finkorniga jordar, Statens Geotekniska Institut, Report Linköping.

Leroueil, S., Kabbaj, M., Tavenas, F. & Bouchard, R. (1985). Stress-strain-strain rate for the compressibility of sensitive clays, *Géotechnique,* Vol. 35, No. 2, pp. 159-180.

Leroueil, S., & Marques, M. E. S. (1996). State of the art: Importance of strain rate and temperature effects in geotechnical engineering. Washington, D.C., pp. 1-60.

Länsivaara, T. (1995). Stress-strain-strain rate relation in oedometer tests. *Proceedings, 70 Years of Soil Mechanics, International Symposium*, Istanbul, pp. 109-118.

Länsivaara, T. (1999). A study of the mechanical behaviour of soft clay, Ph.D. Thesis, Department of Geotechnical Engineering, The Norwegian University of Science and Technology, Trondheim.

Magnan, J. P., Baghery, S., Brucy, M. & Tavenas, F. (1979). Etude numerique de la consolidationunidimensionelle en tenant compte des variations de la perméabilité et de la compressibilité du sol, dufluage et dela non-saturation. *Bulletin de Liaison* Vol. No. 103, pp. 83-94.

Mesri, G., & Castro, A. (1987). C_α/C_c concept and K_0 during secondary compression, *Journal of Geotechnical Engineering,* Vol. 113, No. 2, March, pp. 230-247.

Mesri, G., & Choi, Y. K. (1985). The uniqueness of the end-of-primary (EOP) void ratio-effective stress relationship. *Proc. of the 11th Int. Conf. on Soil Mechanics and Foundation Engineering*, San Fransisco, pp. 587-590.

Mesri, G., & Godlewski, P. (1977). Time- and stress-compressibility interrelationship, *Journal of the Geotechnical Engineering Division, Proceeding of the American Society of Civil Engineers,* Vol. 103, No GT5, May, pp. 417-430.

Mesri, G., Choi, Y. K., & Lo, D. O. K. (1989). The ILLICON Computer Program, Dep. of Civil Engineering, University of Illinois at Urbana-Champaign, Urbana, Illinios.

Mesri, G., Kwan Lo, D.O. & Feng, T.-W. (1994). Settlement of embankments on soft clays Vertical and horizontal deformations of foundations and embankments. *Proceedings of Settlements '94, Vertical and Horizontal Deformations of Foundations and Embankments,* Vol. 1, Collage Station, Texas, pp. 8-56.

Runesson, K. (1978). On non-linear consolidation of soft clay, Ph.D. Thesis, Department of Structural Mechanics, Chalmers University of Technology, Göteborg.

SGI (1981). Rv E6 Göteborg - Uddevalla, delen Bratteröd - Bräcke, Göteborgs och Bohuslän, Tekniskt PM, Report Linköping.

SIS (1991). Svensk standard SS 02 71 26, Geotechnical tests - Compression properties - Oedometer test, CRS test - Cohesive soil, BST, Byggstandardiseringen, Stockholm.

Smith, R. E., & Wahls, H. E. (1969). Consolidation under Constant Rate of Strain. *J. Soil Mechanics and Foundation, Div. ASCE*, Ann Arbor, Michigan, pp. 519-539.

Suklje, L. (1957). The Analysis of the Consolidation Process by the Isotaches Method. *Proc. of the fourth Int. Con. on Soil Mechanics and Foundation Engineering*, London, pp. 200-206.

Svanö, G., & Emdal, A. (1987). KRYKON Ver.02, A FEM Program for One-Dimensional Consolidation Analysis including creep effects, Div. of Geotechnical Engineering, SINTEF, Report STF69 F88009, Trondheim.

Svanö, G., Christensen, S. & Nordahl, S. (1991). A soil model for consolidation and creep. *Proceeding of the 10th European Conference on Soil Mechanics and Foundation Engineering*, Florens, pp. 269-272.

Sällfors, G. (1975). Preconsolidation pressure of soft, high-plastic clays, Ph. D. Thesis, Department of Geotechnical Engineering, Chalmers University of Technology, Göteborg.

Tavenas, F., Leroueil, S., La Rochelle, P. & Roy, M. (1978). Creep behaviour of an undisturbed lightly overconsolidated clay, *Canadian Geotechnical Journal* Vol. 15, No. 3, pp. 402-423.

Taylor, D. W. (1942). Research on consolidation of clays, Massachusetts Institute of Technology, Deparment of Civil Engineering, Report 82, Cambridge, Massachusetts.

Taylor, D. W. (1948). Fundamentals of Soil Mechanics, 9th printing 1956, John Wiley & Sons, Inc, New York, Cambridge, Massachusetts.

Taylor, D. W. & Merchant, W. (1940). A theory of consolidation accounting for secondary compression, *Journal of Mathematics and Physics,* Vol. 19, No. 3, pp. 167-185.

Terzaghi, K. (1923). Die Berechnung der Durchlässigkeitsziffer des Tones aus dem Verlauf der hydrodynamishen Spannungserscheinungen. Akademie der Wisenschaften in Wien. *Mathematisch-Naturwissenschaftliche Klasse*. Seitungberichte. Abteilung IIa Vol. 132, No. 3/4, pp. 125-138.

Terzaghi, K. (1943). Theoretical Soil Mechanics, 7th printing 1954, John Wiley & Sons, Inc, New York, Cambridge, Massachusetts,

Terzaghi, K., & Fröhlich, O. K. (1936). Theorie der Setzung von Tonschichten, Report Vienna: Deuticke.

Tidfors, M., & Sällfors, G. (1989). Temperature effects on the preconsolidation pressure, *Geotechnical Testing Journal,* Vol. 12, No. 1, pp. 93-97.

Wissa, A. (1969). A New One-Dimensional Consolidation Test. *Proc. 8th Int. Conf. Soil Mechanics and Foundation Engineering*, Mexico City, p. 524.

Yin J.H. & Graham, J. (1989). Viscous-elastic-plastic modelling of one-dimensional time dependent behaviour of clays, *Canadian Geotechnical Journal,* Vol. 26, No. 2, pp. 199-209.

Yin, J.H., & Graham, J. (1994). Equivalent times and one-dimensional elastic visco-plastic modelling of time-dependent stress-strain behaviour of clays *Canadian Geotechnical Journal* Vol. 31, No. Number 1, February, pp. 42-52.

Yin, J.H., & Graham, J. (1996). Elastic visco-plastic modelling of one-dimensional consolidation, *Géotechnique,* Vol. 46, No. 3, pp. 515-527.

Yin, J.-H., & Graham, J. (1999). Elastic visco-plastic modelling of the time-dependent stress-strain behaviour of soils, *Canadian Geotechnical Journal,* Vol. 36, No. Number 4, August, pp. 736-745.

Åhnberg, H., & Holm, G. (1988). Cellplastbank i Bratteröd, E6 Göteborg - Uddevalla, Resultat av sättningsberäkning och uppföljning, SGI, Report Linköping.

APPENDICES

Appendix A: The Änggårdens test site, results from geotechnical investigations borehole CTH12.

Appendix B: The Bratteröd test site, results from geotechnical investigations borehole CTH02 and CTH03.

Appendix C: Evaluated in-situ effective stress and preconsolidation pressure for borehole 101, Lundby Strand, and for kv Guldet, Lilla Bommen.

APPENDIX A

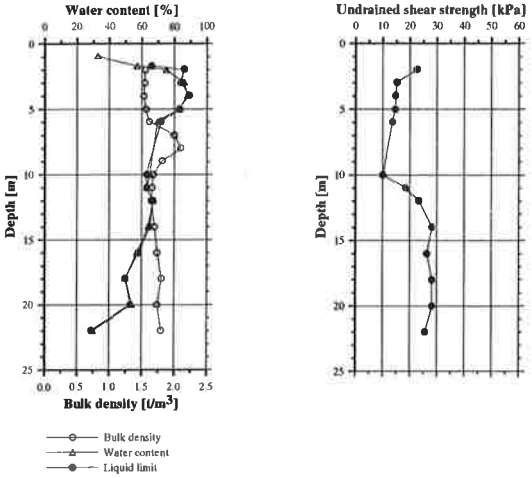

Figure A1 *Soil parameters for borehole CTH12, the Änggården test site.*

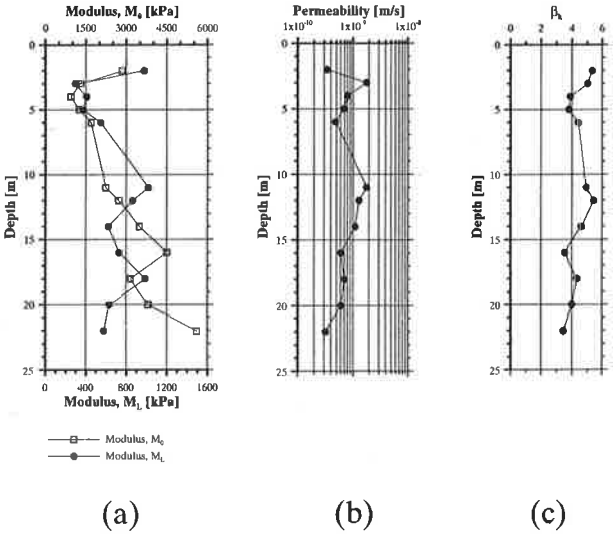

Figure A2 *Interpreted values of compression moduli, permeability and the coefficient of permeability change for borehole CTH12 at the Änggården test site.*

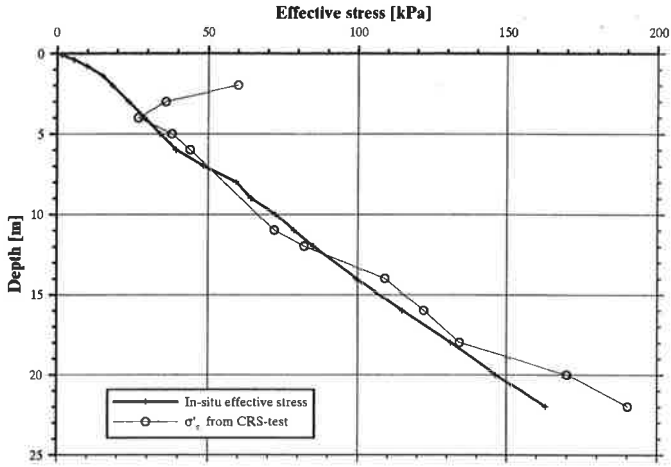

Figure A3 *Evaluated in-situ effective stress and preconsolidation pressure for borehole CTH12 at the Änggården test site.*

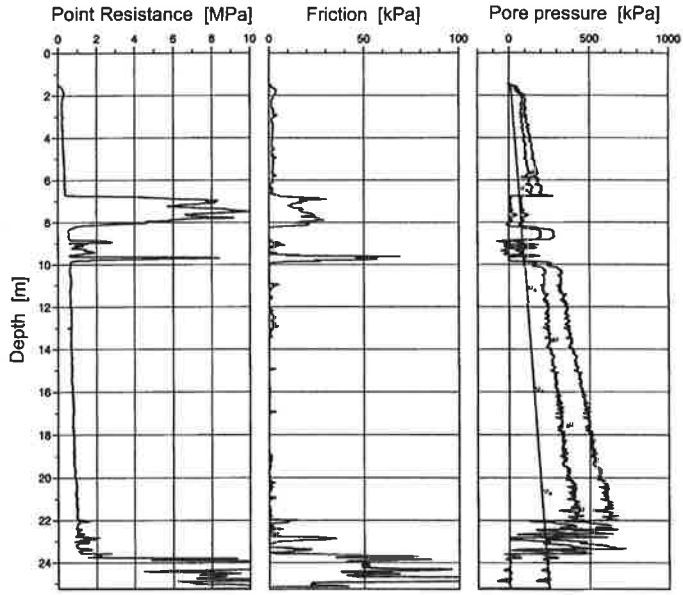

Figure A4 *Results of CPT test for borehole CTH12 at the Änggården test site.*

APPENDIX B

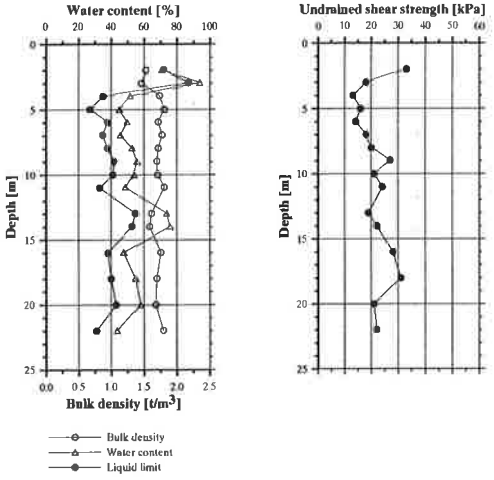

Figure B1 *Soil parameters for borehole CTH02, the Bratteröd test site.*

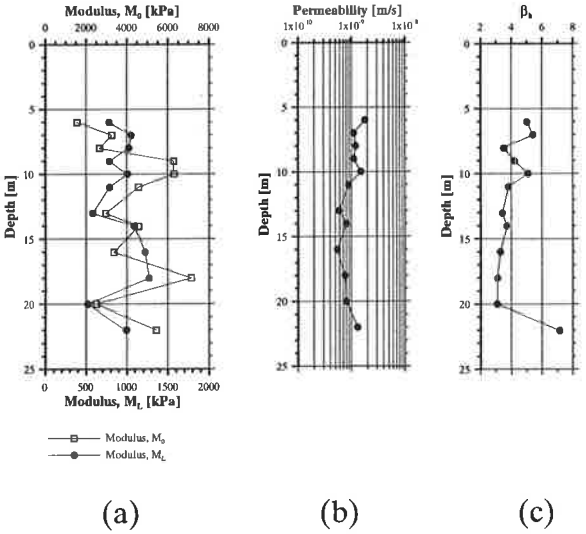

Figure B2 *Interpreted values of compression moduli, permeability and the coefficient of permeability change for borehole CTH02 at the Bratteröd test site.*

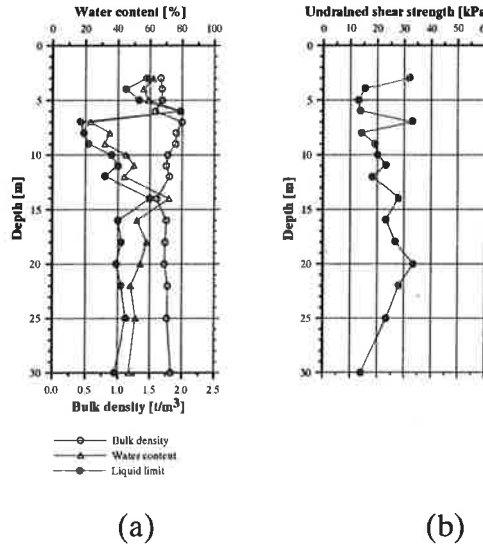

Figure B3 *Soil parameters for borehole CTH03, the Bratteröd test site.*

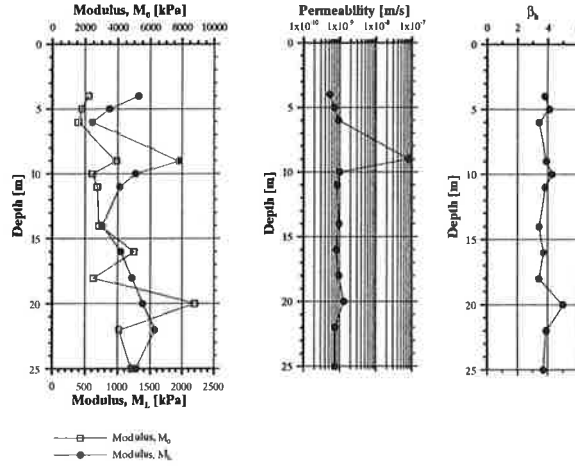

Figure B4 *Interpreted values of compression moduli, permeability and the coefficient of permeability change for borehole CTH03 at the Bratteröd test site.*

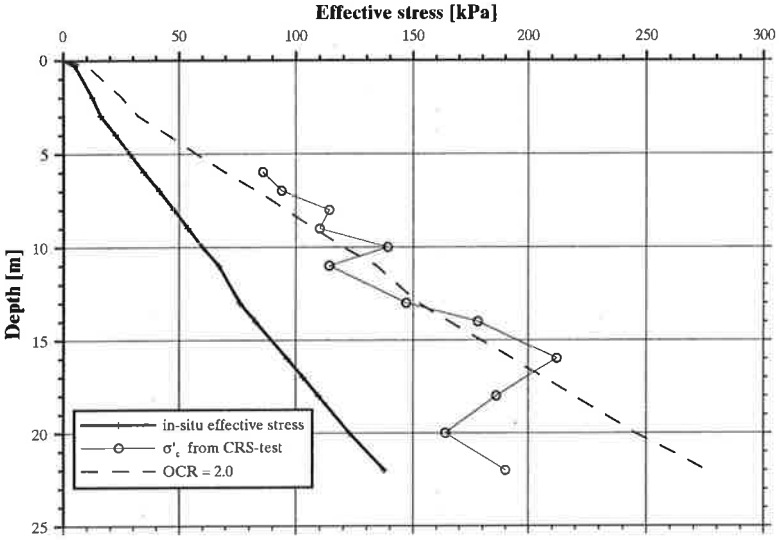

Figure B5 *Evaluated in-situ effective stress and preconsolidation pressure for borehole CTH02 at the Bratteröd test site.*

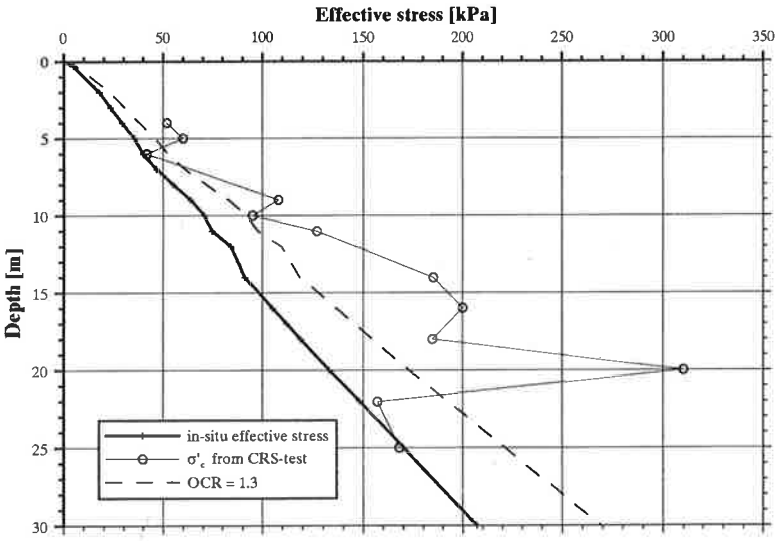

Figure B6 *Evaluated in-situ effective stress and preconsolidation pressure for borehole CTH03 at the Bratteröd test site.*

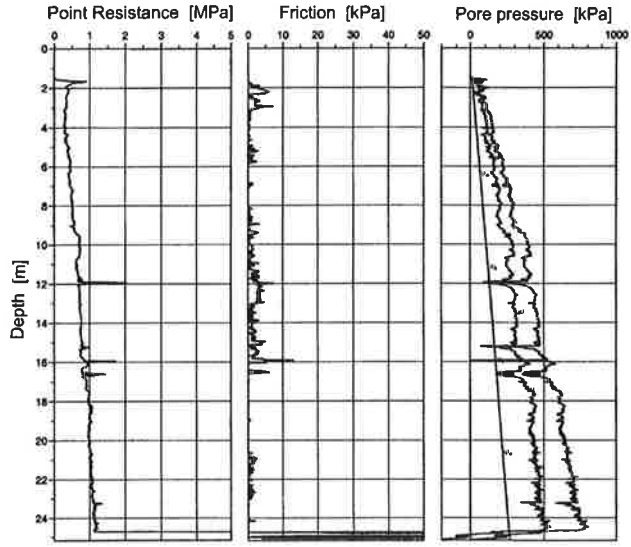

Figure B7 *Results of CPT test for borehole CTH02 at the Bratteröd test site.*

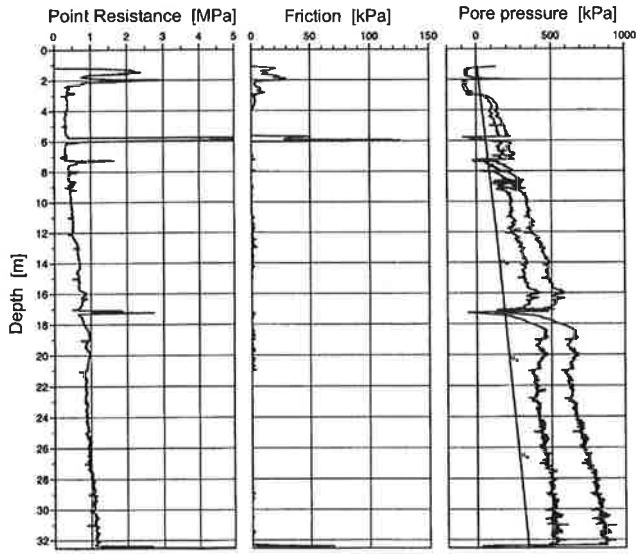

Figure B8 *Results of CPT test for borehole CTH03 at the Bratteröd test site.*

APPENDIX C

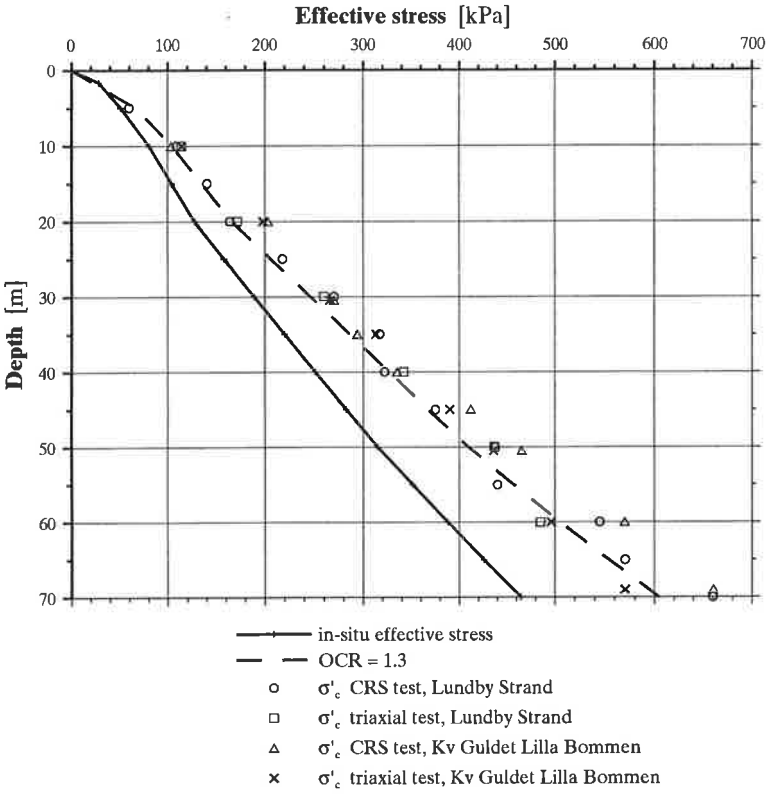

Figure C1 *Evaluated in-situ effective stress and preconsolidation pressure for borehole 101 at the Lundy Strand test site and for Kv Guldet Lilla Bommen.*

CHALMERS UNIVERSITY OF TECHNOLOGY
SE-412 96 Göteborg, Sweden
Telephone: +46-(0)31 772 10 00
www.chalmers.se